

PDF hosted at the Radboud Repository of the Radboud University Nijmegen

The following full text is a publisher's version.

For additional information about this publication click this link.

<http://hdl.handle.net/2066/147393>

Please be advised that this information was generated on 2017-12-05 and may be subject to change.



Search for the associated production of the Higgs boson with a top quark pair in multilepton final states with the ATLAS detector



ATLAS Collaboration ^{*}

ARTICLE INFO

Article history:

Received 19 June 2015

Received in revised form 29 July 2015

Accepted 31 July 2015

Available online 5 August 2015

Editor: W.-D. Schlatter

ABSTRACT

A search for the associated production of the Higgs boson with a top quark pair is performed in multilepton final states using 20.3 fb^{-1} of proton–proton collision data recorded by the ATLAS experiment at $\sqrt{s} = 8 \text{ TeV}$ at the Large Hadron Collider. Five final states, targeting the decays $H \rightarrow WW^*$, $\tau\tau$, and ZZ^* , are examined for the presence of the Standard Model (SM) Higgs boson: two same-charge light leptons (e or μ) without a hadronically decaying τ lepton; three light leptons; two same-charge light leptons with a hadronically decaying τ lepton; four light leptons; and one light lepton and two hadronically decaying τ leptons. No significant excess of events is observed above the background expectation. The best fit for the $t\bar{t}H$ production cross section, assuming a Higgs boson mass of 125 GeV, is $2.1^{+1.4}_{-1.2}$ times the SM expectation, and the observed (expected) upper limit at the 95% confidence level is 4.7 (2.4) times the SM rate. The p -value for compatibility with the background-only hypothesis is 1.8σ ; the expectation in the presence of a Standard Model signal is 0.9σ .

© 2015 CERN for the benefit of the ATLAS Collaboration. Published by Elsevier B.V. This is an open access article under the CC BY license (<http://creativecommons.org/licenses/by/4.0/>). Funded by SCOAP³.

1. Introduction

The discovery of a new particle H with a mass of about 125 GeV in searches for the Standard Model (SM) [1–3] Higgs boson [4–7] at the LHC was reported by the ATLAS [8] and CMS [9] Collaborations in July 2012. The particle has been observed in the decays $H \rightarrow \gamma\gamma$ [10,11], $H \rightarrow ZZ^* \rightarrow 4\ell$ [12,13], and $H \rightarrow WW^* \rightarrow \ell\nu\ell\nu$ [14,15], and evidence has been reported for $H \rightarrow \tau\tau$ [16,17], consistent with the rates expected for the SM Higgs boson.

The observation of the process in which the Higgs boson is produced in association with a pair of top quarks ($t\bar{t}H$) would permit a direct measurement of the top quark–Higgs boson Yukawa coupling in a process that is tree-level at the lowest order, which is otherwise accessible primarily through loop effects. Having both the tree- and loop-level measurements would allow disambiguation of new physics effects that could affect the two differently, such as dimension-six operators contributing to the ggH vertex. This letter describes a search for the SM Higgs boson in the $t\bar{t}H$ production mode in multilepton final states. The five final states considered are: two same-charge-sign light leptons (e or μ) with no additional hadronically decaying τ lepton; three light leptons; two same-sign light leptons with one hadronically decaying τ lepton; four light leptons; and one light lepton with two hadronically decaying τ candidates. These channels are sensitive to the Higgs decays $H \rightarrow WW^*$, $\tau\tau$, and ZZ^* produced in association

with a top quark pair decaying to one or two leptons. A similar search has been performed by the CMS Collaboration [18].

The selections of this search are designed to avoid overlap with ATLAS searches for $t\bar{t}H$ in $H \rightarrow b\bar{b}$ [19] and $H \rightarrow \gamma\gamma$ [20] decays. The main backgrounds to the signal arise from $t\bar{t}$ production with additional jets and non-prompt leptons, associated production of a top quark pair and a vector boson W or Z (collectively denoted $t\bar{t}V$), and other processes where the electron charge is incorrectly measured or where quark or gluon jets are incorrectly identified as τ candidates.

2. ATLAS detector and dataset

The features of the ATLAS detector [21] most relevant to this analysis are briefly summarized here. The detector consists of an inner tracking detector system surrounded by a superconducting solenoid, electromagnetic and hadronic calorimeters, and a muon spectrometer. Charged particles in the pseudorapidity¹ range $|\eta| < 2.5$ are reconstructed with the inner tracking detector, which is immersed in a 2 T magnetic field parallel to the detector axis

¹ The ATLAS experiment uses a right-handed coordinate system with its origin at the nominal interaction point (IP) in the centre of the detector, and the z -axis along the beam line. The x -axis points from the IP to the centre of the LHC ring, and the y -axis points upwards. Cylindrical coordinates (r, ϕ) are used in the transverse plane, ϕ being the azimuthal angle around the z -axis. Observables labelled “transverse” are projected onto the x - y plane. The pseudorapidity is defined in terms of the polar angle θ as $\eta = -\ln \tan \theta/2$. The transverse momentum is defined as $p_T = p \sin \theta = p/\cosh \eta$, and the transverse energy E_T has an analogous definition.

^{*} E-mail address: atlas.publications@cern.ch.

and consists of pixel and strip semiconductor detectors as well as a straw-tube transition radiation tracker. The solenoid is surrounded by a calorimeter system covering $|\eta| < 4.9$, which provides three-dimensional reconstruction of particle showers. Lead/liquid-argon (LAr) sampling technology is used for the electromagnetic component. Iron/scintillator-tile sampling calorimeters are used for the hadronic component for $|\eta| < 1.7$, and copper/LAr and tungsten/LAr technology is used for $|\eta| > 1.5$. Outside the calorimeter system, air-core toroids provide a magnetic field for the muon spectrometer. Three stations of precision drift tubes and cathode-strip chambers provide a measurement of the muon track position and curvature in the region $|\eta| < 2.7$. Resistive-plate and thin-gap chambers provide muon triggering capability up to $|\eta| = 2.4$.

This search uses data collected by the ATLAS experiment in 2012 at a centre-of-mass energy of $\sqrt{s} = 8$ TeV. All events considered were recorded while the detector and trigger systems were fully functional; the integrated luminosity of this dataset is 20.3 fb^{-1} .

3. Cross sections for signal and background processes

The cross section for the production of $t\bar{t}H$ in pp collisions has been calculated at next-to-leading order (NLO) in quantum chromodynamics (QCD) [22–26]. Uncertainties on the cross section are evaluated by varying the renormalization and factorization scales by factors of two and by varying the input parton distribution functions (PDF) of the proton. A Higgs boson mass of $m_H = 125$ GeV is assumed; this gives a predicted $t\bar{t}H$ production cross section at $\sqrt{s} = 8$ TeV of 129_{-12}^{+5} (scale) ± 10 (PDF) fb [27]. This assumed Higgs boson mass is consistent with the combined ATLAS and CMS measurement [28].

In this letter the associated production of single top quarks with a Higgs boson is considered a background process and set to the Standard Model rate. The production of $tHqb$ and tHW is taken into account. In the Standard Model these rates are very small compared to $t\bar{t}H$ production. These processes are simulated with the same parameters as used by the ATLAS $t\bar{t}H$, $H \rightarrow \gamma\gamma$ search [20]. The cross sections for both are computed using the MG5_AMC@NLO generator [29] at NLO in QCD. For $tHqb$, the renormalization and factorization scales are set to 75 GeV and the process is computed in the four-flavour scheme, yielding $\sigma(tHqb) = 17.2_{-1.4}^{+0.8}$ (scale) $_{-0.9}^{+1.2}$ (PDF) fb. For tHW , dynamic factorization and renormalization scales are used, and the process is computed in the five-flavour scheme; the result is $\sigma(tHW) = 4.7_{-0.3}^{+0.4}$ (scale) $_{-0.6}^{+0.8}$ (PDF) fb. The interference of tHW production with $t\bar{t}H$, which appears at NLO for tHW in diagrams with an additional b -quark in the final state, is not considered.

The production of $t\bar{t}W$ and $t\bar{t}(Z/\gamma^*) \rightarrow t\bar{t}\ell^+\ell^-$ yield multi-lepton final states with b -quarks and are major backgrounds to the $t\bar{t}H$ signal. For simplicity of notation the latter process is referred to as $t\bar{t}Z$ throughout this letter with off-shell Z and photon components also included except where noted otherwise. The $t\bar{t}W$ process includes both $t\bar{t}W^+$ and $t\bar{t}W^-$ components. Next-to-leading-order cross sections are used for $t\bar{t}W$ [30] and $t\bar{t}Z$ [31]. The MG5_AMC@NLO generator is used to reproduce the QCD scale uncertainties of these calculations and determine uncertainties due to the PDF. For $t\bar{t}W$ production the value 232 ± 28 (scale) ± 18 (PDF) fb is used, and for $t\bar{t}Z$ production² the value is 206 ± 23 (scale) ± 18 (PDF) fb.

² The NLO cross section is only evaluated for $t\bar{t}Z$ production with on-shell Z . The cross section obtained for $t\bar{t}(Z/\gamma^*)$ production including off-shell Z/γ^* contributions in a leading-order simulation is scaled by a K -factor of 1.35 obtained as the ratio of NLO and LO on-shell cross sections. The K -factor differs from that of Ref. [31] due to a different choice of PDF.

The associated production of a single top quark and a Z boson is a subleading background for the most sensitive channels. The cross section has been calculated at NLO for the t - and s -channels [32]. The resulting values used in this work are 160 ± 7 (scale) ± 11 (PDF) fb for tZ and 76 ± 4 (scale) ± 5 (PDF) fb for $\bar{t}Z$. The cross section for the production of tWZ is computed at leading order (LO) using the MADGRAPH v5 generator [33] and found to be 4.1 fb.

The cross section for inclusive production of vector boson pairs WW , WZ , and ZZ is computed using MCFM [34]. Contributions from virtual photons and off-shell Z bosons are included. The uncertainties on the acceptance for these processes in the signal regions (which favour production with additional b - or c -quarks) dominate over the inclusive cross-section uncertainty (see Section 7.2) and so the latter is neglected in the analysis.

The inclusive $t\bar{t}$ cross section is calculated at next-to-next-to-leading order (NNLO) in QCD which includes resummation of next-to-next-to-leading logarithmic (NNLL) soft gluon terms using TOP++ [35], yielding 253_{-15}^{+13} pb for $\sqrt{s} = 8$ TeV. The single-top-quark samples are normalized to the approximate NNLO theoretical cross sections [36–38] using the MSTW2008 [39] NNLO PDF set. The production of $Z \rightarrow \ell^+\ell^- + \text{jets}$ and $W \rightarrow \ell\nu + \text{jets}$ is normalized using NNLO cross sections as computed by FEWZ [40].

4. Event generation

The event generator configurations used for simulating the signal and main background processes are shown in Table 1. Additional information is given below.

The $t\bar{t}H$ signal event simulation samples contain all Higgs boson decays with branching fractions set to values computed at NNLO in QCD [26,66–69]. The factorization (μ_F) and renormalization (μ_R) scales are set to $m_t + m_H/2$. Higgs boson and top quark masses of 125 and 172.5 GeV, respectively, are used. These samples are the same as those used by other ATLAS $t\bar{t}H$ searches [19, 20].

Production of single top quarks with Higgs bosons is simulated as follows. For $tHqb$, events are generated at leading order with MADGRAPH in the four-flavour scheme. For tHW , events are generated at NLO with MG5_AMC@NLO in the five-flavour scheme. Higgs boson and top quark masses are set as for $t\bar{t}H$ production.

The main irreducible backgrounds are production of $t\bar{t}W$ and $t\bar{t}Z$ ($t\bar{t}V$). For the $t\bar{t}W$ process, events are generated at leading order with zero, one, or two extra partons in the final state, while for $t\bar{t}Z$ zero or one extra parton is generated. The important contribution from off-shell $\gamma^*/Z \rightarrow \ell^+\ell^-$ is included. The tZ process is simulated with the same setup, without extra partons.

For diboson processes, the full matrix element for $\ell^+\ell^-$ production, including γ^* and off-shell Z contributions, is used. The SHERPA $q\bar{q}$ and qg samples include diagrams with additional partons in the final state at the matrix-element (ME) level, and include b - and c -quark mass effects. SHERPA was found to have better agreement with data than POWHEG for WZ , while the SHERPA and POWHEG descriptions of ZZ production are similar.

A $t\bar{t} + \text{jets}$ sample generated with the POWHEG NLO generator [61] is used; the top quark mass is set to 172.5 GeV. Small corrections to the $t\bar{t}$ system and top quark p_T spectra are applied based on discrepancies in differential distributions observed between data and simulation at 7 TeV [70]. Double-counting between the $t\bar{t}$ and Wt single top production final states is eliminated using the diagram-removal method [71].

Samples of $Z \rightarrow \ell^+\ell^- + \text{jets}$ and $W \rightarrow \ell\nu + \text{jets}$ events are generated with up to five additional partons using the ALPGEN v2.14 [65] leading order (LO) generator. Samples are merged with matrix element-parton shower overlaps removed using MLM

Table 1

Configurations used for event generation of signal and background processes. If only one parton distribution function is shown, the same one is used for both the matrix element (ME) and parton shower generators; if two are shown, the first is used for the matrix element calculation and the second for the parton shower. “Tune” refers to the underlying-event tune of the parton shower generator. “PYTHIA 6” refers to version 6.425; “PYTHIA 8” refers to version 8.1; “HERWIG++” refers to version 2.6; “MADGRAPH” refers to version 5; “ALPGEN” refers to version 2.14; “SHERPA” refers to version 1.4; “GGZZ” refers to version 2.0.

Process	ME generator	Parton shower	PDF	Tune
$t\bar{t}H$	HELAC-OneLoop [41,42] + POWHEG-BOX [48–50] MADGRAPH [33]	PYTHIA 8 [43]	CT10 [44]/CTEQ6L1 [45,46]	AU2 [47]
$tHqb$	MADGRAPH [33]	PYTHIA 8	CT10	AU2
tHW	MG5_AMC@NLO [29]	HERWIG++ [51]	CT10/MRST LO** [52]	UE-EE-4 [53]
$t\bar{t}W + \leq 2$ partons	MADGRAPH	PYTHIA 6 [54]	CTEQ6L1	AUET2B [55]
$t\bar{t}(Z/\gamma^*) + \leq 1$ parton	MADGRAPH	PYTHIA 6	CTEQ6L1	AUET2B
$t(Z/\gamma^*)$	MADGRAPH	PYTHIA 6	CTEQ6L1	AUET2B
$q\bar{q}, qg \rightarrow WW, WZ$	SHERPA [56]	SHERPA	CT10	SHERPA default
$qq \rightarrow qqWW, qqWZ, qqZZ$	SHERPA	SHERPA	CT10	SHERPA default
$q\bar{q}, qg \rightarrow ZZ$	POWHEG-BOX [57]	PYTHIA 8	CT10	AU2
$gg \rightarrow ZZ$	GGZZ [58]	HERWIG [59]	CT10	AUET2 [60]
$t\bar{t}$	POWHEG-BOX [61]	PYTHIA 6	CT10/CTEQ6L1	Perugia2011C [62]
$s-, t$ -channel, Wt single top	POWHEG-BOX [63,64]	PYTHIA 6	CT10/CTEQ6L1	Perugia2011C
$Z \rightarrow \ell^+\ell^- + \leq 5$ partons	ALPGEN [65]	PYTHIA 6	CTEQ6L1	Perugia2011C
$W \rightarrow \ell\nu + \leq 5$ partons	ALPGEN	PYTHIA 6	CTEQ6L1	Perugia2011C

matching [72]. Production of b - and c -quarks is also computed at matrix-element level, and overlaps between ME and parton shower production are handled by separating the kinematic regimes based on the angular separation of additional heavy partons. The resulting “light” and “heavy” flavour samples are normalized by comparing the resulting b -tagged jet spectra with data.

All simulated samples with PYTHIA 6 and HERWIG [59] parton showering use PHOTOS 2.15 [73] to model photon radiation and TAUOLA 1.20 [74] for τ decays. The HERWIG++ samples model photon radiation with PHOTOS but use the internal τ decay model. Samples using PYTHIA 8.1 and SHERPA use those generators’ internal τ lepton decay and photon radiation generators. For HERWIG samples, multiple parton interactions are modelled with JIMMY [75].

Showered and hadronized events are passed through simulations of the ATLAS detector (either full GEANT4 [76] simulation or a hybrid simulation with parameterized calorimeter showers and GEANT4 simulation of the tracking systems [77,78]). Additional minimum-bias pp interactions (pileup) are modelled with the PYTHIA 8.1 generator with the MSTW2008 LO PDF set and the A2 tune [79]. They are added to the signal and background simulated events according to the luminosity profile of the recorded data, with additional overall scaling to achieve a good match to observed calorimetry and tracking variables. The contributions from pileup interactions both within the same bunch crossing as the hard-scattering process and in neighbouring bunch crossings are included in the simulation.

5. Object selection

Electron candidates are reconstructed from energy clusters in the electromagnetic calorimeter associated with reconstructed tracks in the inner detector. They are required to have $|\eta_{\text{cluster}}| < 2.47$. Candidates in the transition region $1.37 < |\eta_{\text{cluster}}| < 1.52$ between sections of the electromagnetic calorimeter are excluded. A multivariate discriminant based on shower shape and track information is used to distinguish electrons from hadronic showers [80,81]. Only electron candidates with transverse energy E_T greater than 10 GeV are considered. To reduce the background from non-prompt electrons, i.e. from decays of hadrons (including heavy flavour) produced in jets, electron candidates are required to be isolated. Two isolation variables, based on calorimetric and tracking variables, are computed. The first (E_T^{cone}) is based on the sum of transverse energies of calorimeter cells within a cone of radius $\Delta R \equiv \sqrt{(\Delta\phi)^2 + (\Delta\eta)^2} = 0.2$ around the electron candidate direction. This energy sum excludes cells associated with the

electron and is corrected for leakage from the electromagnetic shower and ambient energy in the event. The second (p_T^{cone}) is defined based on tracks with $p_T > 1$ GeV within a cone of radius $\Delta R = 0.2$ around the electron candidate. Both isolation energies are separately required to be less than $0.05 \times E_T$. The longitudinal impact parameter of the electron track with respect to the selected event primary vertex, multiplied by the sine of the polar angle, $|z_0 \sin\theta|$, is required to be less than 1 mm. The transverse impact parameter divided by the estimated uncertainty on its measurement, $|d_0|/\sigma(d_0)$, must be less than 4. If two electrons closer than $\Delta R = 0.1$ are selected, only the one with the higher p_T is considered. An electron is rejected if, after passing all the above selections, it lies within $\Delta R = 0.1$ of a selected muon.

Muon candidates are reconstructed by combining inner detector tracks with track segments or full tracks in the muon spectrometer [82]. Only candidates with $|\eta| < 2.5$ and $p_T > 10$ GeV are kept. Additionally, muons are required to be separated by at least $\Delta R > 0.04 + (10 \text{ GeV})/p_{T,\mu}$ from any selected jets (see below for details on jet reconstruction and selection). The cut value is optimized to maximize the acceptance for prompt muons at a fixed rejection factor for non-prompt and fake muon candidates. Furthermore, muons must satisfy similar E_T^{cone} and p_T^{cone} isolation criteria as for electrons, with both required to be less than $0.10 \times p_T$. The value of $|z_0 \sin\theta|$ is required to be less than 1 mm, while $|d_0|/\sigma(d_0)$ must be less than 3.

Hadronically decaying τ candidates (τ_{had}) are reconstructed using clusters in the electromagnetic and hadronic calorimeters. The τ candidates are required to have p_T greater than 25 GeV and $|\eta| < 2.47$. The number of charged tracks associated with the τ candidates is required to be one or three and the charge of the τ candidates, determined from the associated tracks, must be ± 1 . The τ identification uses calorimeter cluster and tracking-based variables, combined using a boosted decision tree (BDT) [83]. An additional BDT which uses combined calorimeter and track quantities is employed to reject electrons reconstructed as one-prong hadronically decaying τ leptons.

Jets are reconstructed from calibrated topological clusters [21] built from energy deposits in the calorimeters, using the anti- k_t algorithm [84–86] with a radius parameter $R = 0.4$. Prior to jet finding, a local cluster calibration scheme [87,88] is applied to correct the topological cluster energies for the effects of non-compensating calorimeter response, inactive material and out-of-cluster leakage. The jets are calibrated using energy and η -dependent calibration factors, derived from simulations, to the mean energy of stable particles inside the jets. Additional correc-

tions to account for the difference between simulation and data are derived from in-situ techniques [89,90]. After energy calibration, jets are required to have $p_T > 25$ GeV and $|\eta| < 2.5$.

To reduce the contamination from jets originating in pp interactions within the same bunch crossing (pileup), the scalar sum of the p_T of tracks matched to the jet and originating from the primary vertex must be at least 50% of the scalar sum of the p_T of all tracks matched to the jet. This criterion is only applied to jets with $p_T < 50$ GeV (those most likely to originate from pileup) and $|\eta| < 2.4$ (to avoid inefficiency at the edge of tracking acceptance).

The calorimeter energy deposits from electrons are typically also reconstructed as jets; in order to eliminate double counting, any jets within $\Delta R = 0.3$ of a selected electron are not considered.

Jets containing b -hadrons are identified (b -tagged) via a multivariate discriminant [91] that combines information from the impact parameters of displaced tracks with topological properties of secondary and tertiary decay vertices reconstructed within the jet. The working point used for this search corresponds to approximately 70% efficiency to tag a b -hadron jet, with a light-jet mistag rate of $\approx 1\%$ and a charm-jet rejection factor of 5, as determined for b -tagged jets with p_T of 20–100 GeV and $|\eta| < 2.5$ in simulated $t\bar{t}$ events. To avoid inefficiencies associated with the edge of the tracking coverage, only jets with $|\eta| < 2.4$ are considered as possible b -tagged jets in this analysis. The efficiency and mistag rates of the b -tagging algorithm are measured in data [91,92] and correction factors are applied to the simulated events.

6. Event selection and classification

All events considered in this analysis are required to pass single-lepton (e or μ) triggers. These achieve their maximal plateau efficiency for lepton $p_T > 25$ GeV.

This analysis primarily targets the $H \rightarrow WW^*$ and $\tau\tau$ decay modes. Considering the decay of the $t\bar{t}$ system as well, these $t\bar{t}H$ events contain either $WWWWb\bar{b}$ or $\tau\tau WWb\bar{b}$. The strategy is to target final states that cannot be produced in $t\bar{t}$ decay alone – i.e., three or more leptons, or two same-sign leptons – thus suppressing what would otherwise be the largest single background.

The analysis categories are classified by the number of light leptons and hadronic τ decay candidates. The leptons are selected using the criteria described earlier. Events are initially classified by counting the number of light leptons with $p_T > 10$ GeV. At least one light lepton is required to match a lepton selected by the trigger system. After initial sorting into analysis categories, in some cases the lepton selection criteria are tightened by raising the p_T threshold, tightening isolation selections or restricting the allowed $|\eta|$ range, as explained in the following per-category descriptions. The analysis includes five distinct categories: two same-sign light leptons with no τ_{had} ($2\ell 0\tau_{\text{had}}$), three light leptons (3ℓ), two same-sign light leptons and one τ_{had} ($2\ell 1\tau_{\text{had}}$), four light leptons (4ℓ), and one light lepton and two τ_{had} ($1\ell 2\tau_{\text{had}}$). The categories with τ_{had} candidates target the $H \rightarrow \tau\tau$ decay; the others are primarily sensitive to $H \rightarrow WW^*$ with a very small contribution from $H \rightarrow ZZ^*$. The contributions to each category from different Higgs boson decay modes are shown in Table 2. These selection criteria ensure that an event can only contribute to a single category. The contamination from gluon fusion, vector boson fusion, and associated VH production mechanisms for the Higgs boson is predicted to be negligible. Summed over all categories, the total expected number of reconstructed signal events assuming Standard Model $t\bar{t}H$ production is 10.2, corresponding to 0.40% of all produced $t\bar{t}H$ events. The detailed criteria for each category are described below.

Table 2

Fraction of the expected $t\bar{t}H$ signal arising from different Higgs boson decay modes in each analysis category. The six $2\ell 0\tau_{\text{had}}$ categories are combined together, as are the two 4ℓ categories. The decays contributing to the “other” column are dominantly $H \rightarrow \mu\mu$ and $H \rightarrow b\bar{b}$. Rows may not add to 100% due to rounding.

Category	Higgs boson decay mode			
	WW^*	$\tau\tau$	ZZ^*	Other
$2\ell 0\tau_{\text{had}}$	80%	15%	3%	2%
3ℓ	74%	15%	7%	4%
$2\ell 1\tau_{\text{had}}$	35%	62%	2%	1%
4ℓ	69%	14%	14%	4%
$1\ell 2\tau_{\text{had}}$	4%	93%	0%	3%

6.1. $2\ell 0\tau_{\text{had}}$ categories

Selected events are required to include exactly two light leptons, which must have the same charge. Events with τ_{had} candidates are vetoed. To reduce the background from non-prompt leptons, the leading (subleading) lepton is required to satisfy $p_T > 25$ (20) GeV, and the muon isolation requirements are tightened to $E_T^{\text{cone}}/p_T < 0.05$ and $p_T^{\text{cone}}/p_T < 0.05$. The angular acceptance of electron candidates is restricted to $|\eta| < 1.37$ in order to suppress $t\bar{t}$ background events where the sign of the electron charge is misreconstructed, as the charge misidentification rate increases at high pseudorapidity.

In order to suppress the lower-multiplicity $t\bar{t} + \text{jets}$ and $t\bar{t}W$ backgrounds, events must include at least four reconstructed jets. In order to suppress diboson and single-boson backgrounds, at least one of these jets must be b -tagged. The selected events are separated by lepton flavour ($e^\pm e^\pm$, $e^\pm \mu^\pm$, and $\mu^\pm \mu^\pm$) and number of jets (exactly four jets, at least five jets) into six categories with different signal-to-background ratio, resulting in higher overall sensitivity to the $t\bar{t}H$ signal.

6.2. 3ℓ category

Selected events are required to include exactly three light leptons with total charge equal to ± 1 . Candidate events arising from non-prompt leptons overwhelmingly originate as opposite-sign dilepton events with one additional non-prompt lepton. As a result, the non-prompt lepton is generally one of the two leptons with the same charge. To reduce these backgrounds, a higher momentum threshold $p_T > 20$ GeV is applied to the two leptons with the same charge. No requirements are imposed on the number of τ_{had} candidates. In order to suppress the $t\bar{t} + \text{jets}$ and $t\bar{t}V$ backgrounds, selected events are required to include either at least four jets of which at least one must be b -tagged, or exactly three jets of which at least two are b -tagged. To suppress the $t\bar{t}Z$ background, events that contain an opposite-sign same-flavour lepton pair with the dilepton invariant mass within 10 GeV of the Z mass are vetoed. Events containing an opposite-sign lepton pair with invariant mass below 12 GeV are also removed to suppress background from resonances that decay to light leptons.

6.3. $2\ell 1\tau_{\text{had}}$ category

Selected events are required to include exactly two light leptons, with the same charge and leading (subleading) $p_T > 25$ (15) GeV, and exactly one hadronic τ candidate. The reconstructed charge of the τ_{had} candidate has to be opposite to that of the light leptons. In order to reduce $t\bar{t} + \text{jets}$ and $t\bar{t}V$ backgrounds, events must include at least four reconstructed jets. In order to suppress diboson and single-boson backgrounds, at least one jet must be b -tagged. To suppress the $Z \rightarrow \ell^+ \ell^- + \text{jets}$ background, events with dielectron invariant mass within 10 GeV of the Z mass are vetoed.

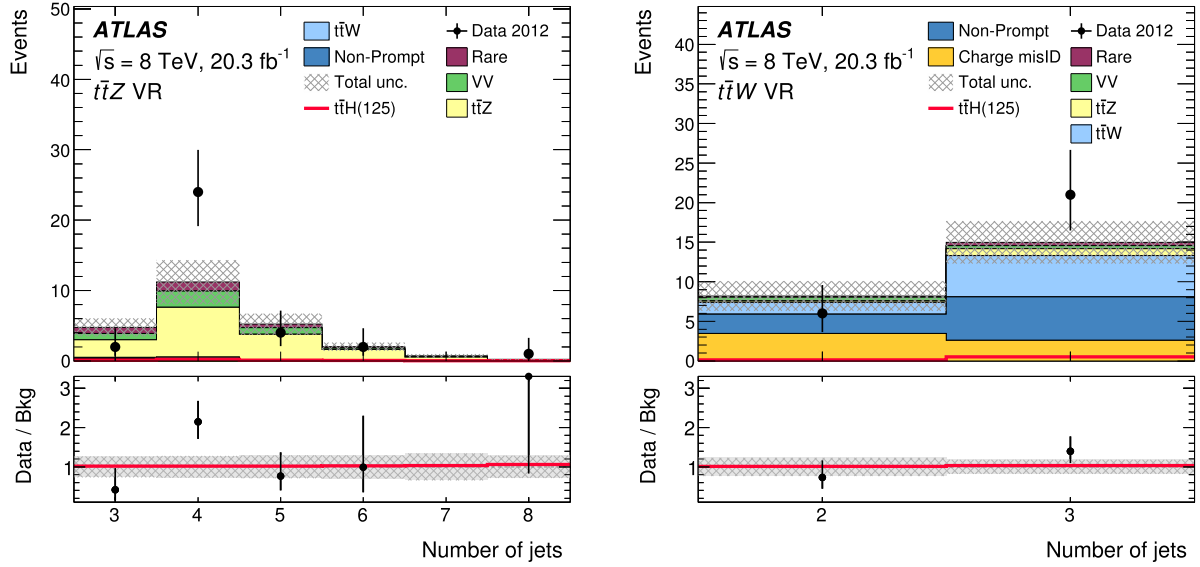


Fig. 1. The spectrum of the number of jets expected and observed in the $t\bar{t}Z$ (left) and $t\bar{t}W$ (right) validation regions (VR). The hatched band represents the total uncertainty on the background prediction in each bin. The “non-prompt” backgrounds are those with a lepton arising from a hadron decay or from a photon conversion in detector material. Rare processes include tZ , $t\bar{t}WW$, triboson, $t\bar{t}t$, and tH production. The overlaid red line corresponds to the $t\bar{t}H$ signal predicted by the SM. (For interpretation of the references to color in this figure legend, the reader is referred to the web version of this article.)

6.4. 4ℓ categories

Selected events are required to include exactly four light leptons with total charge equal to zero and leading (subleading) $p_T > 25$ (15) GeV. No requirements are applied on the number of τ_{had} candidates. In order to suppress the $t\bar{t} + \text{jets}$ and $t\bar{t}V$ backgrounds, the selected events are required to include at least two jets of which at least one must be b -tagged. To suppress the $t\bar{t}Z$ background, events that contain an opposite-sign same-flavour lepton pair with dilepton invariant mass within 10 GeV of the Z mass are vetoed. In order to suppress background contributions from resonances that decay to light leptons, all opposite-sign same-flavour lepton pairs are required to have a dilepton invariant mass greater than 10 GeV. The four-lepton invariant mass is required to be between 100 and 500 GeV, which gives high acceptance for $t\bar{t}H$, $H \rightarrow WW^* \rightarrow \ell\nu\ell\nu$, but rejects $Z \rightarrow 4\ell$ and high-mass $t\bar{t}Z$ events. Selected events are separated by the presence or absence of a same-flavour, opposite-sign lepton pair into two categories, referred to respectively as the Z -enriched and Z -depleted categories. In both cases the Z mass veto is applied, but background events in the Z -enriched category can arise from off-shell Z and $\gamma^* \rightarrow \ell^+\ell^-$ processes while in the Z -depleted category these backgrounds are absent.

6.5. $1\ell 2\tau_{\text{had}}$ category

Selected events are required to include exactly one light lepton with $p_T > 25$ GeV and exactly two hadronic τ candidates. The τ_{had} candidates must have opposite charge. In order to suppress the $t\bar{t} + \text{jets}$ and $t\bar{t}V$ backgrounds, events must include at least three reconstructed jets. In order to suppress diboson and single-boson backgrounds, at least one of the jets must be b -tagged. This final state is primarily sensitive to $H \rightarrow \tau^+\tau^-$ decays, allowing use of the invariant mass of the visible decay products of the $\tau_{\text{had}}\tau_{\text{had}}$ system (m_{vis}) as a signal discriminant. Signal events are required to satisfy $60 < m_{\text{vis}} < 120$ GeV.

7. Background estimation

Important irreducible backgrounds include $t\bar{t}V$ and diboson production and are estimated from MC simulation. Validation regions enriched in these backgrounds are used to verify proper modelling of data by simulation. Reducible backgrounds are due to non-prompt lepton production and electron charge misidentification, and are estimated from data, with input from simulation in some categories. In the $1\ell 2\tau_{\text{had}}$ category the primary concern is fake τ_{had} candidates, which are modelled using simulation and validated against a data-driven estimate.

7.1. $t\bar{t}V$ and tZ

The primary backgrounds with prompt leptons stem from the production of $t\bar{t}W$ and $t\bar{t}Z$. The $t\bar{t}W$ background tends to have lower jet multiplicity than the signal and so the leading contribution comes from events with additional high- p_T jets; it is the major $t\bar{t}V$ contribution in the $2\ell 0\tau_{\text{had}}$ categories and comparable to $t\bar{t}Z$ in the $2\ell 1\tau_{\text{had}}$ category. The $t\bar{t}Z$ process has similar multiplicity to the $t\bar{t}H$ signal but can only contribute to the signal categories when the Z boson decays leptonically, so the on-shell contribution can be removed by vetoing events with opposite-sign dilepton pairs with invariant mass near the Z pole. This is the larger of the two $t\bar{t}V$ contributions for the 3ℓ , 4ℓ , and $1\ell 2\tau_{\text{had}}$ categories. The tZ process makes a subleading contribution to both channels. A validation region is used to verify the modelling of $t\bar{t}Z$ using on-shell Z decays. Agreement is seen within the large statistical uncertainty. No region of equivalent purity and statistical power exists for $t\bar{t}W$ production; nevertheless the expectations are cross-checked with a validation region defined with the $2\ell 0\tau_{\text{had}}$ selection except with two or more b -tagged jets and either two or three jets, where the $t\bar{t}W$ purity is $\approx 30\%$, and are found to be consistent within uncertainties. The spectra of the number of jets in these validation regions are shown in Fig. 1.

Uncertainties on the $t\bar{t}V$ background contributions arise from both the overall cross section uncertainties (see Section 3) and the acceptance uncertainties. The latter are estimated by comparing particle-level samples after showering produced by three different pairs of generators: a) the nominal MADGRAPH LO merged

Table 3
Expected and observed yields in each channel. Uncertainties shown are the sum in quadrature of systematic uncertainties and Monte Carlo simulation statistical uncertainties. “Non-prompt” includes the misidentified τ_{had} background to the $1\ell 2\tau_{\text{had}}$ category. Rare processes (tZ , $t\bar{t}WW$, triboson production, $t\bar{t}t$, tH) are not shown as a separate column but are included in the total expected background estimate.

Category	q mis-id	Non-prompt	$t\bar{t}W$	$t\bar{t}Z$	Diboson	Expected bkg.	$t\bar{t}H$ ($\mu = 1$)	Observed
$ee + \geq 5j$	1.1 ± 0.5	2.3 ± 1.2	1.4 ± 0.4	0.98 ± 0.26	0.47 ± 0.29	6.5 ± 1.8	0.73 ± 0.14	10
$e\mu + \geq 5j$	0.85 ± 0.35	6.7 ± 2.4	4.8 ± 1.2	2.1 ± 0.5	0.38 ± 0.30	15 ± 3	2.13 ± 0.41	22
$\mu\mu + \geq 5j$	–	2.9 ± 1.4	3.8 ± 0.9	0.95 ± 0.25	0.69 ± 0.39	8.6 ± 2.2	1.41 ± 0.28	11
$ee + 4j$	1.8 ± 0.7	3.4 ± 1.7	2.0 ± 0.4	0.75 ± 0.20	0.74 ± 0.42	9.1 ± 2.1	0.44 ± 0.06	9
$e\mu + 4j$	1.4 ± 0.6	12 ± 4	6.2 ± 1.0	1.5 ± 0.3	1.9 ± 1.0	24 ± 5	1.16 ± 0.14	26
$\mu\mu + 4j$	–	6.3 ± 2.6	4.7 ± 0.9	0.80 ± 0.22	0.53 ± 0.30	12.7 ± 2.9	0.74 ± 0.10	20
3ℓ	–	3.2 ± 0.7	2.3 ± 0.7	3.9 ± 0.8	0.86 ± 0.55	11.4 ± 2.3	2.34 ± 0.35	18
$2\ell 1\tau_{\text{had}}$	–	$0.4^{+0.6}_{-0.4}$	0.38 ± 0.12	0.37 ± 0.08	0.12 ± 0.11	1.4 ± 0.6	0.47 ± 0.08	1
$1\ell 2\tau_{\text{had}}$	–	15 ± 5	0.17 ± 0.06	0.37 ± 0.09	0.41 ± 0.42	16 ± 5	0.68 ± 0.13	10
$4\ell Z$ -enr.	–	$\lesssim 10^{-3}$	$\lesssim 3 \times 10^{-3}$	0.43 ± 0.12	0.05 ± 0.02	0.55 ± 0.15	0.17 ± 0.02	1
$4\ell Z$ -dep.	–	$\lesssim 10^{-4}$	$\lesssim 10^{-3}$	0.002 ± 0.002	$\lesssim 2 \times 10^{-5}$	0.007 ± 0.005	0.025 ± 0.003	0

sample versus an equivalent LO merged sample generated with SHERPA 2.1.1, to account for ME-parton shower matching effects; b) the LO merged SHERPA sample versus a SHERPA+OPENLOOPS [93] NLO sample, to compare LO merged and NLO acceptance; and c) MG5_AMC@NLO with PYTHIA 8 parton shower versus HERWIG++ parton shower, to compare p_T -ordered versus angular-ordered parton showers. Each of these variations is input independently into the final fit. When summed in quadrature they have an impact of 5–23% depending on the category and background source ($t\bar{t}W$ versus $t\bar{t}Z$). Uncertainties arising from changes in the acceptance due to the choice of QCD scale and PDF are also evaluated; these have an impact of 1.3–6.7% for scale and 0.9–4.8% for PDF.

7.2. Other prompt lepton contributions

Other backgrounds with prompt leptons arise from multiboson processes (WZ , ZZ , and triboson production) in association with heavy-flavour jets, or with a misidentified light-flavour jet. The main process affecting the final result is WZ + jets. Validation regions with three leptons including a Z candidate and either zero or one b -tagged jet are studied. The number of jets in WZ + $0b$ events is reproduced well in the highly populated bins (up to 4 jets), leading to the conclusion that the jet radiation spectrum is well modelled. The dominant uncertainty on the prediction in the signal region is expected to arise from the WZ + b cross section. Data constrain this component with roughly 100% uncertainty. As a result a 100% uncertainty is assigned to the WZ + b cross section, giving a 50% uncertainty on the total WZ yield, correlated across categories. The cross sections for production of WW + b and ZZ + b are also assigned 50% uncertainties; these have negligible impact on the final result.

7.3. Charge sign misidentification

The process $e^\pm \rightarrow e^\pm \gamma \rightarrow e^\pm e^+ e^-$ occurring in detector material can result in an electron produced with nearly the same momentum as the parent electron but with opposite charge. In these cases the observed electron has opposite charge to that of the primary electron (charge mis-id). The analogous processes $\mu^\pm \rightarrow \mu^\pm e^+ e^-$ and $\mu^\pm \rightarrow \mu^\pm \mu^+ \mu^-$ have negligible rates for the selected events. The $t\bar{t}$ and $Z/\gamma^* \rightarrow \ell^+ \ell^-$ + jets events that undergo this process contribute to $2\ell 0\tau_{\text{had}}$ in the ee and $e\mu$ categories. As electrons pass through more material at high $|\eta|$, the charge mis-id rate increases as well, and so the electron $|\eta| < 1.37$ requirement significantly reduces the impact of this background. The charge mis-id rate due to track curvature mismeasurement for electrons and muons is negligible.

The charge mis-id probability is determined by a maximum-likelihood fit using $Z \rightarrow ee$ events reconstructed as same-sign and as opposite-sign pairs, as a function of electron η and p_T . This probability function is then applied to a sample of events passing the $2\ell 0\tau_{\text{had}}$ selection except that the lepton pair is required to be opposite sign. The charge mis-id probability from the relatively low momentum Z daughters is extrapolated to higher p_T using scaling functions extracted from Monte Carlo simulations. The dominant uncertainty is due to the statistical precision of the charge mis-id probability determination, and is $\approx 40\%$ in the signal regions.

7.4. Non-prompt light leptons

A significant background arises from leptons not produced in decays of electroweak bosons (non-prompt leptons), which can promote (for example) a single-lepton $t\bar{t}$ event into a $2\ell 0\tau_{\text{had}}$ category or a dilepton $t\bar{t}$ event to the 3ℓ or $2\ell 1\tau_{\text{had}}$ categories. These backgrounds in the signal regions are expected to be dominated by $t\bar{t}$ or single top quark production with leptons produced in decays of heavy-flavour hadrons. Production of $t\bar{t}$ with an additional photon which converts in the detector material is a subdominant contribution. With the tight object selection requirements applied in this analysis, almost all reconstructed electron and muon objects correspond to real electrons and muons; the fraction arising from incorrect particle identification is negligible. Estimates of these backgrounds are obtained from data. Each channel has a slightly different procedure, motivated by the specific event topology and the statistical power available in the control regions. The methods are discussed below, and the expected non-prompt lepton contributions to the various categories are shown in Table 3. In the following, a *tight* lepton is a lepton that passes the nominal selection, a *sideband* lepton is defined as a lepton candidate which satisfies different criteria than the tight lepton selection (identification selection, isolation, or p_T), and (sideband) *control regions* either require one or more sideband leptons to replace a tight lepton in the signal region selection, or have the same lepton selection as the signal region but different jet requirements.

7.4.1. $2\ell 0\tau_{\text{had}}$ categories

The non-prompt lepton yields in the signal regions are estimated by extrapolating from sideband control regions in data which are enriched in $t\bar{t}$ non-prompt contributions. For electrons, sideband objects are selected by inverting the electron identification and isolation requirements; for muons the sideband objects have low transverse momentum, $6 < p_T < 10$ GeV, but otherwise are selected the same way as nominal muons. Transfer factors are used to extrapolate from events with one tight and one sideband

lepton, but which otherwise pass the signal region selections, to the signal regions with two tight leptons. These transfer factors are determined from additional data control regions (tight + sideband and two tight leptons) with lower jet multiplicity ($1 \leq n_{\text{jet}} \leq 3$ for electrons, $2 \leq n_{\text{jet}} \leq 3$ for muons). In all regions the expected contribution from processes producing prompt leptons is subtracted before extracting transfer factors or using the yields for extrapolation. For channels with electrons, the charge mis-id background is also subtracted, and a dilepton mass veto is applied in the control regions to suppress contributions from $Z \rightarrow e^+e^-$ decays. A cross-check on the muon estimate, using an extrapolation in muon isolation instead of muon p_T , agrees well with the nominal procedure and provides additional confidence in the estimate.

The systematic uncertainties on this procedure are estimated by checking a) its ability to successfully predict the non-prompt background in $t\bar{t}$ simulation and b) the stability of the prediction using data when the selection of the control regions is altered. For the former, different parton shower and b -hadron decay models were checked, as was the result of removing the b -tagged jet requirement. In addition, for electrons, the effects of relaxing the pseudorapidity requirement to $|\eta| < 2.5$ and of raising the p_T threshold were studied. These checks show stability at the 25–30% level, limited by the statistical precision of the simulations. The stability in data is checked by altering the p_T required for the b -tagged jet, applying a requirement on missing transverse momentum³ E_T^{miss} , extracting the transfer factors only from events with three jets, or (for muons) using 10–15 GeV muons as the sideband objects. This check shows stability of the predictions to 14% for muons and 19% for electrons. Additional systematic uncertainties in the prediction arise from the statistical uncertainties on the yields in the control regions and the subtraction of prompt and charge mis-id contributions. The overall uncertainties on the non-prompt yield prediction in any given category range from 32% to 52%, and correlations between the categories due to uncertainties in the transfer factors are included in the fit (see Section 9).

7.4.2. 3ℓ category

Sideband leptons are defined by reversing the isolation requirement for electrons and muons and, for electrons, requiring that the candidate fail the tight electron identification discriminant requirement of the analysis but pass a looser selection. The non-prompt lepton contribution in the signal region is estimated by extrapolating from data regions with two tight and one sideband lepton, using transfer factors estimated from Monte Carlo simulation. These events typically contain two prompt opposite-sign leptons and one non-prompt lepton, which necessarily must be of the same sign as one of the prompt leptons. Therefore the non-prompt lepton estimation procedure is applied only to the two same-sign leptons. The simulation-derived transfer factor is validated in a region of lower jet multiplicity ($2 \leq n_{\text{jet}} \leq 3$ and exactly one b -tagged jet). Good agreement is observed in this validation region between the prediction (11.8 ± 2.3) and the observed yield (9.8 ± 4.9 events after prompt background subtraction). Systematic uncertainties in the procedure are derived by studying the agreement between data and simulation in the variables used for the extrapolation, which is $\approx 20\%$ for both electrons and muons. Additional uncertainties arise from the statistical uncertainties on the yields in the control regions and in the $t\bar{t}$ simulation.

7.4.3. $2\ell 1\tau_{\text{had}}$ category

Reconstructing two same-sign light leptons from $t\bar{t}$ production or similar sources requires that one of the light leptons is non-prompt or has its charge misidentified. In the $2\ell 1\tau_{\text{had}}$ category, the charge mis-id contribution is negligible and the primary concern is non-prompt light leptons. Around half of the τ_{had} candidates in these events come from $W \rightarrow \tau\nu$ decays, while the remainder arise from misidentified light-quark or gluon jets. Regardless of whether the τ_{had} candidate is a fake, there is also a non-prompt light lepton. Due to this fact, sidebands in the light-lepton selection criteria are used, analogously to the $2\ell 0\tau_{\text{had}}$ and 3ℓ categories. Since the ratio of real and fake τ_{had} candidates is similar in the signal and all control regions, fake τ_{had} candidates are not accounted for separately; the small variations in the ratio in the control regions are found to have negligible impact on the total estimate in the signal region. In order to maintain similar origin composition of the non-prompt leptons, the E_T isolation requirement is inverted, the p_T isolation requirement is relaxed, and for electrons the identification criteria are also relaxed to a looser working point. The low jet multiplicity region $2 \leq n_{\text{jet}} \leq 3$ is used to determine a transfer factor from sideband to tight lepton selections. The expected non-prompt lepton yield in the signal region is obtained by using this transfer factor to extrapolate from a control region with the same jet selection as the signal region but with one tight and one sideband light lepton. The procedure is validated by checking that it correctly reproduces the signal region yield expected in $t\bar{t}$ simulations. The assigned systematic uncertainty (27%) is dominated by the statistical precision of this test. The overall uncertainty on the non-prompt background prediction is dominated by the limited statistics of the high jet multiplicity control region.

7.4.4. 4ℓ category

The non-prompt lepton contribution in this category is expected to be negligible and is estimated to be $\lesssim 10^{-3}$ events in the Z -enriched sample and $\lesssim 10^{-4}$ events in the Z -depleted sample. In both cases this represents $\lesssim 2\%$ of the total background expectation. These estimates are obtained using the transfer factors from the 3ℓ channel and appropriate control regions with two loose leptons and relaxed jet multiplicity requirements.

7.5. τ_{had} misidentification in the $1\ell 2\tau_{\text{had}}$ category

The nominal estimate for the fake τ_{had} yield is derived from $t\bar{t}$ simulation. To obtain a sufficiently large sample size, fast simulation using parameterized calorimeter showers is used. At all preselection stages the simulation is found to give an acceptable description of the $t\bar{t}$ background, both in kinematic distributions and total yield. This estimate is cross-checked with the data-driven method described below.

Of the two τ_{had} candidates, one is opposite in sign to the light lepton (OS) and the other has the same sign (SS). The SS candidate is almost always a fake τ_{had} , while the light lepton is prompt and the OS τ_{had} candidate is often real ($\approx 30\%$). A sideband τ_{had} is defined as a candidate passing a loose identification BDT selection but not the nominal tight one. Assuming the τ_{had} candidate fake probabilities are not correlated between jets identified as OS and SS candidates, control regions can be used to predict yields in the signal region. There are three control regions, depending on whether only the OS, only the SS, or both the OS and SS τ_{had} candidates are sideband objects. The two regions with sideband OS τ_{had} candidates are used to obtain the transfer factor for the SS τ_{had} candidate, which is then applied to the region with a tight OS and sideband SS candidate to obtain the prediction for the signal region where both are tight. The transfer factor is measured

³ This is calculated using calorimeter energy deposits, calibrated according to associated reconstructed physics objects, and also including the transverse momenta of reconstructed muons.

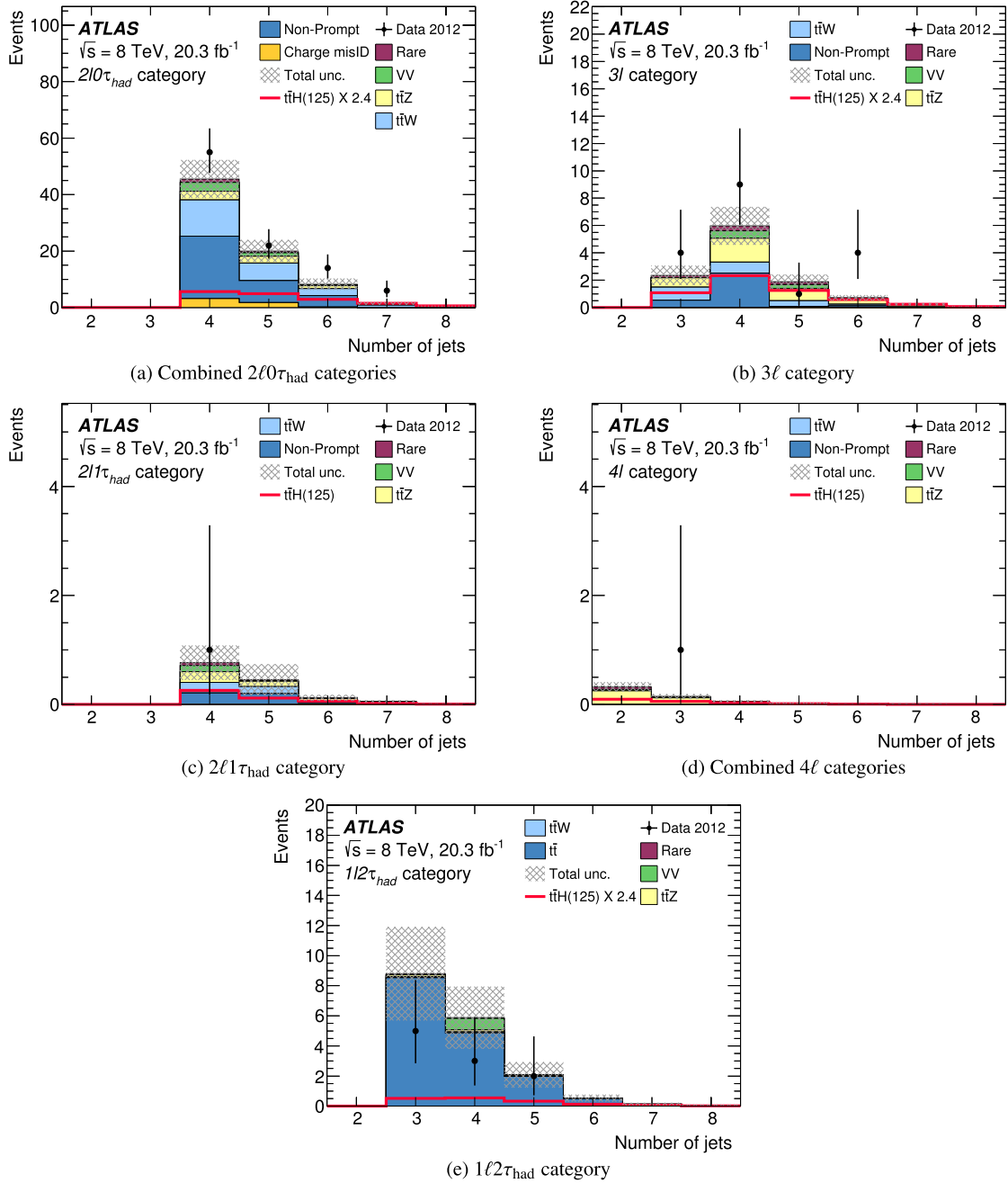


Fig. 2. The spectrum of the number of jets expected and observed in each signal region. For display purposes the six $2\ell 0\tau_{\text{had}}$ categories ($ee/e\mu/\mu\mu$ and $=4/\geq 5$ jets) are combined into one plot, as are the two 4ℓ categories (Z -enriched and Z -depleted). The hatched bands show the total uncertainty on the background prediction in each bin. The non-prompt and charge mis-id background spectra are taken from simulation of $t\bar{t}$, single top, $Z \rightarrow \ell^+\ell^- + \text{jets}$, and other small backgrounds, with normalization as described in the text (in particular the $=4/\geq 5$ jet regions of the $2\ell 0\tau_{\text{had}}$ plot have the ratio given by the data-driven prediction). The overlaid red line shows the $t\bar{t}H$ signal from the Standard Model. For visibility, the $t\bar{t}H$ signal is multiplied by a factor of 2.4 in the $2\ell 0\tau_{\text{had}}$, 3ℓ , and $1\ell 2\tau_{\text{had}}$ plots. (For interpretation of the references to color in this figure legend, the reader is referred to the web version of this article.)

as a function of the p_T , η , number of tracks, and b -tag discriminant value of the $SS \tau_{\text{had}}$ candidate. The data-driven method is cross-checked in $t\bar{t}$ simulation and found to successfully predict the yields in the signal region. The main limitation of this method is the statistical power of the control regions.

The simulation-driven method is taken as the primary estimate, as the validation of the method at preselection stages is more precise than the data-driven method due to larger event yield for the former. The comparison of the simulation- and data-driven techniques gives a 36% uncertainty in the prediction in the sig-

nal region, which is taken as the systematic uncertainty on the estimate.

8. Other systematic uncertainties

Systematic uncertainties not already discussed are summarized below.

The uncertainty on the integrated luminosity is 2.8%. This uncertainty is derived from a calibration of the luminosity scale derived from beam-separation scans performed in November 2012, following the same methodology as that detailed in Ref. [94].

Lepton reconstruction and identification uncertainties are obtained from $Z \rightarrow \ell\ell$, $Z \rightarrow \ell\ell\gamma$, $\Upsilon \rightarrow \ell\ell$, and $J/\psi \rightarrow \ell\ell$ events [80–82]. Uncertainties on the detector response are assessed similarly to other ATLAS analyses. The modelling of the efficiency of the tight isolation requirements in simulation is explicitly checked as a function of the number of jets in the event. These corrections are found to be very small, with uncertainties limited by data statistics.

The largest jet-related systematic uncertainty arises from the jet energy scale, in particular contributions from the in-situ calibration in data, the different response to quark and gluon jets, and the pileup subtraction. The impact of the b -tagging efficiency uncertainty on the signal strength $\mu = \sigma_{\bar{t}\bar{t}H, \text{obs}}/\sigma_{\bar{t}\bar{t}H, \text{SM}}$ at the best-fit value of μ is $\Delta\mu = {}^{+0.08}_{-0.06}$. Because only one (of typically two) b -jets present in signal or $\bar{t}\bar{t}V$ events is required to be tagged, the uncertainty on the b -tagging efficiency (while included) does not have as large an effect in this analysis as it does in other $\bar{t}\bar{t}H$ searches such as those targeting the $H \rightarrow b\bar{b}$ decay.

The uncertainties on the inclusive $\bar{t}\bar{t}H$ production cross section are discussed in Section 3. Additionally, the effects of PDF uncertainty, QCD scale choice, and parton shower algorithm on the signal acceptance in each analysis category are considered. The resulting relative uncertainties on the acceptance are 0.3–1.4% for PDF, 0.1–2.7% for scale choice, and 1.5–13% for parton shower algorithm.

For most backgrounds the uncertainties from Monte Carlo simulation sample sizes are negligible. For the diboson backgrounds, however, these can reach 50% of the total diboson yield uncertainties shown in Table 3.

9. Results

The observed yields, and a comparison with the expected backgrounds and $\bar{t}\bar{t}H$ signal, are shown in Table 3. The distributions of the number of jets in the events passing signal region selections are shown in Fig. 2. The best-fit value of the signal strength $\mu = \sigma_{\bar{t}\bar{t}H, \text{obs}}/\sigma_{\bar{t}\bar{t}H, \text{SM}}$ is determined using a maximum likelihood fit to the data yields of the categories listed in Table 3, which are treated as independent Poisson terms in the likelihood. The fit is based on the profile-likelihood approach where the systematic uncertainties are treated as nuisance parameters with prior uncertainties that can be further constrained by the fit [95]. The $\mu = 1$ hypothesis assumes Standard Model Higgs boson production and decay with $m_H = 125$ GeV; for all other values of μ only the $\bar{t}\bar{t}H$ production cross section is scaled (the Higgs boson branching fractions are fixed to their SM values).

Systematic uncertainties are allowed to float in the fit as nuisance parameters and take on their best-fit values. The only constraints on nuisance parameter uncertainties found by the fit are for non-prompt lepton transfer factors and normalization region yields in the $2\ell 0\tau_{\text{had}}$ categories and the fake τ_{had} background yield in the $1\ell 2\tau_{\text{had}}$ category. The former all have large statistical components and so the additional information from the signal regions is expected to constrain them. The latter has a very large initial uncertainty which the fit is able to constrain as μ is required to be the same in all categories. The largest difference between pre- and post-fit nuisance parameter values is in the $1\ell 2\tau_{\text{had}}$ fake estimate, which shifts by -1.0σ due to the deficit of observed relative to expected events. The next largest effect is a $+0.4\sigma$ shift in the $2\ell 0\tau_{\text{had}}$ non-prompt μ transfer factor.

The results of the fit are shown in Fig. 3. The impact of the most important systematic uncertainties on the measured value of μ in the combined fit is shown in Table 4. In each category, the uncertainties on μ are mainly statistical, except for the combined $2\ell 0\tau_{\text{had}}$ result where the statistical and systematic uncertainties

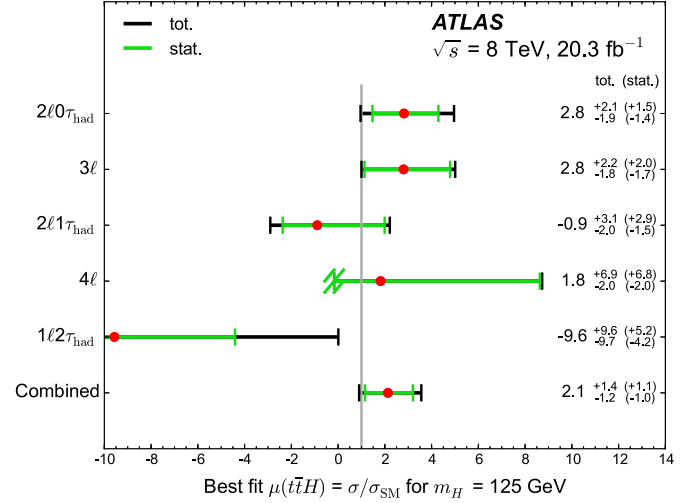


Fig. 3. Best-fit values of the signal strength parameter $\mu = \sigma_{\bar{t}\bar{t}H, \text{obs}}/\sigma_{\bar{t}\bar{t}H, \text{SM}}$. For the 4ℓ Z-depleted category, $\mu < -0.17$ results in a negative expected total yield and so the lower uncertainty is truncated at this point.

Table 4

Leading sources of systematic uncertainty and their impact on the measured value of μ .

Source	$\Delta\mu$	
$2\ell 0\tau_{\text{had}}$ non-prompt muon transfer factor	+0.38	-0.35
$\bar{t}\bar{t}W$ acceptance	+0.26	-0.21
$\bar{t}\bar{t}H$ inclusive cross section	+0.28	-0.15
Jet energy scale	+0.24	-0.18
$2\ell 0\tau_{\text{had}}$ non-prompt electron transfer factor	+0.26	-0.16
$\bar{t}\bar{t}H$ acceptance	+0.22	-0.15
$\bar{t}\bar{t}Z$ inclusive cross section	+0.19	-0.17
$\bar{t}\bar{t}W$ inclusive cross section	+0.18	-0.15
Muon isolation efficiency	+0.19	-0.14
Luminosity	+0.18	-0.14

are of comparable size. In the 4ℓ Z-depleted category, a (non-physical) signal strength $\mu < -0.17$ results in a negative expected total yield and a discontinuity in the profiled likelihood; the error bar is therefore truncated at this point. The results are compatible with the Standard Model expectation and with previous searches for $\bar{t}\bar{t}H$ production in multilepton final states [18]. Combined over all categories, the value of μ is found to be $2.1^{+1.4}_{-1.2}$. In the presence of a signal of SM strength, the combined fit is expected to return $\mu = 1.0^{+1.2}_{-1.1}$. The $\mu = 0$ hypothesis has an observed (expected) p -value of 0.037 (0.18), corresponding to 1.8σ (0.9σ). The $\mu = 1$ hypothesis (the SM) has an observed p -value of 0.18, corresponding to 0.9σ . The likelihood function can be used to obtain 95% confidence level (CL) upper limits on μ using the CL_s method [95,96], leading to the results in Table 5. The observed (expected) upper limit, combining all channels, is $\mu < 4.7$ (2.4).

This analysis is a search for $\bar{t}\bar{t}H$ production; as such, production of $tHq\bar{b}$ and tHW is considered as a background and set to Standard Model expectation. Including this contribution as a background induces a shift of $\Delta\mu = -0.04$ compared to setting it to zero. A full extraction of limits on the top quark Yukawa coupling including the relevant modifications of single top plus Higgs boson production is reported in Ref. [97].

The results are sensitive to the assumed cross sections for $\bar{t}\bar{t}W$ and $\bar{t}\bar{t}Z$ production, and use theoretical predictions for these values as experimental measurements do not yet have sufficient precision. The best-fit μ value as a function of these cross sections is

Table 5
Observed and expected 95% CL upper limits, derived using the CL_s method, on the strength parameter $\mu = \sigma_{t\bar{t}H, \text{obs}}/\sigma_{t\bar{t}H, \text{SM}}$ for a Higgs boson of mass $m_H = 125$ GeV. The last column shows the median expected limit in the presence of a $t\bar{t}H$ signal of Standard Model strength.

Channel	Observed limit	Expected limit		Median	+1 σ	+2 σ	Median ($\mu = 1$)
		-2 σ	-1 σ				
2 ℓ 0 τ_{had}	6.7	2.1	2.8	3.9	5.7	8.4	5.0
3 ℓ	6.8	2.0	2.7	3.8	5.7	8.5	5.1
2 ℓ 1 τ_{had}	7.5	4.5	6.1	8.4	13	21	10
4 ℓ	18	8.0	11	15	23	39	17
1 ℓ 2 τ_{had}	13	10	13	18	26	40	19
Combined	4.7	1.3	1.8	2.4	3.6	5.3	3.7

$$\mu(t\bar{t}H) = 2.1 - 1.4 \left(\frac{\sigma(t\bar{t}W)}{232 \text{ fb}} - 1 \right) - 1.3 \left(\frac{\sigma(t\bar{t}Z)}{206 \text{ fb}} - 1 \right).$$

10. Conclusions

A search for $t\bar{t}H$ production in multilepton final states has been performed using 20.3 fb⁻¹ of proton–proton collision data at $\sqrt{s} = 8$ TeV recorded by the ATLAS experiment at the LHC. The best-fit value of the ratio μ of the observed production rate to that predicted by the Standard Model is $2.1^{+1.4}_{-1.2}$. This result is consistent with the Standard Model expectation. A 95% confidence level limit of $\mu < 4.7$ is set. The expected limit in the absence of $t\bar{t}H$ signal is $\mu < 2.4$. The observed (expected) p -value of the no-signal hypothesis corresponds to 1.8 σ (0.9 σ).

Acknowledgements

We thank CERN for the very successful operation of the LHC, as well as the support staff from our institutions without whom ATLAS could not be operated efficiently.

We acknowledge the support of ANPCyT, Argentina; YerPhI, Armenia; ARC, Australia; BMWFW and FWF, Austria; ANAS, Azerbaijan; SSTC, Belarus; CNPq and FAPESP, Brazil; NSERC, NRC and CFI, Canada; CERN; CONICYT, Chile; CAS, MOST and NSFC, China; COLCIENCIAS, Colombia; MSMT CR, MPO CR and VSC CR, Czech Republic; DNRF, DNSRC and Lundbeck Foundation, Denmark; EPLANET, ERC and NSRF, European Union; IN2P3–CNRS, CEA–DSM/IRFU, France; GNSF, Georgia; BMBF, DFG, HGF, MPG and AvH Foundation, Germany; GSRT and NSRF, Greece; RGC, Hong Kong SAR, China; ISF, MINERVA, GIF, I-CORE and Benozio Center, Israel; INFN, Italy; MEXT and JSPS, Japan; CNRST, Morocco; FOM and NWO, Netherlands; BRF and RCN, Norway; MNiSW and NCN, Poland; GRICES and FCT, Portugal; MNE/IFA, Romania; MES of Russia and NRC KI, Russian Federation; JINR; MSTP, Serbia; MSSR, Slovakia; ARRS and MIZŠ, Slovenia; DST/NRF, South Africa; MINECO, Spain; SRC and Wallenberg Foundation, Sweden; SER, SNSF and Cantons of Bern and Geneva, Switzerland; NSC, Taiwan; TAEK, Turkey; STFC, the Royal Society and Leverhulme Trust, United Kingdom; DOE and NSF, United States of America.

The crucial computing support from all WLCG partners is acknowledged gratefully, in particular from CERN and the ATLAS Tier-1 facilities at TRIUMF (Canada), NDGF (Denmark, Norway, Sweden), CC-IN2P3 (France), KIT/GridKA (Germany), INFN-CNAF (Italy), NL-T1 (Netherlands), PIC (Spain), ASGC (Taiwan), RAL (UK) and BNL (USA) and in the Tier-2 facilities worldwide.

References

- [1] S.L. Glashow, Partial symmetries of weak interactions, Nucl. Phys. 22 (1961) 579.
- [2] S. Weinberg, A model of leptons, Phys. Rev. Lett. 19 (1967) 1264.
- [3] A. Salam, Weak and electromagnetic interactions, in: N. Svartholm (Ed.), Elementary Particle Theory: Relativistic Groups and Analyticity. Proceedings of the Eighth Nobel Symposium, Almqvist & Wiksell, Stockholm, 1968, p. 367.

- [4] F. Englert, R. Brout, Broken symmetry and the mass of gauge vector mesons, Phys. Rev. Lett. 13 (1964) 321.
- [5] P.W. Higgs, Broken symmetries, massless particles and gauge fields, Phys. Rev. Lett. 12 (1964) 132.
- [6] P.W. Higgs, Broken symmetries and the masses of gauge bosons, Phys. Rev. Lett. 13 (1964) 508.
- [7] G. Guralnik, C.R. Hagen, T.W.B. Kibble, Global conservation laws and massless particles, Phys. Rev. Lett. 13 (1964) 585.
- [8] ATLAS Collaboration, Observation of a new particle in the search for the Standard Model Higgs boson with the ATLAS detector at the LHC, Phys. Lett. B 716 (2012) 1, arXiv:1207.7214 [hep-ex].
- [9] CMS Collaboration, Observation of a new boson at a mass of 125 GeV with the CMS experiment at the LHC, Phys. Lett. B 716 (2012) 30, arXiv:1207.7235 [hep-ex].
- [10] ATLAS Collaboration, Measurement of Higgs boson production in the diphoton decay channel in pp collisions at center-of-mass energies of 7 and 8 TeV with the ATLAS detector, Phys. Rev. D 90 (2014) 112015, arXiv:1408.7084 [hep-ex].
- [11] CMS Collaboration, Observation of the diphoton decay of the Higgs boson and measurement of its properties, Eur. Phys. J. C 74 (2014) 3076, arXiv:1407.0558 [hep-ex].
- [12] ATLAS Collaboration, Measurements of Higgs boson production and couplings in the four-lepton channel in pp collisions at center-of-mass energies of 7 and 8 TeV with the ATLAS detector, Phys. Rev. D 91 (2015) 012006, arXiv:1408.5191 [hep-ex].
- [13] CMS Collaboration, Measurement of the properties of a Higgs boson in the four-lepton final state, Phys. Rev. D 89 (2014) 092007, arXiv:1312.5353 [hep-ex].
- [14] ATLAS Collaboration, Observation and measurement of Higgs boson decays to WW^* with the ATLAS detector, Phys. Rev. D 92 (2015) 012006, arXiv:1412.2641 [hep-ex].
- [15] CMS Collaboration, Measurement of Higgs boson production and properties in the WW decay channel with leptonic final states, J. High Energy Phys. 1401 (2014) 096, arXiv:1312.1129 [hep-ex].
- [16] ATLAS Collaboration, Evidence for the Higgs-boson Yukawa coupling to tau leptons with the ATLAS detector, J. High Energy Phys. 1504 (2015) 117, arXiv:1501.04943 [hep-ex].
- [17] CMS Collaboration, Evidence for the 125 GeV Higgs boson decaying to a pair of τ leptons, J. High Energy Phys. 1405 (2014) 104, arXiv:1401.5041 [hep-ex].
- [18] CMS Collaboration, Search for the associated production of the Higgs boson with a top-quark pair, J. High Energy Phys. 1409 (2014) 087, arXiv:1408.1682 [hep-ex], Erratum: J. High Energy Phys. 1410 (2014) 106.
- [19] ATLAS Collaboration, Search for the standard model Higgs boson produced in association with top quarks and decaying into $b\bar{b}$ in pp collisions at $\sqrt{s} = 8$ TeV with the ATLAS detector, Eur. Phys. J. C 75 (2015) 349, <http://dx.doi.org/10.1140/epjc/s10052-015-3543-1>, arXiv:1503.05066 [hep-ex].
- [20] ATLAS Collaboration, Search for $H \rightarrow \gamma\gamma$ produced in association with top quarks and constraints on the Yukawa coupling between the top quark and the Higgs boson using data taken at 7 TeV and 8 TeV with the ATLAS detector, Phys. Lett. B 740 (2015) 222, arXiv:1409.3122 [hep-ex].
- [21] ATLAS Collaboration, ATLAS experiment at the CERN Large Hadron Collider, J. Instrum. 3 (2008) S08003.
- [22] S. Dawson, C. Jackson, L. Orr, L. Reina, D. Wackerth, Associated Higgs production with top quarks at the Large Hadron Collider: NLO QCD corrections, Phys. Rev. D 68 (2003) 034022, arXiv:hep-ph/0305087.
- [23] L. Reina, S. Dawson, Next-to-leading order results for $t\bar{t}H$ production at the Tevatron, Phys. Rev. Lett. 87 (2001) 201804, arXiv:hep-ph/0107101.
- [24] W. Beenakker, et al., NLO QCD corrections to $t\bar{t}H$ production in hadron collisions, Nucl. Phys. B 653 (2003) 151, arXiv:hep-ph/0211352.
- [25] W. Beenakker, et al., Higgs radiation off top quarks at the Tevatron and the LHC, Phys. Rev. Lett. 87 (2001) 201805, arXiv:hep-ph/0107081.
- [26] LHC Higgs Cross Section Working Group Collaboration, S. Dittmaier, et al., Handbook of LHC Higgs cross sections: 1. Inclusive observables, arXiv:1101.0593 [hep-ph].

- [27] LHC Higgs Cross Section Working Group Collaboration, S. Heinemeyer, et al., Handbook of LHC Higgs cross sections: 3. Higgs properties, arXiv:1307.1347 [hep-ph].
- [28] ATLAS, CMS Collaborations, Combined measurement of the Higgs boson mass in pp collisions at $\sqrt{s} = 7$ and 8 TeV with the ATLAS and CMS experiments, Phys. Rev. Lett. 114 (2015) 191803, <http://dx.doi.org/10.1103/PhysRevLett.114.191803>, arXiv:1503.07589 [hep-ex].
- [29] J. Alwall, et al., The automated computation of tree-level and next-to-leading order differential cross sections, and their matching to parton shower simulations, J. High Energy Phys. 1407 (2014) 079, arXiv:1405.0301 [hep-ph].
- [30] J.M. Campbell, R.K. Ellis, $t\bar{t}W^\pm$ production and decay at NLO, J. High Energy Phys. 1207 (2012) 052, arXiv:1204.5678 [hep-ph].
- [31] M. Garzelli, A. Kardos, C. Papadopoulos, Z. Trocsanyi, $t\bar{t}W^\pm$ and $t\bar{t}Z$ hadroproduction at NLO accuracy in QCD with parton shower and hadronization effects, J. High Energy Phys. 1211 (2012) 056, arXiv:1208.2665 [hep-ph].
- [32] J.M. Campbell, R.K. Ellis, R. Röntsch, Single top production in association with a Z boson at the LHC, Phys. Rev. D 87 (2013) 114006, arXiv:1302.3856 [hep-ph].
- [33] J. Alwall, M. Herquet, F. Maltoni, O. Mattelaer, T. Stelzer, MadGraph 5: going beyond, J. High Energy Phys. 1106 (2011) 128, arXiv:1106.0522 [hep-ex].
- [34] J.M. Campbell, R.K. Ellis, C. Williams, Vector boson pair production at the LHC, J. High Energy Phys. 1107 (2011) 018, arXiv:1105.0020 [hep-ph].
- [35] M. Czakon, A. Mitov, Top++: a program for the calculation of the top-pair cross-section at hadron colliders, Comput. Phys. Commun. 185 (2014) 2930, arXiv:1112.5675 [hep-ph].
- [36] N. Kidonakis, NNLL resummation for s-channel single top quark production, Phys. Rev. D 81 (2010) 054028, arXiv:1001.5034 [hep-ph].
- [37] N. Kidonakis, Next-to-next-to-leading-order collinear and soft gluon corrections for t-channel single top quark production, Phys. Rev. D 83 (2011) 091503, arXiv:1103.2792 [hep-ph].
- [38] N. Kidonakis, Two-loop soft anomalous dimensions for single top quark associated production with a W or H, Phys. Rev. D 82 (2010) 054018, arXiv:1005.4451 [hep-ph].
- [39] A. Martin, W.J. Stirling, R.S. Thorne, G. Watt, Parton distributions for the LHC, Eur. Phys. J. C 63 (2009) 189, arXiv:0901.0002 [hep-ph].
- [40] C. Anastasiou, L.J. Dixon, K. Melnikov, F. Petriello, High precision QCD at hadron colliders: electroweak gauge boson rapidity distributions at NNLO, Phys. Rev. D 69 (2004) 094008, arXiv:hep-ph/0312266.
- [41] G. Bevilacqua, et al., HELAC-NLO, Comput. Phys. Commun. 184 (2013) 986, arXiv:1110.1499 [hep-ph].
- [42] M. Garzelli, A. Kardos, C. Papadopoulos, Z. Trocsanyi, Standard model Higgs boson production in association with a top anti-top pair at NLO with parton showering, Europhys. Lett. 96 (2011) 11001, arXiv:1108.0387 [hep-ph].
- [43] T. Sjöstrand, S. Mrenna, P. Skands, A brief introduction to PYTHIA 8.1, Comput. Phys. Commun. 178 (2008) 852, arXiv:0710.3820 [hep-ph].
- [44] H.-L. Lai, et al., New parton distributions for collider physics, Phys. Rev. D 82 (2010) 074024, arXiv:1007.2241 [hep-ph].
- [45] J. Pumplin, D.R. Stump, J. Huston, H.-L. Lai, P.M. Nadolsky, W.K. Tung, New generation of parton distributions with uncertainties from global QCD analysis, J. High Energy Phys. 0207 (2012) 012, arXiv:hep-ph/0201195.
- [46] P.M. Nadolsky, et al., Implications of CTEQ global analysis for collider observables, Phys. Rev. D 78 (2008) 013004, arXiv:0802.0007 [hep-ph].
- [47] ATLAS Collaboration, Summary of ATLAS Pythia 8 tunes, ATL-PHYS-PUB-2012-003, <https://cds.cern.ch/record/1474107>.
- [48] P. Nason, A new method for combining NLO QCD with shower Monte Carlo algorithms, J. High Energy Phys. 0411 (2004) 040, arXiv:hep-ph/0409146.
- [49] S. Frixione, P. Nason, C. Oleari, Matching NLO QCD computations with Parton Shower simulations: the POWHEG method, J. High Energy Phys. 0711 (2007) 070, arXiv:0709.2092 [hep-ph].
- [50] S. Alioli, et al., A general framework for implementing NLO calculations in shower Monte Carlo programs: the POWHEG BOX, J. High Energy Phys. 1006 (2010) 043, arXiv:1002.2581 [hep-ph].
- [51] M. Bahr, et al., Herwig++ physics and manual, Eur. Phys. J. C 58 (2008) 639, arXiv:0803.0883 [hep-ph].
- [52] A. Sherstnev, R. Thorne, Parton distributions for LO generators, Eur. Phys. J. C 55 (2008) 553, arXiv:0711.2473 [hep-ph].
- [53] S. Gieseke, C. Rohr, A. Siodmok, Colour reconnections in Herwig++, Eur. Phys. J. C 72 (2012) 2225, arXiv:1206.0041 [hep-ph].
- [54] T. Sjöstrand, et al., High-energy-physics event generation with Pythia 6.1, Comput. Phys. Commun. 135 (2001) 238, arXiv:hep-ph/0010017.
- [55] ATLAS Collaboration, ATLAS tunes of PYTHIA 6 and PYTHIA8 for MC11, ATL-PHYS-PUB-2011-009, <http://cds.cern.ch/record/1363300>.
- [56] T. Gleisberg, et al., Event generation with SHERPA 1.1, J. High Energy Phys. 0902 (2009) 007, arXiv:0811.4622 [hep-ph].
- [57] T. Melia, P. Nason, R. Röntsch, G. Zanderighi, W^+W^- , WZ and ZZ production in the POWHEG BOX, J. High Energy Phys. 1111 (2011) 078, arXiv:1107.5051 [hep-ph].
- [58] T. Binoth, N. Kauer, P. Mertsch, Gluon-induced QCD corrections to $pp \rightarrow ZZ \rightarrow \mu\mu\tau\tau$, arXiv:0807.0024 [hep-ph].
- [59] G. Corcella, et al., HERWIG 6.5: an event generator for hadron emission reactions with interfering gluons (including supersymmetric processes), J. High Energy Phys. 0101 (2001) 010, arXiv:hep-ph/0011363.
- [60] ATLAS Collaboration, New ATLAS event generator tunes to 2010 data, ATL-PHYS-PUB-2011-008, <http://cds.cern.ch/record/1345343>.
- [61] S. Frixione, G. Ridolfi, P. Nason, A positive-weight next-to-leading-order Monte Carlo for heavy flavour hadroproduction, J. High Energy Phys. 0709 (2009) 126, arXiv:0707.3088 [hep-ph].
- [62] P. Skands, Tuning Monte Carlo generators: the Perugia tunes, Phys. Rev. D 82 (2010) 074018, arXiv:1005.3457 [hep-ph].
- [63] E. Re, Single-top Wt -channel production matched with parton showers using the POWHEG method, Eur. Phys. J. C 71 (2011) 1547, arXiv:1009.2450 [hep-ph].
- [64] S. Alioli, P. Nason, C. Oleari, E. Re, NLO single-top production matched with shower in POWHEG: s- and t-channel contributions, J. High Energy Phys. 0909 (2009) 111, arXiv:0907.4076 [hep-ph], Erratum: J. High Energy Phys. 1002 (2010) 011.
- [65] M.L. Mangano, et al., ALPGEN, a generator for hard multiparton processes in hadronic collisions, J. High Energy Phys. 0307 (2003) 001, arXiv:hep-ph/0206293.
- [66] A. Djouadi, J. Kalinowski, M. Spira, HDECAY: a program for Higgs boson decays in the standard model and its supersymmetric extension, Comput. Phys. Commun. 108 (1998) 56, arXiv:hep-ph/9704448.
- [67] A. Bredenstein, A. Denner, S. Dittmaier, M. Weber, Precise predictions for the Higgs-boson decay $H \rightarrow WW/ZZ \rightarrow 4$ leptons, Phys. Rev. D 74 (2006) 013004, arXiv:hep-ph/0604011.
- [68] S. Actis, G. Passarino, C. Sturm, S. Uccirati, NNLO computational techniques: the cases $H \rightarrow \gamma\gamma$ and $H \rightarrow gg$, Nucl. Phys. B 811 (2009) 182, arXiv:0809.3667 [hep-ph].
- [69] A. Denner, S. Heinemeyer, I. Puljak, D. Rebuszi, M. Spira, Standard model Higgs-boson branching ratios with uncertainties, Eur. Phys. J. C 71 (2011) 1753, arXiv:1107.5909 [hep-ph].
- [70] ATLAS Collaboration, Measurements of normalized differential cross sections for $t\bar{t}$ production in pp collisions at $\sqrt{s} = 7$ TeV using the ATLAS detector, Phys. Rev. D 90 (2014) 072004, arXiv:1407.0371 [hep-ex].
- [71] S. Frixione, E. Laenen, P. Motylinski, B.R. Webber, C.D. White, Single-top hadroproduction in association with a W boson, J. High Energy Phys. 0807 (2008) 029, arXiv:0805.3067 [hep-ph].
- [72] M.L. Mangano, et al., Multijet matrix elements and shower evolution in hadronic collisions: $Wb\bar{b} + n$ jets as a case study, Nucl. Phys. B 632 (2002) 343, arXiv:hep-ph/0108069.
- [73] P. Golonka, Z. Was, PHOTOS Monte Carlo: a precision tool for QED corrections in Z and W decays, Eur. Phys. J. C 45 (2006) 97, arXiv:hep-ph/0506026.
- [74] J. Stanisław, J. Kühn, Z. Was, TAUOLA – a library of Monte Carlo programs to simulate decays of polarized τ leptons, Comput. Phys. Commun. 64 (1991) 275.
- [75] J. Butterworth, J.R. Forshaw, M. Seymour, Multiparton interactions in photoproduction at HERA, Z. Phys. C 72 (1996) 637, arXiv:hep-ph/9601371.
- [76] S. Agostinelli, et al., Geant4: a simulation toolkit, Nucl. Instrum. Methods Phys. Res., Sect. A, Accel. Spectrom. Detect. Assoc. Equip. 506 (2003) 250.
- [77] ATLAS Collaboration, The ATLAS simulation infrastructure, Eur. Phys. J. C 70 (2010) 823, arXiv:1005.4568 [physics.ins-det].
- [78] ATLAS Collaboration, The simulation principle and performance of the ATLAS fast calorimeter simulation FastCaloSim, ATL-PHYS-PUB-2010-013, <http://cds.cern.ch/record/1300517>.
- [79] ATLAS Collaboration, Further ATLAS tunes of PYTHIA 6 and Pythia 8, ATL-PHYS-PUB-2011-014, <https://cds.cern.ch/record/1400677>.
- [80] ATLAS Collaboration, Electron reconstruction and identification efficiency measurements with the ATLAS detector using the 2011 LHC proton–proton collision data, Eur. Phys. J. C 74 (2014) 2941, arXiv:1404.2240 [hep-ex].
- [81] ATLAS Collaboration, Electron efficiency measurements with the ATLAS detector using the 2012 LHC proton–proton collision data, ATLAS-CONF-2014-032, <http://cds.cern.ch/record/1706245>.
- [82] ATLAS Collaboration, Measurement of the muon reconstruction performance of the ATLAS detector using 2011 and 2012 LHC proton–proton collision data, Eur. Phys. J. C 74 (2014) 3130, arXiv:1407.3935 [hep-ex].
- [83] ATLAS Collaboration, Identification and energy calibration of hadronically decaying tau leptons with the ATLAS experiment in pp collisions at $\sqrt{s} = 8$ TeV, Eur. Phys. J. C 75 (2014) 303, <http://dx.doi.org/10.1140/epjc/s10052-015-3500-z>, arXiv:1412.7086 [hep-ph].
- [84] M. Cacciari, G.P. Salam, G. Soyez, The anti- k_t jet clustering algorithm, J. High Energy Phys. 0804 (2008) 063, arXiv:0802.1189 [hep-ph].
- [85] M. Cacciari, G.P. Salam, Dispelling the N^3 myth for the k_t jet-finder, Phys. Lett. B 641 (2006) 57, arXiv:hep-ph/0512210 [hep-ph].
- [86] M. Cacciari, G.P. Salam, G. Soyez, FastJet user manual, Eur. Phys. J. C 72 (2012) 1896, arXiv:1111.6097 [hep-ph].
- [87] C. Cojocaru, et al., Hadronic calibration of the ATLAS liquid argon end-cap calorimeter in the pseudorapidity region $1.6 < |\eta| < 1.8$ in beam tests, Nucl. Instrum. Methods Phys. Res., Sect. A, Accel. Spectrom. Detect. Assoc. Equip. 531 (2004) 481, arXiv:physics/0407009 [physics].

- [88] T. Barillari, et al., Local hadronic calibration, ATL-LARG-PUB-2009-001, <http://cds.cern.ch/record/1112035>.
- [89] ATLAS Collaboration, Jet energy measurement with the ATLAS detector in proton–proton collisions at $\sqrt{s} = 7$ TeV, *Eur. Phys. J. C* 73 (2013) 2304, arXiv:1112.6426 [hep-ex].
- [90] ATLAS Collaboration, Jet energy resolution in proton–proton collisions at $\sqrt{s} = 7$ TeV recorded in 2010 with the ATLAS detector, *Eur. Phys. J. C* 73 (2013) 2306, arXiv:1210.6210 [hep-ex].
- [91] ATLAS Collaboration, Calibration of the performance of b -tagging for c and light-flavour jets in the 2012 ATLAS data, ATLAS-CONF-2014-046, <http://cds.cern.ch/record/1741020>.
- [92] ATLAS Collaboration, Calibration of b -tagging using dileptonic top pair events in a combinatorial likelihood approach with the ATLAS experiment, ATLAS-CONF-2014-004, <http://cds.cern.ch/record/1664335>.
- [93] F. Cascioli, P. Maierhöfer, S. Pozzorini, Scattering amplitudes with Open Loops, *Phys. Rev. Lett.* 108 (2012) 111601, arXiv:1111.5206 [hep-ph].
- [94] ATLAS Collaboration, Improved luminosity determination in pp collisions at $\sqrt{s} = 7$ TeV using the ATLAS detector at the LHC, *Eur. Phys. J. C* 73 (2013) 2518, arXiv:1302.4393 [hep-ex].
- [95] G. Cowan, K. Cranmer, E. Gross, O. Vitells, Asymptotic formulae for likelihood-based tests of new physics, *Eur. Phys. J. C* 71 (2011) 1554, arXiv:1007.1727 [physics.data-an], Erratum: *Eur. Phys. J. C* 73 (2013) 2501.
- [96] A.L. Read, Presentation of search results: the CL(s) technique, *J. Phys. G* 28 (2002) 2693.
- [97] ATLAS Collaboration, Measurements of the Higgs boson production and decay rates and coupling strengths using pp collision data at $\sqrt{s} = 7$ and 8 TeV in the ATLAS experiment, submitted to *Eur. Phys. J. C* (2015), arXiv:1507.04548 [hep-ex].

ATLAS Collaboration

G. Aad⁸⁵, B. Abbott¹¹³, J. Abdallah¹⁵¹, O. Abdinov¹¹, R. Aben¹⁰⁷, M. Abolins⁹⁰, O.S. AbouZeid¹⁵⁸, H. Abramowicz¹⁵³, H. Abreu¹⁵², R. Abreu³⁰, Y. Abulaiti^{146a,146b}, B.S. Acharya^{164a,164b,a}, L. Adamczyk^{38a}, D.L. Adams²⁵, J. Adelman¹⁰⁸, S. Adomeit¹⁰⁰, T. Adye¹³¹, A.A. Affolder⁷⁴, T. Agatonovic-Jovin¹³, J.A. Aguilar-Saavedra^{126a,126f}, S.P. Ahlen²², F. Ahmadov^{65,b}, G. Aielli^{133a,133b}, H. Akerstedt^{146a,146b}, T.P.A. Åkesson⁸¹, G. Akimoto¹⁵⁵, A.V. Akimov⁹⁶, G.L. Alberghi^{20a,20b}, J. Albert¹⁶⁹, S. Albrand⁵⁵, M.J. Alconada Verzini⁷¹, M. Aleksa³⁰, I.N. Aleksandrov⁶⁵, C. Alexa^{26a}, G. Alexander¹⁵³, T. Alexopoulos¹⁰, M. Alhroob¹¹³, G. Alimonti^{91a}, L. Alio⁸⁵, J. Alison³¹, S.P. Alkire³⁵, B.M.M. Allbrooke¹⁸, P.P. Allport⁷⁴, A. Aloisio^{104a,104b}, A. Alonso³⁶, F. Alonso⁷¹, C. Alpigiani⁷⁶, A. Altheimer³⁵, B. Alvarez Gonzalez³⁰, D. Álvarez Piqueras¹⁶⁷, M.G. Alviggi^{104a,104b}, B.T. Amadio¹⁵, K. Amako⁶⁶, Y. Amaral Coutinho^{24a}, C. Amelung²³, D. Amidei⁸⁹, S.P. Amor Dos Santos^{126a,126c}, A. Amorim^{126a,126b}, S. Amoroso⁴⁸, N. Amram¹⁵³, G. Amundsen²³, C. Anastopoulos¹³⁹, L.S. Ancu⁴⁹, N. Andari³⁰, T. Andeen³⁵, C.F. Anders^{58b}, G. Anders³⁰, J.K. Anders⁷⁴, K.J. Anderson³¹, A. Andreazza^{91a,91b}, V. Andrei^{58a}, S. Angelidakis⁹, I. Angelozzi¹⁰⁷, P. Anger⁴⁴, A. Angerami³⁵, F. Anghinolfi³⁰, A.V. Anisenkov^{109,c}, N. Anjos¹², A. Annovi^{124a,124b}, M. Antonelli⁴⁷, A. Antonov⁹⁸, J. Antos^{144b}, F. Anulli^{132a}, M. Aoki⁶⁶, L. Aperio Bella¹⁸, G. Arabidze⁹⁰, Y. Arai⁶⁶, J.P. Araque^{126a}, A.T.H. Arce⁴⁵, F.A. Arduh⁷¹, J-F. Arguin⁹⁵, S. Argyropoulos⁴², M. Arik^{19a}, A.J. Armbruster³⁰, O. Arnaez³⁰, V. Arnal⁸², H. Arnold⁴⁸, M. Arratia²⁸, O. Arslan²¹, A. Artamonov⁹⁷, G. Artoni²³, S. Asai¹⁵⁵, N. Asbah⁴², A. Ashkenazi¹⁵³, B. Åsman^{146a,146b}, L. Asquith¹⁴⁹, K. Assamagan²⁵, R. Astalos^{144a}, M. Atkinson¹⁶⁵, N.B. Atlay¹⁴¹, B. Auerbach⁶, K. Augsten¹²⁸, M. Auresseau^{145b}, G. Avolio³⁰, B. Axen¹⁵, M.K. Ayoub¹¹⁷, G. Azuelos^{95,d}, M.A. Baak³⁰, A.E. Baas^{58a}, C. Bacci^{134a,134b}, H. Bachacou¹³⁶, K. Bachas¹⁵⁴, M. Backes³⁰, M. Backhaus³⁰, P. Bagiacchi^{132a,132b}, P. Bagnaia^{132a,132b}, Y. Bai^{33a}, T. Bain³⁵, J.T. Baines¹³¹, O.K. Baker¹⁷⁶, P. Balek¹²⁹, T. Balestri¹⁴⁸, F. Balli⁸⁴, E. Banas³⁹, Sw. Banerjee¹⁷³, A.A.E. Bannoura¹⁷⁵, H.S. Bansil¹⁸, L. Barak³⁰, E.L. Barberio⁸⁸, D. Barberis^{50a,50b}, M. Barbero⁸⁵, T. Barillari¹⁰¹, M. Barisonzi^{164a,164b}, T. Barklow¹⁴³, N. Barlow²⁸, S.L. Barnes⁸⁴, B.M. Barnett¹³¹, R.M. Barnett¹⁵, Z. Barnovska⁵, A. Baroncelli^{134a}, G. Barone⁴⁹, A.J. Barr¹²⁰, F. Barreiro⁸², J. Barreiro Guimarães da Costa⁵⁷, R. Bartoldus¹⁴³, A.E. Barton⁷², P. Bartos^{144a}, A. Basalae¹²³, A. Bassalat¹¹⁷, A. Basye¹⁶⁵, R.L. Bates⁵³, S.J. Batista¹⁵⁸, J.R. Batley²⁸, M. Battaglia¹³⁷, M. Bauce^{132a,132b}, F. Bauer¹³⁶, H.S. Bawa^{143,e}, J.B. Beacham¹¹¹, M.D. Beattie⁷², T. Beau⁸⁰, P.H. Beauchemin¹⁶¹, R. Beccherle^{124a,124b}, P. Bechtel²¹, H.P. Beck^{17,f}, K. Becker¹²⁰, M. Becker⁸³, S. Becker¹⁰⁰, M. Beckingham¹⁷⁰, C. Becot¹¹⁷, A.J. Beddall^{19c}, A. Beddall^{19c}, V.A. Bednyakov⁶⁵, C.P. Bee¹⁴⁸, L.J. Beemster¹⁰⁷, T.A. Beermann¹⁷⁵, M. Begel²⁵, J.K. Behr¹²⁰, C. Belanger-Champagne⁸⁷, W.H. Bell⁴⁹, G. Bella¹⁵³, L. Bellagamba^{20a}, A. Bellerive²⁹, M. Bellomo⁸⁶, K. Belotskiy⁹⁸, O. Beltramello³⁰, O. Benary¹⁵³, D. Benchechroun^{135a}, M. Bender¹⁰⁰, K. Bendtz^{146a,146b}, N. Benekos¹⁰, Y. Benhammou¹⁵³, E. Benhar Noccioli⁴⁹, J.A. Benitez Garcia^{159b}, D.P. Benjamin⁴⁵, J.R. Bensinger²³, S. Bentvelsen¹⁰⁷, L. Beresford¹²⁰, M. Beretta⁴⁷, D. Berge¹⁰⁷, E. Bergeaas Kuutmann¹⁶⁶, N. Berger⁵, F. Berghaus¹⁶⁹, J. Beringer¹⁵, C. Bernard²², N.R. Bernard⁸⁶, C. Bernius¹¹⁰, F.U. Bernlochner²¹, T. Berry⁷⁷, P. Berta¹²⁹, C. Bertella⁸³, G. Bertoli^{146a,146b}, F. Bertolucci^{124a,124b}, C. Bertsche¹¹³, D. Bertsche¹¹³, M.I. Besana^{91a}, G.J. Besjes¹⁰⁶, O. Bessidskaia Bylund^{146a,146b}, M. Bessner⁴², N. Besson¹³⁶, C. Betancourt⁴⁸, S. Bethke¹⁰¹, A.J. Bevan⁷⁶, W. Bhimji⁴⁶, R.M. Bianchi¹²⁵, L. Bianchini²³, M. Bianco³⁰, O. Biebel¹⁰⁰, S.P. Bieniek⁷⁸, M. Biglietti^{134a}, J. Bilbao De Mendizabal⁴⁹,

H. Bilokon⁴⁷, M. Bindi⁵⁴, S. Binet¹¹⁷, A. Bingul^{19c}, C. Bini^{132a,132b}, C.W. Black¹⁵⁰, J.E. Black¹⁴³, K.M. Black²², D. Blackburn¹³⁸, R.E. Blair⁶, J.-B. Blanchard¹³⁶, J.E. Blanco⁷⁷, T. Blazek^{144a}, I. Bloch⁴², C. Blocker²³, W. Blum^{83,*}, U. Blumenschein⁵⁴, G.J. Bobbink¹⁰⁷, V.S. Bobrovnikov^{109,c}, S.S. Bocchetta⁸¹, A. Bocci⁴⁵, C. Bock¹⁰⁰, M. Boehler⁴⁸, J.A. Bogaerts³⁰, A.G. Bogdanchikov¹⁰⁹, C. Boehm^{146a}, V. Boisvert⁷⁷, T. Bold^{38a}, V. Boldea^{26a}, A.S. Boldyrev⁹⁹, M. Bomben⁸⁰, M. Bona⁷⁶, M. Boonekamp¹³⁶, A. Borisov¹³⁰, G. Borissov⁷², S. Borroni⁴², J. Bortfeldt¹⁰⁰, V. Bortolotto^{60a,60b,60c}, K. Bos¹⁰⁷, D. Boscherini^{20a}, M. Bosman¹², J. Boudreau¹²⁵, J. Bouffard², E.V. Bouhova-Thacker⁷², D. Boumediene³⁴, C. Bourdarios¹¹⁷, N. Bousson¹¹⁴, A. Boveia³⁰, J. Boyd³⁰, I.R. Boyko⁶⁵, I. Bozic¹³, J. Bracinik¹⁸, A. Brandt⁸, G. Brandt⁵⁴, O. Brandt^{58a}, U. Bratzler¹⁵⁶, B. Brau⁸⁶, J.E. Brau¹¹⁶, H.M. Braun^{175,*}, S.F. Brazzale^{164a,164c}, K. Brendlinger¹²², A.J. Brennan⁸⁸, L. Brenner¹⁰⁷, R. Brenner¹⁶⁶, S. Bressler¹⁷², K. Bristow^{145c}, T.M. Bristow⁴⁶, D. Britton⁵³, D. Britzger⁴², F.M. Brochu²⁸, I. Brock²¹, R. Brock⁹⁰, J. Bronner¹⁰¹, G. Brooijmans³⁵, T. Brooks⁷⁷, W.K. Brooks^{32b}, J. Brosamer¹⁵, E. Brost¹¹⁶, J. Brown⁵⁵, P.A. Bruckman de Renstrom³⁹, D. Bruncko^{144b}, R. Bruneliere⁴⁸, A. Bruni^{20a}, G. Bruni^{20a}, M. Bruschi^{20a}, L. Bryngemark⁸¹, T. Buanes¹⁴, Q. Buat¹⁴², P. Buchholz¹⁴¹, A.G. Buckley⁵³, S.I. Buda^{26a}, I.A. Budagov⁶⁵, F. Buehrer⁴⁸, L. Bugge¹¹⁹, M.K. Bugge¹¹⁹, O. Bulekov⁹⁸, D. Bullock⁸, H. Burckhart³⁰, S. Burdin⁷⁴, B. Burghgrave¹⁰⁸, S. Burke¹³¹, I. Burmeister⁴³, E. Busato³⁴, D. Büscher⁴⁸, V. Büscher⁸³, P. Bussey⁵³, J.M. Butler²², A.I. Butt³, C.M. Buttar⁵³, J.M. Butterworth⁷⁸, P. Butti¹⁰⁷, W. Buttinger²⁵, A. Buzatu⁵³, A.R. Buzykaev^{109,c}, S. Cabrera Urbán¹⁶⁷, D. Caforio¹²⁸, V.M. Cairo^{37a,37b}, O. Cakir^{4a}, P. Calafiura¹⁵, A. Calandri¹³⁶, G. Calderini⁸⁰, P. Calfayan¹⁰⁰, L.P. Caloba^{24a}, D. Calvet³⁴, S. Calvet³⁴, R. Camacho Toro³¹, S. Camarda⁴², P. Camarri^{133a,133b}, D. Cameron¹¹⁹, L.M. Caminada¹⁵, R. Caminal Armadans¹², S. Campana³⁰, M. Campanelli⁷⁸, A. Campoverde¹⁴⁸, V. Canale^{104a,104b}, A. Canepa^{159a}, M. Cano Bret⁷⁶, J. Cantero⁸², R. Cantrill^{126a}, T. Cao⁴⁰, M.D.M. Capeans Garrido³⁰, I. Caprini^{26a}, M. Caprini^{26a}, M. Capua^{37a,37b}, R. Caputo⁸³, R. Cardarelli^{133a}, T. Carli³⁰, G. Carlino^{104a}, L. Carminati^{91a,91b}, S. Caron¹⁰⁶, E. Carquin^{32a}, G.D. Carrillo-Montoya⁸, J.R. Carter²⁸, J. Carvalho^{126a,126c}, D. Casadei⁷⁸, M.P. Casado¹², M. Casolino¹², E. Castaneda-Miranda^{145b}, A. Castelli¹⁰⁷, V. Castillo Gimenez¹⁶⁷, N.F. Castro^{126a,g}, P. Catastini⁵⁷, A. Catinaccio³⁰, J.R. Catmore¹¹⁹, A. Cattai³⁰, J. Caudron⁸³, V. Cavaliere¹⁶⁵, D. Cavalli^{91a}, M. Cavalli-Sforza¹², V. Cavasinni^{124a,124b}, F. Ceradini^{134a,134b}, B.C. Cerio⁴⁵, K. Cerny¹²⁹, A.S. Cerqueira^{24b}, A. Cerri¹⁴⁹, L. Cerrito⁷⁶, F. Cerutti¹⁵, M. Cerv³⁰, A. Cervelli¹⁷, S.A. Cetin^{19b}, A. Chafaq^{135a}, D. Chakraborty¹⁰⁸, I. Chalupkova¹²⁹, P. Chang¹⁶⁵, B. Chapleau⁸⁷, J.D. Chapman²⁸, D.G. Charlton¹⁸, C.C. Chau¹⁵⁸, C.A. Chavez Barajas¹⁴⁹, S. Cheatham¹⁵², A. Chegwidden⁹⁰, S. Chekanov⁶, S.V. Chekulaev^{159a}, G.A. Chelkov^{65,h}, M.A. Chelstowska⁸⁹, C. Chen⁶⁴, H. Chen²⁵, K. Chen¹⁴⁸, L. Chen^{33d,i}, S. Chen^{33c}, X. Chen^{33f}, Y. Chen⁶⁷, H.C. Cheng⁸⁹, Y. Cheng³¹, A. Cheplakov⁶⁵, E. Cheremushkina¹³⁰, R. Cherkaoui El Moursli^{135e}, V. Chernyatin^{25,*}, E. Cheu⁷, L. Chevalier¹³⁶, V. Chiarella⁴⁷, J.T. Childers⁶, G. Chiodini^{73a}, A.S. Chisholm¹⁸, R.T. Chislett⁷⁸, A. Chitan^{26a}, M.V. Chizhov⁶⁵, K. Choi⁶¹, S. Chouridou⁹, B.K.B. Chow¹⁰⁰, V. Christodoulou⁷⁸, D. Chromek-Burckhart³⁰, M.L. Chu¹⁵¹, J. Chudoba¹²⁷, A.J. Chuinard⁸⁷, J.J. Chwastowski³⁹, L. Chytka¹¹⁵, G. Ciapetti^{132a,132b}, A.K. Ciftci^{4a}, D. Cinca⁵³, V. Cindro⁷⁵, I.A. Cioara²¹, A. Ciocio¹⁵, Z.H. Citron¹⁷², M. Ciubancan^{26a}, A. Clark⁴⁹, B.L. Clark⁵⁷, P.J. Clark⁴⁶, R.N. Clarke¹⁵, W. Cleland¹²⁵, C. Clement^{146a,146b}, Y. Coadou⁸⁵, M. Cobal^{164a,164c}, A. Coccaro¹³⁸, J. Cochran⁶⁴, L. Coffey²³, J.G. Cogan¹⁴³, B. Cole³⁵, S. Cole¹⁰⁸, A.P. Colijn¹⁰⁷, J. Collot⁵⁵, T. Colombo^{58c}, G. Compostella¹⁰¹, P. Conde Muiño^{126a,126b}, E. Coniavitis⁴⁸, S.H. Connell^{145b}, I.A. Connelly⁷⁷, S.M. Consonni^{91a,91b}, V. Consorti⁴⁸, S. Constantinescu^{26a}, C. Conta^{121a,121b}, G. Conti³⁰, F. Conventi^{104a,j}, M. Cooke¹⁵, B.D. Cooper⁷⁸, A.M. Cooper-Sarkar¹²⁰, T. Cornelissen¹⁷⁵, M. Corradi^{20a}, F. Corriveau^{87,k}, A. Corso-Radu¹⁶³, A. Cortes-Gonzalez¹², G. Cortiana¹⁰¹, G. Costa^{91a}, M.J. Costa¹⁶⁷, D. Costanzo¹³⁹, D. Côté⁸, G. Cottin²⁸, G. Cowan⁷⁷, B.E. Cox⁸⁴, K. Cranmer¹¹⁰, G. Cree²⁹, S. Crépe-Renaudin⁵⁵, F. Crescioli⁸⁰, W.A. Cribbs^{146a,146b}, M. Crispin Ortuzar¹²⁰, M. Cristinziani²¹, V. Croft¹⁰⁶, G. Crosetti^{37a,37b}, T. Cuhadar Donszelmann¹³⁹, J. Cummings¹⁷⁶, M. Curatolo⁴⁷, C. Cuthbert¹⁵⁰, H. Czirr¹⁴¹, P. Czodrowski³, S. D'Auria⁵³, M. D'Onofrio⁷⁴, M.J. Da Cunha Sargedas De Sousa^{126a,126b}, C. Da Via⁸⁴, W. Dabrowski^{38a}, A. Dafinca¹²⁰, T. Dai⁸⁹, O. Dale¹⁴, F. Dallaire⁹⁵, C. Dallapiccola⁸⁶, M. Dam³⁶, J.R. Dandoy³¹, N.P. Dang⁴⁸, A.C. Daniells¹⁸, M. Danninger¹⁶⁸, M. Dano Hoffmann¹³⁶, V. Dao⁴⁸, G. Darbo^{50a}, S. Darmora⁸, J. Dassoulas³, A. Dattagupta⁶¹, W. Davey²¹, C. David¹⁶⁹, T. Davidek¹²⁹, E. Davies^{120,l}, M. Davies¹⁵³, P. Davison⁷⁸, Y. Davygora^{58a}, E. Dawe⁸⁸, I. Dawson¹³⁹,

R.K. Daya-Ishmukhametova⁸⁶, K. De⁸, R. de Asmundis^{104a}, S. De Castro^{20a,20b}, S. De Cecco⁸⁰, N. De Groot¹⁰⁶, P. de Jong¹⁰⁷, H. De la Torre⁸², F. De Lorenzi⁶⁴, L. De Nooij¹⁰⁷, D. De Pedis^{132a}, A. De Salvo^{132a}, U. De Sanctis¹⁴⁹, A. De Santo¹⁴⁹, J.B. De Vivie De Regie¹¹⁷, W.J. Dearnaley⁷², R. Debbé²⁵, C. Debenedetti¹³⁷, D.V. Dedovich⁶⁵, I. Deigaard¹⁰⁷, J. Del Peso⁸², T. Del Prete^{124a,124b}, D. Delgove¹¹⁷, F. Deliot¹³⁶, C.M. Delitzsch⁴⁹, M. Deliyergiyev⁷⁵, A. Dell'Acqua³⁰, L. Dell'Asta²², M. Dell'Orso^{124a,124b}, M. Della Pietra^{104a,j}, D. della Volpe⁴⁹, M. Delmastro⁵, P.A. Delsart⁵⁵, C. Deluca¹⁰⁷, D.A. DeMarco¹⁵⁸, S. Demers¹⁷⁶, M. Demichev⁶⁵, A. Demilly⁸⁰, S.P. Denisov¹³⁰, D. Derendarz³⁹, J.E. Derkaoui^{135d}, F. Derue⁸⁰, P. Dervan⁷⁴, K. Desch²¹, C. Deterre⁴², P.O. Deviveiros³⁰, A. Dewhurst¹³¹, S. Dhaliwal²³, A. Di Ciaccio^{133a,133b}, L. Di Ciaccio⁵, A. Di Domenico^{132a,132b}, C. Di Donato^{104a,104b}, A. Di Girolamo³⁰, B. Di Girolamo³⁰, A. Di Mattia¹⁵², B. Di Micco^{134a,134b}, R. Di Nardo⁴⁷, A. Di Simone⁴⁸, R. Di Sipio¹⁵⁸, D. Di Valentino²⁹, C. Diaconu⁸⁵, M. Diamond¹⁵⁸, F.A. Dias⁴⁶, M.A. Diaz^{32a}, E.B. Diehl⁸⁹, J. Dietrich¹⁶, S. Diglio⁸⁵, A. Dimitrievska¹³, J. Dingfelder²¹, P. Dita^{26a}, S. Dita^{26a}, F. Dittus³⁰, F. Djama⁸⁵, T. Djobava^{51b}, J.I. Djuvsland^{58a}, M.A.B. do Vale^{24c}, D. Dobos³⁰, M. Dobre^{26a}, C. Doglioni⁴⁹, T. Dohmae¹⁵⁵, J. Dolejsi¹²⁹, Z. Dolezal¹²⁹, B.A. Dolgoshein^{98,*}, M. Donadelli^{24d}, S. Donati^{124a,124b}, P. Dondero^{121a,121b}, J. Donini³⁴, J. Dopke¹³¹, A. Doria^{104a}, M.T. Dova⁷¹, A.T. Doyle⁵³, E. Drechsler⁵⁴, M. Dris¹⁰, E. Dubreuil³⁴, E. Duchovni¹⁷², G. Duckeck¹⁰⁰, O.A. Ducu^{26a,85}, D. Duda¹⁷⁵, A. Dudarev³⁰, L. Dufлот¹¹⁷, L. Duguid⁷⁷, M. Dührssen³⁰, M. Dunford^{58a}, H. Duran Yildiz^{4a}, M. Düren⁵², A. Durglishvili^{51b}, D. Duschinger⁴⁴, M. Dyndal^{38a}, C. Eckardt⁴², K.M. Ecker¹⁰¹, R.C. Edgar⁸⁹, W. Edson², N.C. Edwards⁴⁶, W. Ehrenfeld²¹, T. Eifert³⁰, G. Eigen¹⁴, K. Einsweiler¹⁵, T. Ekelof¹⁶⁶, M. El Kacimi^{135c}, M. Ellert¹⁶⁶, S. Elles⁵, F. Ellinghaus⁸³, A.A. Elliot¹⁶⁹, N. Ellis³⁰, J. Elmsheuser¹⁰⁰, M. Elsing³⁰, D. Emelianov¹³¹, Y. Enari¹⁵⁵, O.C. Endner⁸³, M. Endo¹¹⁸, J. Erdmann⁴³, A. Ereditato¹⁷, G. Ernis¹⁷⁵, J. Ernst², M. Ernst²⁵, S. Errede¹⁶⁵, E. Ertel⁸³, M. Escalier¹¹⁷, H. Esch⁴³, C. Escobar¹²⁵, B. Esposito⁴⁷, A.I. Etienne¹³⁶, E. Etzion¹⁵³, H. Evans⁶¹, A. Ezhilov¹²³, L. Fabbri^{20a,20b}, G. Facini³¹, R.M. Fakhruddinov¹³⁰, S. Falciano^{132a}, R.J. Falla⁷⁸, J. Faltova¹²⁹, Y. Fang^{33a}, M. Fanti^{91a,91b}, A. Farbin⁸, A. Farilla^{134a}, T. Farooque¹², S. Farrell¹⁵, S.M. Farrington¹⁷⁰, P. Farthouat³⁰, F. Fassi^{135e}, P. Fassnacht³⁰, D. Fassouliotis⁹, M. Fauci Giannelli⁷⁷, A. Favareto^{50a,50b}, L. Fayard¹¹⁷, P. Federic^{144a}, O.L. Fedin^{123,m}, W. Fedorko¹⁶⁸, S. Feigl³⁰, L. Felgioni⁸⁵, C. Feng^{33d}, E.J. Feng⁶, H. Feng⁸⁹, A.B. Fenyuk¹³⁰, P. Fernandez Martinez¹⁶⁷, S. Fernandez Perez³⁰, J. Ferrando⁵³, A. Ferrari¹⁶⁶, P. Ferrari¹⁰⁷, R. Ferrari^{121a}, D.E. Ferreira de Lima⁵³, A. Ferrer¹⁶⁷, D. Ferrere⁴⁹, C. Ferretti⁸⁹, A. Ferretto Parodi^{50a,50b}, M. Fiascaris³¹, F. Fiedler⁸³, A. Filipčič⁷⁵, M. Filipuzzi⁴², F. Filthaut¹⁰⁶, M. Fincke-Keeler¹⁶⁹, K.D. Finelli¹⁵⁰, M.C.N. Fiolhais^{126a,126c}, L. Fiorini¹⁶⁷, A. Firan⁴⁰, A. Fischer², C. Fischer¹², J. Fischer¹⁷⁵, W.C. Fisher⁹⁰, E.A. Fitzgerald²³, M. Flechl⁴⁸, I. Fleck¹⁴¹, P. Fleischmann⁸⁹, S. Fleischmann¹⁷⁵, G.T. Fletcher¹³⁹, G. Fletcher⁷⁶, T. Flick¹⁷⁵, A. Floderus⁸¹, L.R. Flores Castillo^{60a}, M.J. Flowerdew¹⁰¹, A. Formica¹³⁶, A. Forti⁸⁴, D. Fournier¹¹⁷, H. Fox⁷², S. Fracchia¹², P. Francavilla⁸⁰, M. Franchini^{20a,20b}, D. Francis³⁰, L. Franconi¹¹⁹, M. Franklin⁵⁷, M. Fraternali^{121a,121b}, D. Freeborn⁷⁸, S.T. French²⁸, F. Friedrich⁴⁴, D. Froidevaux³⁰, J.A. Frost¹²⁰, C. Fukunaga¹⁵⁶, E. Fullana Torregrosa⁸³, B.G. Fulsom¹⁴³, J. Fuster¹⁶⁷, C. Gabaldon⁵⁵, O. Gabizon¹⁷⁵, A. Gabrielli^{20a,20b}, A. Gabrielli^{132a,132b}, S. Gadatsch¹⁰⁷, S. Gadomski⁴⁹, G. Gagliardi^{50a,50b}, P. Gagnon⁶¹, C. Galea¹⁰⁶, B. Galhardo^{126a,126c}, E.J. Gallas¹²⁰, B.J. Gallop¹³¹, P. Gallus¹²⁸, G. Galster³⁶, K.K. Gan¹¹¹, J. Gao^{33b,85}, Y. Gao⁴⁶, Y.S. Gao^{143,e}, F.M. Garay Walls⁴⁶, F. Garberon¹⁷⁶, C. García¹⁶⁷, J.E. García Navarro¹⁶⁷, M. Garcia-Sciveres¹⁵, R.W. Gardner³¹, N. Garelli¹⁴³, V. Garonne¹¹⁹, C. Gatti⁴⁷, A. Gaudiello^{50a,50b}, G. Gaudio^{121a}, B. Gaur¹⁴¹, L. Gauthier⁹⁵, P. Gauzzi^{132a,132b}, I.L. Gavrilenko⁹⁶, C. Gay¹⁶⁸, G. Gaycken²¹, E.N. Gazis¹⁰, P. Ge^{33d}, Z. Gece¹⁶⁸, C.N.P. Gee¹³¹, D.A.A. Geerts¹⁰⁷, Ch. Geich-Gimbel²¹, M.P. Geisler^{58a}, C. Gemme^{50a}, M.H. Genest⁵⁵, S. Gentile^{132a,132b}, M. George⁵⁴, S. George⁷⁷, D. Gerbaudo¹⁶³, A. Gershon¹⁵³, H. Ghazlane^{135b}, B. Giacobbe^{20a}, S. Giagu^{132a,132b}, V. Giangiobbe¹², P. Giannetti^{124a,124b}, B. Gibbard²⁵, S.M. Gibson⁷⁷, M. Gilchriese¹⁵, T.P.S. Gillam²⁸, D. Gillberg³⁰, G. Gilles³⁴, D.M. Gingrich^{3,d}, N. Giokaris⁹, M.P. Giordani^{164a,164c}, F.M. Giorgi^{20a}, F.M. Giorgi¹⁶, P.F. Giraud¹³⁶, P. Giromini⁴⁷, D. Giugni^{91a}, C. Giuliani⁴⁸, M. Giulini^{58b}, B.K. Gjelsten¹¹⁹, S. Gkaitatzis¹⁵⁴, I. Gkialas¹⁵⁴, E.L. Gkougkousis¹¹⁷, L.K. Gladilin⁹⁹, C. Glasman⁸², J. Glatzer³⁰, P.C.F. Glaysher⁴⁶, A. Glazov⁴², M. Goblirsch-Kolb¹⁰¹, J.R. Goddard⁷⁶, J. Godlewski³⁹, S. Goldfarb⁸⁹, T. Golling⁴⁹, D. Golubkov¹³⁰, A. Gomes^{126a,126b,126d}, R. Gonçalo^{126a}, J. Goncalves Pinto Firmino Da Costa¹³⁶, L. Gonella²¹, S. González de la Hoz¹⁶⁷, G. Gonzalez Parra¹², S. Gonzalez-Sevilla⁴⁹, L. Goossens³⁰, P.A. Gorbounov⁹⁷, H.A. Gordon²⁵,

I. Gorelov¹⁰⁵, B. Gorini³⁰, E. Gorini^{73a,73b}, A. Gorišek⁷⁵, E. Gornicki³⁹, A.T. Goshaw⁴⁵, C. Gössling⁴³, M.I. Gostkin⁶⁵, D. Goujdami^{135c}, A.G. Goussiou¹³⁸, N. Govender^{145b}, H.M.X. Grabas¹³⁷, L. Graber⁵⁴, I. Grabowska-Bold^{38a}, P. Grafström^{20a,20b}, K.-J. Grahn⁴², J. Gramling⁴⁹, E. Gramstad¹¹⁹, S. Grancagnolo¹⁶, V. Grassi¹⁴⁸, V. Gratchev¹²³, H.M. Gray³⁰, E. Graziani^{134a}, Z.D. Greenwood^{79,n}, K. Gregersen⁷⁸, I.M. Gregor⁴², P. Grenier¹⁴³, J. Griffiths⁸, A.A. Grillo¹³⁷, K. Grimm⁷², S. Grinstein^{12,o}, Ph. Gris³⁴, J.-F. Grivaz¹¹⁷, J.P. Grohs⁴⁴, A. Grohsjean⁴², E. Gross¹⁷², J. Grosse-Knetter⁵⁴, G.C. Grossi⁷⁹, Z.J. Grout¹⁴⁹, L. Guan^{33b}, J. Guenther¹²⁸, F. Guescini⁴⁹, D. Guest¹⁷⁶, O. Gueta¹⁵³, E. Guido^{50a,50b}, T. Guillemin¹¹⁷, S. Guindon², U. Gul⁵³, C. Gumpert⁴⁴, J. Guo^{33e}, S. Gupta¹²⁰, P. Gutierrez¹¹³, N.G. Gutierrez Ortiz⁵³, C. Gutschew⁴⁴, C. Guyot¹³⁶, C. Gwenlan¹²⁰, C.B. Gwilliam⁷⁴, A. Haas¹¹⁰, C. Haber¹⁵, H.K. Hadavand⁸, N. Haddad^{135e}, P. Haefner²¹, S. Hageböck²¹, Z. Hajduk³⁹, H. Hakobyan¹⁷⁷, M. Haleem⁴², J. Haley¹¹⁴, D. Hall¹²⁰, G. Halladjian⁹⁰, G.D. Hallewell⁸⁵, K. Hamacher¹⁷⁵, P. Hamal¹¹⁵, K. Hamano¹⁶⁹, M. Hamer⁵⁴, A. Hamilton^{145a}, G.N. Hamity^{145c}, P.G. Hamnett⁴², L. Han^{33b}, K. Hanagaki¹¹⁸, K. Hanawa¹⁵⁵, M. Hance¹⁵, P. Hanke^{58a}, R. Hanna¹³⁶, J.B. Hansen³⁶, J.D. Hansen³⁶, M.C. Hansen²¹, P.H. Hansen³⁶, K. Hara¹⁶⁰, A.S. Hard¹⁷³, T. Harenberg¹⁷⁵, F. Hariri¹¹⁷, S. Harkusha⁹², R.D. Harrington⁴⁶, P.F. Harrison¹⁷⁰, F. Hartjes¹⁰⁷, M. Hasegawa⁶⁷, S. Hasegawa¹⁰³, Y. Hasegawa¹⁴⁰, A. Hasib¹¹³, S. Hassani¹³⁶, S. Haug¹⁷, R. Hauser⁹⁰, L. Hauswald⁴⁴, M. Havranek¹²⁷, C.M. Hawkes¹⁸, R.J. Hawking³⁰, A.D. Hawkins⁸¹, T. Hayashi¹⁶⁰, D. Hayden⁹⁰, C.P. Hays¹²⁰, J.M. Hays⁷⁶, H.S. Hayward⁷⁴, S.J. Haywood¹³¹, S.J. Head¹⁸, T. Heck⁸³, V. Hedberg⁸¹, L. Heelan⁸, S. Heim¹²², T. Heim¹⁷⁵, B. Heinemann¹⁵, L. Heinrich¹¹⁰, J. Hejbal¹²⁷, L. Helary²², S. Hellman^{146a,146b}, D. Hellmich²¹, C. Hensens³⁰, J. Henderson¹²⁰, R.C.W. Henderson⁷², Y. Heng¹⁷³, C. Hengler⁴², A. Henrichs¹⁷⁶, A.M. Henriques Correia³⁰, S. Henrot-Versille¹¹⁷, G.H. Herbert¹⁶, Y. Hernández Jiménez¹⁶⁷, R. Herrberg-Schubert¹⁶, G. Herten⁴⁸, R. Hertenberger¹⁰⁰, L. Hervas³⁰, G.G. Hesketh⁷⁸, N.P. Hessey¹⁰⁷, J.W. Hetherly⁴⁰, R. Hickling⁷⁶, E. Higón-Rodríguez¹⁶⁷, E. Hill¹⁶⁹, J.C. Hill²⁸, K.H. Hiller⁴², S.J. Hillier¹⁸, I. Hinchliffe¹⁵, E. Hines¹²², R.R. Hinman¹⁵, M. Hirose¹⁵⁷, D. Hirschbuehl¹⁷⁵, J. Hobbs¹⁴⁸, N. Hod¹⁰⁷, M.C. Hodgkinson¹³⁹, P. Hodgson¹³⁹, A. Hoecker³⁰, M.R. Hoferkamp¹⁰⁵, F. Hoenig¹⁰⁰, M. Hohlfeld⁸³, D. Hohn²¹, T.R. Holmes¹⁵, M. Homann⁴³, T.M. Hong¹²⁵, L. Hooft van Huysduynen¹¹⁰, W.H. Hopkins¹¹⁶, Y. Horii¹⁰³, A.J. Horton¹⁴², J.-Y. Hostachy⁵⁵, S. Hou¹⁵¹, A. Hoummada^{135a}, J. Howard¹²⁰, J. Howarth⁴², M. Hrabovsky¹¹⁵, I. Hristova¹⁶, J. Hrivnac¹¹⁷, T. Hryn'ova⁵, A. Hrynevich⁹³, C. Hsu^{145c}, P.J. Hsu^{151,p}, S.-C. Hsu¹³⁸, D. Hu³⁵, Q. Hu^{33b}, X. Hu⁸⁹, Y. Huang⁴², Z. Hubacek³⁰, F. Hubaut⁸⁵, F. Huegging²¹, T.B. Huffman¹²⁰, E.W. Hughes³⁵, G. Hughes⁷², M. Huhtinen³⁰, T.A. Hülsing⁸³, N. Huseynov^{65,b}, J. Huston⁹⁰, J. Huth⁵⁷, G. Iacobucci⁴⁹, G. Iakovidis²⁵, I. Ibragimov¹⁴¹, L. Iconomidou-Fayard¹¹⁷, E. Ideal¹⁷⁶, Z. Idrissi^{135e}, P. Iengo³⁰, O. Igonkina¹⁰⁷, T. Iizawa¹⁷¹, Y. Ikegami⁶⁶, K. Ikematsu¹⁴¹, M. Ikeno⁶⁶, Y. Ilchenko^{31,q}, D. Iliadis¹⁵⁴, N. Ilic¹⁴³, Y. Inamaru⁶⁷, T. Ince¹⁰¹, P. Ioannou⁹, M. Iodice^{134a}, K. Iordanidou³⁵, V. Ippolito⁵⁷, A. Irls Quiles¹⁶⁷, C. Isaksson¹⁶⁶, M. Ishino⁶⁸, M. Ishitsuka¹⁵⁷, R. Ishmukhametov¹¹¹, C. Issever¹²⁰, S. Istin^{19a}, J.M. Iturbe Ponce⁸⁴, R. Iuppa^{133a,133b}, J. Ivarsson⁸¹, W. Iwanski³⁹, H. Iwasaki⁶⁶, J.M. Izen⁴¹, V. Izzo^{104a}, S. Jabbar³, B. Jackson¹²², M. Jackson⁷⁴, P. Jackson¹, M.R. Jaekel³⁰, V. Jain², K. Jakobs⁴⁸, S. Jakobsen³⁰, T. Jakoubek¹²⁷, J. Jakubek¹²⁸, D.O. Jamin¹⁵¹, D.K. Jana⁷⁹, E. Jansen⁷⁸, R.W. Jansky⁶², J. Janssen²¹, M. Janus¹⁷⁰, G. Jarlskog⁸¹, N. Javadov^{65,b}, T. Javůrek⁴⁸, L. Jeanty¹⁵, J. Jejelava^{51a,r}, G.-Y. Jeng¹⁵⁰, D. Jennens⁸⁸, P. Jenni^{48,s}, J. Jentzsch⁴³, C. Jeske¹⁷⁰, S. Jézéquel⁵, H. Ji¹⁷³, J. Jia¹⁴⁸, Y. Jiang^{33b}, S. Jiggins⁷⁸, J. Jimenez Pena¹⁶⁷, S. Jin^{33a}, A. Jinaru^{26a}, O. Jinnouchi¹⁵⁷, M.D. Joergensen³⁶, P. Johansson¹³⁹, K.A. Johns⁷, K. Jon-And^{146a,146b}, G. Jones¹⁷⁰, R.W.L. Jones⁷², T.J. Jones⁷⁴, J. Jongmanns^{58a}, P.M. Jorge^{126a,126b}, K.D. Joshi⁸⁴, J. Jovicevic^{159a}, X. Ju¹⁷³, C.A. Jung⁴³, P. Jussel⁶², A. Juste Rozas^{12,o}, M. Kaci¹⁶⁷, A. Kaczmarska³⁹, M. Kado¹¹⁷, H. Kagan¹¹¹, M. Kagan¹⁴³, S.J. Kahn⁸⁵, E. Kajomovitz⁴⁵, C.W. Kalderon¹²⁰, S. Kama⁴⁰, A. Kamenshchikov¹³⁰, N. Kanaya¹⁵⁵, M. Kaneda³⁰, S. Kaneti²⁸, V.A. Kantserov⁹⁸, J. Kanzaki⁶⁶, B. Kaplan¹¹⁰, A. Kapliy³¹, D. Kar⁵³, K. Karakostas¹⁰, A. Karamaoun³, N. Karastathis^{10,107}, M.J. Kareem⁵⁴, M. Karnevskiy⁸³, S.N. Karpov⁶⁵, Z.M. Karpova⁶⁵, K. Karthik¹¹⁰, V. Kartvelishvili⁷², A.N. Karyukhin¹³⁰, L. Kashif¹⁷³, R.D. Kass¹¹¹, A. Kastanas¹⁴, Y. Kataoka¹⁵⁵, A. Katre⁴⁹, J. Katzy⁴², K. Kawagoe⁷⁰, T. Kawamoto¹⁵⁵, G. Kawamura⁵⁴, S. Kazama¹⁵⁵, V.F. Kazanin^{109,c}, M.Y. Kazarinov⁶⁵, R. Keeler¹⁶⁹, R. Kehoe⁴⁰, J.S. Keller⁴², J.J. Kempster⁷⁷, H. Keoshkerian⁸⁴, O. Kepka¹²⁷, B.P. Kerševan⁷⁵, S. Kersten¹⁷⁵, R.A. Keyes⁸⁷, F. Khalil-zada¹¹, H. Khandanyan^{146a,146b}, A. Khanov¹¹⁴, A.G. Kharlamov^{109,c}, T.J. Khoo²⁸, V. Khovanskij⁹⁷, E. Khramov⁶⁵, J. Khubua^{51b,t}, H.Y. Kim⁸,

H. Kim ^{146a,146b}, S.H. Kim ¹⁶⁰, Y. Kim ³¹, N. Kimura ¹⁵⁴, O.M. Kind ¹⁶, B.T. King ⁷⁴, M. King ¹⁶⁷, R.S.B. King ¹²⁰, S.B. King ¹⁶⁸, J. Kirk ¹³¹, A.E. Kiryunin ¹⁰¹, T. Kishimoto ⁶⁷, D. Kisielowska ^{38a}, F. Kiss ⁴⁸, K. Kiuchi ¹⁶⁰, O. Kivernyk ¹³⁶, E. Kladiva ^{144b}, M.H. Klein ³⁵, M. Klein ⁷⁴, U. Klein ⁷⁴, K. Kleinknecht ⁸³, P. Klimek ^{146a,146b}, A. Klimentov ²⁵, R. Klingenberg ⁴³, J.A. Klinger ⁸⁴, T. Klioutchnikova ³⁰, E.-E. Kluge ^{58a}, P. Kluit ¹⁰⁷, S. Kluth ¹⁰¹, E. Kneringer ⁶², E.B.F.G. Knoops ⁸⁵, A. Knue ⁵³, A. Kobayashi ¹⁵⁵, D. Kobayashi ¹⁵⁷, T. Kobayashi ¹⁵⁵, M. Kobel ⁴⁴, M. Kocian ¹⁴³, P. Kodys ¹²⁹, T. Koffas ²⁹, E. Koffeman ¹⁰⁷, L.A. Kogan ¹²⁰, S. Kohlmann ¹⁷⁵, Z. Kohout ¹²⁸, T. Kohriki ⁶⁶, T. Koi ¹⁴³, H. Kolanoski ¹⁶, I. Koletsou ⁵, A.A. Komar ^{96,*}, Y. Komori ¹⁵⁵, T. Kondo ⁶⁶, N. Kondrashova ⁴², K. Köneke ⁴⁸, A.C. König ¹⁰⁶, S. König ⁸³, T. Kono ^{66,u}, R. Konoplich ^{110,v}, N. Konstantinidis ⁷⁸, R. Kopeliansky ¹⁵², S. Koperny ^{38a}, L. Köpke ⁸³, A.K. Kopp ⁴⁸, K. Korcyl ³⁹, K. Kordas ¹⁵⁴, A. Korn ⁷⁸, A.A. Korol ^{109,c}, I. Korolkov ¹², E.V. Korolkova ¹³⁹, O. Kortner ¹⁰¹, S. Kortner ¹⁰¹, T. Kosek ¹²⁹, V.V. Kostyukhin ²¹, V.M. Kotov ⁶⁵, A. Kotwal ⁴⁵, A. Kourkoumeli-Charalampidi ¹⁵⁴, C. Kourkoumelis ⁹, V. Kouskoura ²⁵, A. Koutsman ^{159a}, R. Kowalewski ¹⁶⁹, T.Z. Kowalski ^{38a}, W. Kozanecki ¹³⁶, A.S. Kozhin ¹³⁰, V.A. Kramarenko ⁹⁹, G. Kramberger ⁷⁵, D. Krasnoperov ⁹⁸, M.W. Krasny ⁸⁰, A. Krasznahorkay ³⁰, J.K. Kraus ²¹, A. Kravchenko ²⁵, S. Kreiss ¹¹⁰, M. Kretz ^{58c}, J. Kretzschmar ⁷⁴, K. Kreutzfeldt ⁵², P. Krieger ¹⁵⁸, K. Krizka ³¹, K. Kroeninger ⁴³, H. Kroha ¹⁰¹, J. Kroll ¹²², J. Kroseberg ²¹, J. Krstic ¹³, U. Kruchonak ⁶⁵, H. Krüger ²¹, N. Krumnack ⁶⁴, Z.V. Krumshteyn ⁶⁵, A. Kruse ¹⁷³, M.C. Kruse ⁴⁵, M. Kruskal ²², T. Kubota ⁸⁸, H. Kucuk ⁷⁸, S. Kuday ^{4c}, S. Kuehn ⁴⁸, A. Kugel ^{58c}, F. Kuger ¹⁷⁴, A. Kuhl ¹³⁷, T. Kuhl ⁴², V. Kukhtin ⁶⁵, Y. Kulchitsky ⁹², S. Kuleshov ^{32b}, M. Kuna ^{132a,132b}, T. Kunigo ⁶⁸, A. Kupco ¹²⁷, H. Kurashige ⁶⁷, Y.A. Kurochkin ⁹², R. Kurumida ⁶⁷, V. Kus ¹²⁷, E.S. Kuwertz ¹⁶⁹, M. Kuze ¹⁵⁷, J. Kvita ¹¹⁵, T. Kwan ¹⁶⁹, D. Kyriazopoulos ¹³⁹, A. La Rosa ⁴⁹, J.L. La Rosa Navarro ^{24d}, L. La Rotonda ^{37a,37b}, C. Lacasta ¹⁶⁷, F. Lacava ^{132a,132b}, J. Lacey ²⁹, H. Lacker ¹⁶, D. Lacour ⁸⁰, V.R. Lacuesta ¹⁶⁷, E. Ladygin ⁶⁵, R. Lafaye ⁵, B. Laforge ⁸⁰, T. Lagouri ¹⁷⁶, S. Lai ⁴⁸, L. Lambourne ⁷⁸, S. Lammers ⁶¹, C.L. Lampen ⁷, W. Lampl ⁷, E. Lançon ¹³⁶, U. Landgraf ⁴⁸, M.P.J. Landon ⁷⁶, V.S. Lang ^{58a}, J.C. Lange ¹², A.J. Lankford ¹⁶³, F. Lanni ²⁵, K. Lantzsich ³⁰, S. Laplace ⁸⁰, C. Lapoire ³⁰, J.F. Laporte ¹³⁶, T. Lari ^{91a}, F. Lasagni Manghi ^{20a,20b}, M. Lassnig ³⁰, P. Laurelli ⁴⁷, W. Lavrijsen ¹⁵, A.T. Law ¹³⁷, P. Laycock ⁷⁴, T. Lazovich ⁵⁷, O. Le Dortz ⁸⁰, E. Le Guirriec ⁸⁵, E. Le Menedeu ¹², M. LeBlanc ¹⁶⁹, T. LeCompte ⁶, F. Ledroit-Guillon ⁵⁵, C.A. Lee ^{145b}, S.C. Lee ¹⁵¹, L. Lee ¹, G. Lefebvre ⁸⁰, M. Lefebvre ¹⁶⁹, F. Legger ¹⁰⁰, C. Leggett ¹⁵, A. Lehan ⁷⁴, G. Lehmann Miotto ³⁰, X. Lei ⁷, W.A. Leight ²⁹, A. Leisos ^{154,w}, A.G. Leister ¹⁷⁶, M.A.L. Leite ^{24d}, R. Leitner ¹²⁹, D. Lellouch ¹⁷², B. Lemmer ⁵⁴, K.J.C. Leney ⁷⁸, T. Lenz ²¹, B. Lenzi ³⁰, R. Leone ⁷, S. Leone ^{124a,124b}, C. Leonidopoulos ⁴⁶, S. Leontsinis ¹⁰, C. Leroy ⁹⁵, C.G. Lester ²⁸, C.M. Lester ¹²², M. Levchenko ¹²³, J. Levêque ⁵, D. Levin ⁸⁹, L.J. Levinson ¹⁷², M. Levy ¹⁸, A. Lewis ¹²⁰, A.M. Leyko ²¹, M. Leyton ⁴¹, B. Li ^{33b,x}, H. Li ¹⁴⁸, H.L. Li ³¹, L. Li ⁴⁵, L. Li ^{33e}, S. Li ⁴⁵, Y. Li ^{33c,y}, Z. Liang ¹³⁷, H. Liao ³⁴, B. Liberti ^{133a}, A. Liblong ¹⁵⁸, P. Lichard ³⁰, K. Lie ¹⁶⁵, J. Liebal ²¹, W. Liebig ¹⁴, C. Limbach ²¹, A. Limosani ¹⁵⁰, S.C. Lin ^{151,z}, T.H. Lin ⁸³, F. Linde ¹⁰⁷, B.E. Lindquist ¹⁴⁸, J.T. Linnemann ⁹⁰, E. Lipeles ¹²², A. Lipniacka ¹⁴, M. Lisovsky ^{58b}, T.M. Liss ¹⁶⁵, D. Lissauer ²⁵, A. Lister ¹⁶⁸, A.M. Litke ¹³⁷, B. Liu ^{151,aa}, D. Liu ¹⁵¹, J. Liu ⁸⁵, J.B. Liu ^{33b}, K. Liu ⁸⁵, L. Liu ¹⁶⁵, M. Liu ⁴⁵, M. Liu ^{33b}, Y. Liu ^{33b}, M. Livan ^{121a,121b}, A. Lleres ⁵⁵, J. Llorente Merino ⁸², S.L. Lloyd ⁷⁶, F. Lo Sterzo ¹⁵¹, E. Lobodzinska ⁴², P. Loch ⁷, W.S. Lockman ¹³⁷, F.K. Loebinger ⁸⁴, A.E. Loevschall-Jensen ³⁶, A. Loginov ¹⁷⁶, T. Lohse ¹⁶, K. Lohwasser ⁴², M. Lokajicek ¹²⁷, B.A. Long ²², J.D. Long ⁸⁹, R.E. Long ⁷², K.A. Looper ¹¹¹, L. Lopes ^{126a}, D. Lopez Mateos ⁵⁷, B. Lopez Paredes ¹³⁹, I. Lopez Paz ¹², J. Lorenz ¹⁰⁰, N. Lorenzo Martinez ⁶¹, M. Losada ¹⁶², P. Loscutoff ¹⁵, P.J. Lösel ¹⁰⁰, X. Lou ^{33a}, A. Lounis ¹¹⁷, J. Love ⁶, P.A. Love ⁷², N. Lu ⁸⁹, H.J. Lubatti ¹³⁸, C. Luci ^{132a,132b}, A. Lucotte ⁵⁵, F. Luehring ⁶¹, W. Lukas ⁶², L. Luminari ^{132a}, O. Lundberg ^{146a,146b}, B. Lund-Jensen ¹⁴⁷, D. Lynn ²⁵, R. Lysak ¹²⁷, E. Lytken ⁸¹, H. Ma ²⁵, L.L. Ma ^{33d}, G. Maccarrone ⁴⁷, A. Macchiolo ¹⁰¹, C.M. Macdonald ¹³⁹, J. Machado Miguens ^{122,126b}, D. Macina ³⁰, D. Madaffari ⁸⁵, R. Madar ³⁴, H.J. Maddocks ⁷², W.F. Mader ⁴⁴, A. Madsen ¹⁶⁶, S. Maeland ¹⁴, T. Maeno ²⁵, A. Maevskiy ⁹⁹, E. Magradze ⁵⁴, K. Mahboubi ⁴⁸, J. Mahlstedt ¹⁰⁷, C. Maiani ¹³⁶, C. Maidantchik ^{24a}, A.A. Maier ¹⁰¹, T. Maier ¹⁰⁰, A. Maio ^{126a,126b,126d}, S. Majewski ¹¹⁶, Y. Makida ⁶⁶, N. Makovec ¹¹⁷, B. Malaescu ⁸⁰, Pa. Malecki ³⁹, V.P. Maleev ¹²³, F. Malek ⁵⁵, U. Mallik ⁶³, D. Malon ⁶, C. Malone ¹⁴³, S. Maltezos ¹⁰, V.M. Malyshev ¹⁰⁹, S. Malyukov ³⁰, J. Mamuzic ⁴², G. Mancini ⁴⁷, B. Mandelli ³⁰, L. Mandelli ^{91a}, I. Mandić ⁷⁵, R. Mandrysch ⁶³, J. Maneira ^{126a,126b}, A. Manfredini ¹⁰¹, L. Manhaes de Andrade Filho ^{24b}, J. Manjarres Ramos ^{159b}, A. Mann ¹⁰⁰, P.M. Manning ¹³⁷, A. Manousakis-Katsikakis ⁹, B. Mansoulie ¹³⁶, R. Mantifel ⁸⁷, M. Mantoani ⁵⁴, L. Mapelli ³⁰, L. March ^{145c},

G. Marchiori⁸⁰, M. Marcisovsky¹²⁷, C.P. Marino¹⁶⁹, M. Marjanovic¹³, F. Marroquim^{24a}, S.P. Marsden⁸⁴, Z. Marshall¹⁵, L.F. Marti¹⁷, S. Marti-Garcia¹⁶⁷, B. Martin⁹⁰, T.A. Martin¹⁷⁰, V.J. Martin⁴⁶, B. Martin dit Latour¹⁴, M. Martinez^{12,o}, S. Martin-Haugh¹³¹, V.S. Martoiu^{26a}, A.C. Martyniuk⁷⁸, M. Marx¹³⁸, F. Marzano^{132a}, A. Marzin³⁰, L. Masetti⁸³, T. Mashimo¹⁵⁵, R. Mashinistov⁹⁶, J. Masik⁸⁴, A.L. Maslennikov^{109,c}, I. Massa^{20a,20b}, L. Massa^{20a,20b}, N. Massol⁵, P. Mastrandrea¹⁴⁸, A. Mastroberardino^{37a,37b}, T. Masubuchi¹⁵⁵, P. Mättig¹⁷⁵, J. Mattmann⁸³, J. Maurer^{26a}, S.J. Maxfield⁷⁴, D.A. Maximov^{109,c}, R. Mazini¹⁵¹, S.M. Mazza^{91a,91b}, L. Mazzaferro^{133a,133b}, G. Mc Goldrick¹⁵⁸, S.P. Mc Kee⁸⁹, A. McCarn⁸⁹, R.L. McCarthy¹⁴⁸, T.G. McCarthy²⁹, N.A. McCubbin¹³¹, K.W. McFarlane^{56,*}, J.A. Mcfayden⁷⁸, G. Mchedlidze⁵⁴, S.J. McMahon¹³¹, R.A. McPherson^{169,k}, M. Medinnis⁴², S. Meehan^{145a}, S. Mehlhase¹⁰⁰, A. Mehta⁷⁴, K. Meier^{58a}, C. Meineck¹⁰⁰, B. Meirose⁴¹, B.R. Mellado Garcia^{145c}, F. Meloni¹⁷, A. Mengarelli^{20a,20b}, S. Menke¹⁰¹, E. Meoni¹⁶¹, K.M. Mercurio⁵⁷, S. Mergelmeyer²¹, P. Mermod⁴⁹, L. Merola^{104a,104b}, C. Meroni^{91a}, F.S. Merritt³¹, A. Messina^{132a,132b}, J. Metcalfe²⁵, A.S. Mete¹⁶³, C. Meyer⁸³, C. Meyer¹²², J.-P. Meyer¹³⁶, J. Meyer¹⁰⁷, R.P. Middleton¹³¹, S. Miglioranza^{164a,164c}, L. Mijović²¹, G. Mikenberg¹⁷², M. Mikestikova¹²⁷, M. Mikuž⁷⁵, M. Milesi⁸⁸, A. Milic³⁰, D.W. Miller³¹, C. Mills⁴⁶, A. Milov¹⁷², D.A. Milstead^{146a,146b}, A.A. Minaenko¹³⁰, Y. Minami¹⁵⁵, I.A. Minashvili⁶⁵, A.I. Mincer¹¹⁰, B. Mindur^{38a}, M. Mineev⁶⁵, Y. Ming¹⁷³, L.M. Mir¹², T. Mitani¹⁷¹, J. Mitrevski¹⁰⁰, V.A. Mitsou¹⁶⁷, A. Miucci⁴⁹, P.S. Miyagawa¹³⁹, J.U. Mjörnmark⁸¹, T. Moa^{146a,146b}, K. Mochizuki⁸⁵, S. Mohapatra³⁵, W. Mohr⁴⁸, S. Molander^{146a,146b}, R. Moles-Valls¹⁶⁷, K. Mönig⁴², C. Monini⁵⁵, J. Monk³⁶, E. Monnier⁸⁵, J. Montejo Berlingen¹², F. Monticelli⁷¹, S. Monzani^{132a,132b}, R.W. Moore³, N. Morange¹¹⁷, D. Moreno¹⁶², M. Moreno Llácer⁵⁴, P. Morettini^{50a}, M. Morgenstern⁴⁴, M. Morii⁵⁷, M. Morinaga¹⁵⁵, V. Morisbak¹¹⁹, S. Moritz⁸³, A.K. Morley¹⁴⁷, G. Mornacchi³⁰, J.D. Morris⁷⁶, S.S. Mortensen³⁶, A. Morton⁵³, L. Morvaj¹⁰³, M. Mosidze^{51b}, J. Moss¹¹¹, K. Motohashi¹⁵⁷, R. Mount¹⁴³, E. Mountricha²⁵, S.V. Mouraviev^{96,*}, E.J.W. Moyses⁸⁶, S. Muanza⁸⁵, R.D. Mudd¹⁸, F. Mueller¹⁰¹, J. Mueller¹²⁵, K. Mueller²¹, R.S.P. Mueller¹⁰⁰, T. Mueller²⁸, D. Muenstermann⁴⁹, P. Mullen⁵³, Y. Munwes¹⁵³, J.A. Murillo Quijada¹⁸, W.J. Murray^{170,131}, H. Musheghyan⁵⁴, E. Musto¹⁵², A.G. Myagkov^{130,ab}, M. Myska¹²⁸, O. Nackenhorst⁵⁴, J. Nadal⁵⁴, K. Nagai¹²⁰, R. Nagai¹⁵⁷, Y. Nagai⁸⁵, K. Nagano⁶⁶, A. Nagarkar¹¹¹, Y. Nagasaka⁵⁹, K. Nagata¹⁶⁰, M. Nagel¹⁰¹, E. Nagy⁸⁵, A.M. Nairz³⁰, Y. Nakahama³⁰, K. Nakamura⁶⁶, T. Nakamura¹⁵⁵, I. Nakano¹¹², H. Namasivayam⁴¹, R.F. Naranjo Garcia⁴², R. Narayan³¹, T. Naumann⁴², G. Navarro¹⁶², R. Nayyar⁷, H.A. Neal⁸⁹, P.Yu. Nechaeva⁹⁶, T.J. Neep⁸⁴, P.D. Nef¹⁴³, A. Negri^{121a,121b}, M. Negrini^{20a}, S. Nektarijevic¹⁰⁶, C. Nellist¹¹⁷, A. Nelson¹⁶³, S. Nemecek¹²⁷, P. Nemethy¹¹⁰, A.A. Nepomuceno^{24a}, M. Nessi^{30,ac}, M.S. Neubauer¹⁶⁵, M. Neumann¹⁷⁵, R.M. Neves¹¹⁰, P. Nevski²⁵, P.R. Newman¹⁸, D.H. Nguyen⁶, R.B. Nickerson¹²⁰, R. Nicolaidou¹³⁶, B. Nicquevert³⁰, J. Nielsen¹³⁷, N. Nikiforou³⁵, A. Nikiforov¹⁶, V. Nikolaenko^{130,ab}, I. Nikolic-Audit⁸⁰, K. Nikolopoulos¹⁸, J.K. Nilsen¹¹⁹, P. Nilsson²⁵, Y. Ninomiya¹⁵⁵, A. Nisati^{132a}, R. Nisius¹⁰¹, T. Nobe¹⁵⁷, M. Nomachi¹¹⁸, I. Nomidis²⁹, T. Nooney⁷⁶, S. Norberg¹¹³, M. Nordberg³⁰, O. Novgorodova⁴⁴, S. Nowak¹⁰¹, M. Nozaki⁶⁶, L. Nozka¹¹⁵, K. Ntekas¹⁰, G. Nunes Hanninger⁸⁸, T. Nunnemann¹⁰⁰, E. Nurse⁷⁸, F. Nuti⁸⁸, B.J. O'Brien⁴⁶, F. O'grady⁷, D.C. O'Neil¹⁴², V. O'Shea⁵³, F.G. Oakham^{29,d}, H. Oberlack¹⁰¹, T. Obermann²¹, J. Ocariz⁸⁰, A. Ochi⁶⁷, I. Ochoa⁷⁸, J.P. Ochoa-Ricoux^{32a}, S. Oda⁷⁰, S. Odaka⁶⁶, H. Ogren⁶¹, A. Oh⁸⁴, S.H. Oh⁴⁵, C.C. Ohm¹⁵, H. Ohman¹⁶⁶, H. Oide³⁰, W. Okamura¹¹⁸, H. Okawa¹⁶⁰, Y. Okumura³¹, T. Okuyama¹⁵⁵, A. Olariu^{26a}, S.A. Olivares Pino⁴⁶, D. Oliveira Damazio²⁵, E. Oliver Garcia¹⁶⁷, A. Olszewski³⁹, J. Olszowska³⁹, A. Onofre^{126a,126e}, P.U.E. Onyisi^{31,q}, C.J. Oram^{159a}, M.J. Oreglia³¹, Y. Oren¹⁵³, D. Orestano^{134a,134b}, N. Orlando¹⁵⁴, C. Oropeza Barrera⁵³, R.S. Orr¹⁵⁸, B. Osculati^{50a,50b}, R. Ospanov⁸⁴, G. Otero y Garzon²⁷, H. Otono⁷⁰, M. Ouchrif^{135d}, E.A. Ouellette¹⁶⁹, F. Ould-Saada¹¹⁹, A. Ouraou¹³⁶, K.P. Oussoren¹⁰⁷, Q. Ouyang^{33a}, A. Ovcharova¹⁵, M. Owen⁵³, R.E. Owen¹⁸, V.E. Ozcan^{19a}, N. Ozturk⁸, K. Pachal¹⁴², A. Pacheco Pages¹², C. Padilla Aranda¹², M. Pagáčová⁴⁸, S. Pagan Griso¹⁵, E. Paganis¹³⁹, C. Pahl¹⁰¹, F. Paige²⁵, P. Pais⁸⁶, K. Pajchel¹¹⁹, G. Palacino^{159b}, S. Palestini³⁰, M. Palka^{38b}, D. Pallin³⁴, A. Palma^{126a,126b}, Y.B. Pan¹⁷³, E. Panagiotopoulou¹⁰, C.E. Pandini⁸⁰, J.G. Panduro Vazquez⁷⁷, P. Pani^{146a,146b}, S. Panitkin²⁵, D. Pantea^{26a}, L. Paolozzi⁴⁹, Th.D. Papadopoulou¹⁰, K. Papageorgiou¹⁵⁴, A. Paramonov⁶, D. Paredes Hernandez¹⁵⁴, M.A. Parker²⁸, K.A. Parker¹³⁹, F. Parodi^{50a,50b}, J.A. Parsons³⁵, U. Parzefall⁴⁸, E. Pasqualucci^{132a}, S. Passaggio^{50a}, F. Pastore^{134a,134b,*}, Fr. Pastore⁷⁷, G. Pásztor²⁹, S. Pataria¹⁷⁵, N.D. Patel¹⁵⁰, J.R. Pater⁸⁴, T. Pauly³⁰, J. Pearce¹⁶⁹, B. Pearson¹¹³, L.E. Pedersen³⁶,

M. Pedersen¹¹⁹, S. Pedraza Lopez¹⁶⁷, R. Pedro^{126a,126b}, S.V. Peleganchuk^{109,c}, D. Pelikan¹⁶⁶, H. Peng^{33b},
 B. Penning³¹, J. Penwell⁶¹, D.V. Perepelitsa²⁵, E. Perez Codina^{159a}, M.T. Pérez García-Estañ¹⁶⁷,
 L. Perini^{91a,91b}, H. Pernegger³⁰, S. Perrella^{104a,104b}, R. Peschke⁴², V.D. Peshekhonov⁶⁵, K. Peters³⁰,
 R.F.Y. Peters⁸⁴, B.A. Petersen³⁰, T.C. Petersen³⁶, E. Petit⁴², A. Petridis^{146a,146b}, C. Petridou¹⁵⁴,
 E. Petrolo^{132a}, F. Petrucci^{134a,134b}, N.E. Pettersson¹⁵⁷, R. Pezoa^{32b}, P.W. Phillips¹³¹, G. Piacquadio¹⁴³,
 E. Pianori¹⁷⁰, A. Picazio⁴⁹, E. Piccaro⁷⁶, M. Piccinini^{20a,20b}, M.A. Pickering¹²⁰, R. Piegaia²⁷,
 D.T. Pignotti¹¹¹, J.E. Pilcher³¹, A.D. Pilkington⁸⁴, J. Pina^{126a,126b,126d}, M. Pinamonti^{164a,164c,ad},
 J.L. Pinfold³, A. Pingel³⁶, B. Pinto^{126a}, S. Pires⁸⁰, M. Pitt¹⁷², C. Pizio^{91a,91b}, L. Plazak^{144a}, M.-A. Pleier²⁵,
 V. Pleskot¹²⁹, E. Plotnikova⁶⁵, P. Plucinski^{146a,146b}, D. Pluth⁶⁴, R. Poettgen⁸³, L. Poggioli¹¹⁷, D. Pohl²¹,
 G. Polesello^{121a}, A. Policicchio^{37a,37b}, R. Polifka¹⁵⁸, A. Polini^{20a}, C.S. Pollard⁵³, V. Polychronakos²⁵,
 K. Pommès³⁰, L. Pontecorvo^{132a}, B.G. Pope⁹⁰, G.A. Popeneciu^{26b}, D.S. Popovic¹³, A. Poppleton³⁰,
 S. Pospisil¹²⁸, K. Potamianos¹⁵, I.N. Potrap⁶⁵, C.J. Potter¹⁴⁹, C.T. Potter¹¹⁶, G. Poulard³⁰, J. Poveda³⁰,
 V. Pozdnyakov⁶⁵, P. Pralavorio⁸⁵, A. Pranko¹⁵, S. Prasad³⁰, S. Prell⁶⁴, D. Price⁸⁴, L.E. Price⁶,
 M. Primavera^{73a}, S. Prince⁸⁷, M. Proissl⁴⁶, K. Prokofiev^{60c}, F. Prokoshin^{32b}, E. Protopapadaki¹³⁶,
 S. Protopopescu²⁵, J. Proudfoot⁶, M. Przybycien^{38a}, E. Ptacek¹¹⁶, D. Puddu^{134a,134b}, E. Pueschel⁸⁶,
 D. Puldon¹⁴⁸, M. Purohit^{25,ae}, P. Puzo¹¹⁷, J. Qian⁸⁹, G. Qin⁵³, Y. Qin⁸⁴, A. Quadt⁵⁴, D.R. Quarrie¹⁵,
 W.B. Quayle^{164a,164b}, M. Queitsch-Maitland⁸⁴, D. Quilty⁵³, S. Raddum¹¹⁹, V. Radeka²⁵, V. Radescu⁴²,
 S.K. Radhakrishnan¹⁴⁸, P. Radloff¹¹⁶, P. Rados⁸⁸, F. Ragusa^{91a,91b}, G. Rahal¹⁷⁸, S. Rajagopalan²⁵,
 M. Rammensee³⁰, C. Rangel-Smith¹⁶⁶, F. Rauscher¹⁰⁰, S. Rave⁸³, T. Ravenscroft⁵³, M. Raymond³⁰,
 A.L. Read¹¹⁹, N.P. Readioff⁷⁴, D.M. Rebutti^{121a,121b}, A. Redelbach¹⁷⁴, G. Redlinger²⁵, R. Reece¹³⁷,
 K. Reeves⁴¹, L. Rehnisch¹⁶, H. Reisin²⁷, M. Relich¹⁶³, C. Rembser³⁰, H. Ren^{33a}, A. Renaud¹¹⁷,
 M. Rescigno^{132a}, S. Resconi^{91a}, O.L. Rezanova^{109,c}, P. Reznicek¹²⁹, R. Rezvani⁹⁵, R. Richter¹⁰¹,
 S. Richter⁷⁸, E. Richter-Was^{38b}, O. Ricken²¹, M. Ridel⁸⁰, P. Rieck¹⁶, C.J. Riegel¹⁷⁵, J. Rieger⁵⁴,
 M. Rijssenbeek¹⁴⁸, A. Rimoldi^{121a,121b}, L. Rinaldi^{20a}, B. Ristić⁴⁹, E. Ritsch⁶², I. Riu¹², F. Rizatdinova¹¹⁴,
 E. Rizvi⁷⁶, S.H. Robertson^{87,k}, A. Robichaud-Veronneau⁸⁷, D. Robinson²⁸, J.E.M. Robinson⁸⁴,
 A. Robson⁵³, C. Roda^{124a,124b}, S. Roe³⁰, O. Røhne¹¹⁹, S. Rolli¹⁶¹, A. Romaniouk⁹⁸, M. Romano^{20a,20b},
 S.M. Romano Saez³⁴, E. Romero Adam¹⁶⁷, N. Rompotis¹³⁸, M. Ronzani⁴⁸, L. Roos⁸⁰, E. Ros¹⁶⁷,
 S. Rosati^{132a}, K. Rosbach⁴⁸, P. Rose¹³⁷, P.L. Rosendahl¹⁴, O. Rosenthal¹⁴¹, V. Rossetti^{146a,146b},
 E. Rossi^{104a,104b}, L.P. Rossi^{50a}, R. Rosten¹³⁸, M. Rotaru^{26a}, I. Roth¹⁷², J. Rothberg¹³⁸, D. Rousseau¹¹⁷,
 C.R. Royon¹³⁶, A. Rozanov⁸⁵, Y. Rozen¹⁵², X. Ruan^{145c}, F. Rubbo¹⁴³, I. Rubinskiy⁴², V.I. Rud⁹⁹,
 C. Rudolph⁴⁴, M.S. Rudolph¹⁵⁸, F. Rühr⁴⁸, A. Ruiz-Martinez³⁰, Z. Rurikova⁴⁸, N.A. Rusakovich⁶⁵,
 A. Ruschke¹⁰⁰, H.L. Russell¹³⁸, J.P. Rutherford⁷, N. Ruthmann⁴⁸, Y.F. Ryabov¹²³, M. Rybar¹²⁹,
 G. Rybkin¹¹⁷, N.C. Ryder¹²⁰, A.F. Saavedra¹⁵⁰, G. Sabato¹⁰⁷, S. Sacerdoti²⁷, A. Saddique³,
 H.F.W. Sadrozinski¹³⁷, R. Sadykov⁶⁵, F. Safai Tehrani^{132a}, M. Saimpert¹³⁶, H. Sakamoto¹⁵⁵,
 Y. Sakurai¹⁷¹, G. Salamanna^{134a,134b}, A. Salamon^{133a}, M. Saleem¹¹³, D. Salek¹⁰⁷, P.H. Sales De Bruin¹³⁸,
 D. Saliagic¹⁰¹, A. Salnikov¹⁴³, J. Salt¹⁶⁷, D. Salvatore^{37a,37b}, F. Salvatore¹⁴⁹, A. Salvucci¹⁰⁶,
 A. Salzburger³⁰, D. Sampsonidis¹⁵⁴, A. Sanchez^{104a,104b}, J. Sánchez¹⁶⁷, V. Sanchez Martinez¹⁶⁷,
 H. Sandaker¹⁴, R.L. Sandbach⁷⁶, H.G. Sander⁸³, M.P. Sanders¹⁰⁰, M. Sandhoff¹⁷⁵, C. Sandoval¹⁶²,
 R. Sandstroem¹⁰¹, D.P.C. Sankey¹³¹, M. Sannino^{50a,50b}, A. Sansoni⁴⁷, C. Santoni³⁴, R. Santonico^{133a,133b},
 H. Santos^{126a}, I. Santoyo Castillo¹⁴⁹, K. Sapp¹²⁵, A. Sapronov⁶⁵, J.G. Saraiva^{126a,126d}, B. Sarrazin²¹,
 O. Sasaki⁶⁶, Y. Sasaki¹⁵⁵, K. Sato¹⁶⁰, G. Sauvage^{5,*}, E. Sauvan⁵, G. Savage⁷⁷, P. Savard^{158,d},
 C. Sawyer¹²⁰, L. Sawyer^{79,n}, J. Saxon³¹, C. Sbarra^{20a}, A. Sbrizzi^{20a,20b}, T. Scanlon⁷⁸, D.A. Scannicchio¹⁶³,
 M. Scarcella¹⁵⁰, V. Scarfone^{37a,37b}, J. Schaarschmidt¹⁷², P. Schacht¹⁰¹, D. Schaefer³⁰, R. Schaefer⁴²,
 J. Schaeffer⁸³, S. Schaepe²¹, S. Schaetzel^{58b}, U. Schäfer⁸³, A.C. Schaffer¹¹⁷, D. Schaile¹⁰⁰,
 R.D. Schamberger¹⁴⁸, V. Scharf^{58a}, V.A. Schegelsky¹²³, D. Scheirich¹²⁹, M. Schernau¹⁶³, C. Schiavi^{50a,50b},
 C. Schillo⁴⁸, M. Schioppa^{37a,37b}, S. Schlenker³⁰, E. Schmidt⁴⁸, K. Schmieden³⁰, C. Schmitt⁸³,
 S. Schmitt^{58b}, S. Schmitt⁴², B. Schneider^{159a}, Y.J. Schnellbach⁷⁴, U. Schnoor⁴⁴, L. Schoeffel¹³⁶,
 A. Schoening^{58b}, B.D. Schoenrock⁹⁰, E. Schopf²¹, A.L.S. Schorlemmer⁵⁴, M. Schott⁸³, D. Schouten^{159a},
 J. Schovancova⁸, S. Schramm¹⁵⁸, M. Schreyer¹⁷⁴, C. Schroeder⁸³, N. Schuh⁸³, M.J. Schultens²¹,
 H.-C. Schultz-Coulon^{58a}, H. Schulz¹⁶, M. Schumacher⁴⁸, B.A. Schumm¹³⁷, Ph. Schune¹³⁶,
 C. Schwanenberger⁸⁴, A. Schwartzman¹⁴³, T.A. Schwarz⁸⁹, Ph. Schwegler¹⁰¹, Ph. Schwemling¹³⁶,
 R. Schwienhorst⁹⁰, J. Schwindling¹³⁶, T. Schwindt²¹, M. Schwoerer⁵, F.G. Sciacca¹⁷, E. Scifo¹¹⁷,

G. Sciolla²³, F. Scuri^{124a,124b}, F. Scutti²¹, J. Searcy⁸⁹, G. Sedov⁴², E. Sedykh¹²³, P. Seema²¹, S.C. Seidel¹⁰⁵, A. Seiden¹³⁷, F. Seifert¹²⁸, J.M. Seixas^{24a}, G. Sekhniaidze^{104a}, K. Sekhon⁸⁹, S.J. Sekula⁴⁰, K.E. Selbach⁴⁶, D.M. Seliverstov^{123,*}, N. Semprini-Cesari^{20a,20b}, C. Serfon³⁰, L. Serin¹¹⁷, L. Serkin^{164a,164b}, T. Serre⁸⁵, M. Sessa^{134a,134b}, R. Seuster^{159a}, H. Severini¹¹³, T. Sfiligoi⁷⁵, F. Sforza¹⁰¹, A. Sfyrla³⁰, E. Shabalina⁵⁴, M. Shamim¹¹⁶, L.Y. Shan^{33a}, R. Shang¹⁶⁵, J.T. Shank²², M. Shapiro¹⁵, P.B. Shatalov⁹⁷, K. Shaw^{164a,164b}, S.M. Shaw⁸⁴, A. Shcherbakova^{146a,146b}, C.Y. Shehu¹⁴⁹, P. Sherwood⁷⁸, L. Shi^{151.af}, S. Shimizu⁶⁷, C.O. Shimmin¹⁶³, M. Shimojima¹⁰², M. Shiyakova⁶⁵, A. Shmeleva⁹⁶, D. Shoaleh Saadi⁹⁵, M.J. Shochet³¹, S. Shojaii^{91a,91b}, S. Shrestha¹¹¹, E. Shulga⁹⁸, M.A. Shupe⁷, S. Shushkevich⁴², P. Sicho¹²⁷, O. Sidiropoulou¹⁷⁴, D. Sidorov¹¹⁴, A. Sidoti^{20a,20b}, F. Siegert⁴⁴, Dj. Sijacki¹³, J. Silva^{126a,126d}, Y. Silver¹⁵³, S.B. Silverstein^{146a}, V. Simak¹²⁸, O. Simard⁵, Lj. Simic¹³, S. Simion¹¹⁷, E. Simioni⁸³, B. Simmons⁷⁸, D. Simon³⁴, R. Simoniello^{91a,91b}, P. Sinervo¹⁵⁸, N.B. Sinev¹¹⁶, G. Siragusa¹⁷⁴, A.N. Sisakyan^{65,*}, S.Yu. Sivoklov⁹⁹, J. Sjölín^{146a,146b}, T.B. Sjurson¹⁴, M.B. Skinner⁷², H.P. Skottowe⁵⁷, P. Skubic¹¹³, M. Slater¹⁸, T. Slavicek¹²⁸, M. Slawinska¹⁰⁷, K. Sliwa¹⁶¹, V. Smakhtin¹⁷², B.H. Smart⁴⁶, L. Smestad¹⁴, S.Yu. Smirnov⁹⁸, Y. Smirnov⁹⁸, L.N. Smirnova^{99.ag}, O. Smirnova⁸¹, M.N.K. Smith³⁵, R.W. Smith³⁵, M. Smizanska⁷², K. Smolek¹²⁸, A.A. Snesarev⁹⁶, G. Snidero⁷⁶, S. Snyder²⁵, R. Sobie^{169.k}, F. Socher⁴⁴, A. Soffer¹⁵³, D.A. Soh^{151.af}, C.A. Solans³⁰, M. Solar¹²⁸, J. Solc¹²⁸, E.Yu. Soldatov⁹⁸, U. Soldevila¹⁶⁷, A.A. Solodkov¹³⁰, A. Soloshenko⁶⁵, O.V. Solovyanov¹³⁰, V. Solovyev¹²³, P. Sommer⁴⁸, H.Y. Song^{33b}, N. Soni¹, A. Sood¹⁵, A. Sopczak¹²⁸, B. Sopko¹²⁸, V. Sopko¹²⁸, V. Sorin¹², D. Sosa^{58b}, M. Sosebee⁸, C.L. Sotiropoulou^{124a,124b}, R. Soualah^{164a,164c}, P. Soueid⁹⁵, A.M. Soukharev^{109.c}, D. South⁴², B.C. Sowden⁷⁷, S. Spagnolo^{73a,73b}, M. Spalla^{124a,124b}, F. Spanò⁷⁷, W.R. Spearman⁵⁷, F. Spettel¹⁰¹, R. Spighi^{20a}, G. Spigo³⁰, L.A. Spiller⁸⁸, M. Spousta¹²⁹, T. Spreitzer¹⁵⁸, R.D. St. Denis^{53,*}, S. Staerz⁴⁴, J. Stahlman¹²², R. Stamen^{58a}, S. Stamm¹⁶, E. Stanecka³⁹, C. Stanescu^{134a}, M. Stanescu-Bellu⁴², M.M. Stanitzki⁴², S. Stapnes¹¹⁹, E.A. Starchenko¹³⁰, J. Stark⁵⁵, P. Staroba¹²⁷, P. Starovoitov⁴², R. Staszewski³⁹, P. Stavina^{144a,*}, P. Steinberg²⁵, B. Stelzer¹⁴², H.J. Stelzer³⁰, O. Stelzer-Chilton^{159a}, H. Stenzel⁵², S. Stern¹⁰¹, G.A. Stewart⁵³, J.A. Stillings²¹, M.C. Stockton⁸⁷, M. Stoebe⁸⁷, G. Stoicea^{26a}, P. Stolte⁵⁴, S. Stonjek¹⁰¹, A.R. Stradling⁸, A. Straessner⁴⁴, M.E. Stramaglia¹⁷, J. Strandberg¹⁴⁷, S. Strandberg^{146a,146b}, A. Strandlie¹¹⁹, E. Strauss¹⁴³, M. Strauss¹¹³, P. Strizeneč^{144b}, R. Ströhmer¹⁷⁴, D.M. Strom¹¹⁶, R. Stroynowski⁴⁰, A. Strubig¹⁰⁶, S.A. Stucci¹⁷, B. Stugu¹⁴, N.A. Styles⁴², D. Su¹⁴³, J. Su¹²⁵, R. Subramaniam⁷⁹, A. Succurro¹², Y. Sugaya¹¹⁸, C. Suhr¹⁰⁸, M. Suk¹²⁸, V.V. Sulín⁹⁶, S. Sultansoy^{4d}, T. Sumida⁶⁸, S. Sun⁵⁷, X. Sun^{33a}, J.E. Sundermann⁴⁸, K. Suruliz¹⁴⁹, G. Susinno^{37a,37b}, M.R. Sutton¹⁴⁹, S. Suzuki⁶⁶, Y. Suzuki⁶⁶, M. Svatos¹²⁷, S. Swedish¹⁶⁸, M. Swiatlowski¹⁴³, I. Sykora^{144a}, T. Sykora¹²⁹, D. Ta⁹⁰, C. Taccini^{134a,134b}, K. Tackmann⁴², J. Taenzer¹⁵⁸, A. Taffard¹⁶³, R. Tafirout^{159a}, N. Taiblum¹⁵³, H. Takai²⁵, R. Takashima⁶⁹, H. Takeda⁶⁷, T. Takeshita¹⁴⁰, Y. Takubo⁶⁶, M. Talby⁸⁵, A.A. Talyshev^{109.c}, J.Y.C. Tam¹⁷⁴, K.G. Tan⁸⁸, J. Tanaka¹⁵⁵, R. Tanaka¹¹⁷, S. Tanaka⁶⁶, B.B. Tannenwald¹¹¹, N. Tannoury²¹, S. Tapprogge⁸³, S. Tarem¹⁵², F. Tarrade²⁹, G.F. Tartarelli^{91a}, P. Tas¹²⁹, M. Tasevsky¹²⁷, T. Tashiro⁶⁸, E. Tassi^{37a,37b}, A. Tavares Delgado^{126a,126b}, Y. Tayalati^{135d}, F.E. Taylor⁹⁴, G.N. Taylor⁸⁸, W. Taylor^{159b}, F.A. Teischinger³⁰, M. Teixeira Dias Castanheira⁷⁶, P. Teixeira-Dias⁷⁷, K.K. Temming⁴⁸, H. Ten Kate³⁰, P.K. Teng¹⁵¹, J.J. Teoh¹¹⁸, F. Tepel¹⁷⁵, S. Terada⁶⁶, K. Terashi¹⁵⁵, J. Terron⁸², S. Terzo¹⁰¹, M. Testa⁴⁷, R.J. Teuscher^{158.k}, J. Therhaag²¹, T. Theveneaux-Pelzer³⁴, J.P. Thomas¹⁸, J. Thomas-Wilsker⁷⁷, E.N. Thompson³⁵, P.D. Thompson¹⁸, R.J. Thompson⁸⁴, A.S. Thompson⁵³, L.A. Thomsen¹⁷⁶, E. Thomson¹²², M. Thomson²⁸, R.P. Thun^{89,*}, M.J. Tibbetts¹⁵, R.E. Ticse Torres⁸⁵, V.O. Tikhomirov^{96.ah}, Yu.A. Tikhonov^{109.c}, S. Timoshenko⁹⁸, E. Tiouchichine⁸⁵, P. Tipton¹⁷⁶, S. Tisserant⁸⁵, T. Todorov^{5,*}, S. Todorova-Nova¹²⁹, J. Tojo⁷⁰, S. Tokár^{144a}, K. Tokushuku⁶⁶, K. Tollefson⁹⁰, E. Tolley⁵⁷, L. Tomlinson⁸⁴, M. Tomoto¹⁰³, L. Tompkins^{143.ai}, K. Toms¹⁰⁵, E. Torrence¹¹⁶, H. Torres¹⁴², E. Torrón Pastor¹⁶⁷, J. Toth^{85.aj}, F. Touchard⁸⁵, D.R. Tovey¹³⁹, T. Trefzger¹⁷⁴, L. Tremblet³⁰, A. Tricoli³⁰, I.M. Trigger^{159a}, S. Trincaz-Duvoid⁸⁰, M.F. Tripiana¹², W. Trischuk¹⁵⁸, B. Trocme⁵⁵, C. Troncon^{91a}, M. Trotter-McDonald¹⁵, M. Trovatelli^{134a,134b}, P. True⁹⁰, L. Truong^{164a,164c}, M. Trzebinski³⁹, A. Trzupek³⁹, C. Tsarouchas³⁰, J.C.-L. Tseng¹²⁰, P.V. Tsiarehka⁹², D. Tsionou¹⁵⁴, G. Tsipolitis¹⁰, N. Tsirintanis⁹, S. Tsiskaridze¹², V. Tsiskaridze⁴⁸, E.G. Tskhadadze^{51a}, I.I. Tsukerman⁹⁷, V. Tsulaia¹⁵, S. Tsuno⁶⁶, D. Tsybychev¹⁴⁸, A. Tudorache^{26a}, V. Tudorache^{26a}, A.N. Tuna¹²², S.A. Tupputi^{20a,20b}, S. Turchikhin^{99.ag}, D. Turecek¹²⁸, R. Turra^{91a,91b}, A.J. Turvey⁴⁰, P.M. Tuts³⁵, A. Tykhonov⁴⁹, M. Tylmad^{146a,146b}, M. Tyndel¹³¹, I. Ueda¹⁵⁵, R. Ueno²⁹, M. Ughetto^{146a,146b},

M. Uglund¹⁴, M. Uhlenbrock²¹, F. Ukegawa¹⁶⁰, G. Unal³⁰, A. Undrus²⁵, G. Unel¹⁶³, F.C. Ungaro⁴⁸, Y. Unno⁶⁶, C. Unverdorben¹⁰⁰, J. Urban^{144b}, P. Urquijo⁸⁸, P. Urrejola⁸³, G. Usai⁸, A. Usanova⁶², L. Vacavant⁸⁵, V. Vacek¹²⁸, B. Vachon⁸⁷, C. Valderanis⁸³, N. Valencic¹⁰⁷, S. Valentineti^{20a,20b}, A. Valero¹⁶⁷, L. Valery¹², S. Valkar¹²⁹, E. Valladolid Gallego¹⁶⁷, S. Vallecorsa⁴⁹, J.A. Valls Ferrer¹⁶⁷, W. Van Den Wollenberg¹⁰⁷, P.C. Van Der Deijl¹⁰⁷, R. van der Geer¹⁰⁷, H. van der Graaf¹⁰⁷, R. Van Der Leeuw¹⁰⁷, N. van Eldik¹⁵², P. van Gemmeren⁶, J. Van Nieuwkoop¹⁴², I. van Vulpen¹⁰⁷, M.C. van Woerden³⁰, M. Vanadia^{132a,132b}, W. Vandelli³⁰, R. Vanguri¹²², A. Vaniachine⁶, F. Vannucci⁸⁰, G. Vardanyan¹⁷⁷, R. Vari^{132a}, E.W. Varnes⁷, T. Varol⁴⁰, D. Varouchas⁸⁰, A. Vartapetian⁸, K.E. Varvell¹⁵⁰, F. Vazeille³⁴, T. Vazquez Schroeder⁸⁷, J. Veatch⁷, L.M. Veloce¹⁵⁸, F. Veloso^{126a,126c}, T. Velz²¹, S. Veneziano^{132a}, A. Ventura^{73a,73b}, D. Ventura⁸⁶, M. Venturi¹⁶⁹, N. Venturi¹⁵⁸, A. Venturini²³, V. Vercesi^{121a}, M. Verducci^{132a,132b}, W. Verkerke¹⁰⁷, J.C. Vermeulen¹⁰⁷, A. Vest⁴⁴, M.C. Vetterli^{142,d}, O. Viazlo⁸¹, I. Vichou¹⁶⁵, T. Vickey¹³⁹, O.E. Vickey Boeriu¹³⁹, G.H.A. Viehhauser¹²⁰, S. Viel¹⁵, R. Vigne³⁰, M. Villa^{20a,20b}, M. Villaplana Perez^{91a,91b}, E. Vilucchi⁴⁷, M.G. Vincter²⁹, V.B. Vinogradov⁶⁵, I. Vivarelli¹⁴⁹, F. Vives Vaque³, S. Vlachos¹⁰, D. Vladoiu¹⁰⁰, M. Vlasak¹²⁸, M. Vogel^{32a}, P. Vokac¹²⁸, G. Volpi^{124a,124b}, M. Volpi⁸⁸, H. von der Schmitt¹⁰¹, H. von Radziewski⁴⁸, E. von Toerne²¹, V. Vorobel¹²⁹, K. Vorobev⁹⁸, M. Vos¹⁶⁷, R. Voss³⁰, J.H. Vosseveld⁷⁴, N. Vranjes¹³, M. Vranjes Milosavljevic¹³, V. Vrba¹²⁷, M. Vreeswijk¹⁰⁷, R. Vuillermet³⁰, I. Vukotic³¹, Z. Vykydal¹²⁸, P. Wagner²¹, W. Wagner¹⁷⁵, H. Wahlberg⁷¹, S. Wahrmund⁴⁴, J. Wakabayashi¹⁰³, J. Walder⁷², R. Walker¹⁰⁰, W. Walkowiak¹⁴¹, C. Wang^{33c}, F. Wang¹⁷³, H. Wang¹⁵, H. Wang⁴⁰, J. Wang⁴², J. Wang^{33a}, K. Wang⁸⁷, R. Wang⁶, S.M. Wang¹⁵¹, T. Wang²¹, X. Wang¹⁷⁶, C. Wanotayaroj¹¹⁶, A. Warburton⁸⁷, C.P. Ward²⁸, D.R. Wardrope⁷⁸, M. Warsinsky⁴⁸, A. Washbrook⁴⁶, C. Wasicki⁴², P.M. Watkins¹⁸, A.T. Watson¹⁸, I.J. Watson¹⁵⁰, M.F. Watson¹⁸, G. Watts¹³⁸, S. Watts⁸⁴, B.M. Waugh⁷⁸, S. Webb⁸⁴, M.S. Weber¹⁷, S.W. Weber¹⁷⁴, J.S. Webster³¹, A.R. Weidberg¹²⁰, B. Weinert⁶¹, J. Weingarten⁵⁴, C. Weiser⁴⁸, H. Weits¹⁰⁷, P.S. Wells³⁰, T. Wenaus²⁵, T. Wengler³⁰, S. Wenig³⁰, N. Wermes²¹, M. Werner⁴⁸, P. Werner³⁰, M. Wessels^{58a}, J. Wetter¹⁶¹, K. Whalen²⁹, A.M. Wharton⁷², A. White⁸, M.J. White¹, R. White^{32b}, S. White^{124a,124b}, D. Whiteson¹⁶³, F.J. Wickens¹³¹, W. Wiedenmann¹⁷³, M. Wielers¹³¹, P. Wienemann²¹, C. Wiglesworth³⁶, L.A.M. Wiik-Fuchs²¹, A. Wildauer¹⁰¹, H.G. Wilkens³⁰, H.H. Williams¹²², S. Williams¹⁰⁷, C. Willis⁹⁰, S. Willocq⁸⁶, A. Wilson⁸⁹, J.A. Wilson¹⁸, I. Wingerter-Seez⁵, F. Winklmeier¹¹⁶, B.T. Winter²¹, M. Wittgen¹⁴³, J. Wittkowski¹⁰⁰, S.J. Wollstadt⁸³, M.W. Wolter³⁹, H. Wolters^{126a,126c}, B.K. Wosiek³⁹, J. Wotschack³⁰, M.J. Woudstra⁸⁴, K.W. Wozniak³⁹, M. Wu⁵⁵, M. Wu³¹, S.L. Wu¹⁷³, X. Wu⁴⁹, Y. Wu⁸⁹, T.R. Wyatt⁸⁴, B.M. Wynne⁴⁶, S. Xella³⁶, D. Xu^{33a}, L. Xu^{33b,ak}, B. Yabsley¹⁵⁰, S. Yacoob^{145b,al}, R. Yakabe⁶⁷, M. Yamada⁶⁶, Y. Yamaguchi¹¹⁸, A. Yamamoto⁶⁶, S. Yamamoto¹⁵⁵, T. Yamanaka¹⁵⁵, K. Yamauchi¹⁰³, Y. Yamazaki⁶⁷, Z. Yan²², H. Yang^{33e}, H. Yang¹⁷³, Y. Yang¹⁵¹, L. Yao^{33a}, W-M. Yao¹⁵, Y. Yasu⁶⁶, E. Yatsenko⁵, K.H. Yau Wong²¹, J. Ye⁴⁰, S. Ye²⁵, I. Yeletsikh⁶⁵, A.L. Yen⁵⁷, E. Yildirim⁴², K. Yorita¹⁷¹, R. Yoshida⁶, K. Yoshihara¹²², C. Young¹⁴³, C.J.S. Young³⁰, S. Youssef²², D.R. Yu¹⁵, J. Yu⁸, J.M. Yu⁸⁹, J. Yu¹¹⁴, L. Yuan⁶⁷, A. Yurkewicz¹⁰⁸, I. Yusuff^{28,am}, B. Zabinski³⁹, R. Zaidan⁶³, A.M. Zaitsev^{130,ab}, J. Zalieckas¹⁴, A. Zaman¹⁴⁸, S. Zambito⁵⁷, L. Zanello^{132a,132b}, D. Zanzi⁸⁸, C. Zeitnitz¹⁷⁵, M. Zeman¹²⁸, A. Zemla^{38a}, K. Zengel²³, O. Zenin¹³⁰, T. Ženiš^{144a}, D. Zerwas¹¹⁷, D. Zhang⁸⁹, F. Zhang¹⁷³, J. Zhang⁶, L. Zhang⁴⁸, R. Zhang^{33b}, X. Zhang^{33d}, Z. Zhang¹¹⁷, X. Zhao⁴⁰, Y. Zhao^{33d,117}, Z. Zhao^{33b}, A. Zhemchugov⁶⁵, J. Zhong¹²⁰, B. Zhou⁸⁹, C. Zhou⁴⁵, L. Zhou³⁵, L. Zhou⁴⁰, N. Zhou¹⁶³, C.G. Zhu^{33d}, H. Zhu^{33a}, J. Zhu⁸⁹, Y. Zhu^{33b}, X. Zhuang^{33a}, K. Zhukov⁹⁶, A. Zibell¹⁷⁴, D. Zieminska⁶¹, N.I. Zimine⁶⁵, C. Zimmermann⁸³, S. Zimmermann⁴⁸, Z. Zinonos⁵⁴, M. Zinser⁸³, M. Ziolkowski¹⁴¹, L. Živković¹³, G. Zobernig¹⁷³, A. Zoccoli^{20a,20b}, M. zur Nedden¹⁶, G. Zurzolo^{104a,104b}, L. Zwalinski³⁰

¹ Department of Physics, University of Adelaide, Adelaide, Australia

² Physics Department, SUNY Albany, Albany, NY, United States

³ Department of Physics, University of Alberta, Edmonton, AB, Canada

⁴ (a) Department of Physics, Ankara University, Ankara; (c) Istanbul Aydin University, Istanbul; (d) Division of Physics, TOBB University of Economics and Technology, Ankara, Turkey

⁵ LAPP, CNRS/IN2P3 and Université Savoie Mont Blanc, Annecy-le-Vieux, France

⁶ High Energy Physics Division, Argonne National Laboratory, Argonne, IL, United States

⁷ Department of Physics, University of Arizona, Tucson, AZ, United States

⁸ Department of Physics, The University of Texas at Arlington, Arlington, TX, United States

⁹ Physics Department, University of Athens, Athens, Greece

¹⁰ Physics Department, National Technical University of Athens, Zografou, Greece

¹¹ Institute of Physics, Azerbaijan Academy of Sciences, Baku, Azerbaijan

¹² Institut de Física d'Altes Energies and Departament de Física de la Universitat Autònoma de Barcelona, Barcelona, Spain

- ¹³ Institute of Physics, University of Belgrade, Belgrade, Serbia
- ¹⁴ Department for Physics and Technology, University of Bergen, Bergen, Norway
- ¹⁵ Physics Division, Lawrence Berkeley National Laboratory and University of California, Berkeley, CA, United States
- ¹⁶ Department of Physics, Humboldt University, Berlin, Germany
- ¹⁷ Albert Einstein Center for Fundamental Physics and Laboratory for High Energy Physics, University of Bern, Bern, Switzerland
- ¹⁸ School of Physics and Astronomy, University of Birmingham, Birmingham, United Kingdom
- ¹⁹ ^(a) Department of Physics, Bogazici University, Istanbul; ^(b) Department of Physics, Dogus University, Istanbul; ^(c) Department of Physics Engineering, Gaziantep University, Gaziantep, Turkey
- ²⁰ ^(a) INFN Sezione di Bologna; ^(b) Dipartimento di Fisica e Astronomia, Università di Bologna, Bologna, Italy
- ²¹ Physikalisches Institut, University of Bonn, Bonn, Germany
- ²² Department of Physics, Boston University, Boston, MA, United States
- ²³ Department of Physics, Brandeis University, Waltham, MA, United States
- ²⁴ ^(a) Universidade Federal do Rio De Janeiro COPPE/EE/IF, Rio de Janeiro; ^(b) Electrical Circuits Department, Federal University of Juiz de Fora (UFJF), Juiz de Fora; ^(c) Federal University of Sao Joao del Rei (UFSJ), Sao Joao del Rei; ^(d) Instituto de Fisica, Universidade de Sao Paulo, Sao Paulo, Brazil
- ²⁵ Physics Department, Brookhaven National Laboratory, Upton, NY, United States
- ²⁶ ^(a) National Institute of Physics and Nuclear Engineering, Bucharest; ^(b) National Institute for Research and Development of Isotopic and Molecular Technologies, Physics Department, Cluj Napoca; ^(c) University Politehnica Bucharest, Bucharest; ^(d) West University in Timisoara, Timisoara, Romania
- ²⁷ Departamento de Física, Universidad de Buenos Aires, Buenos Aires, Argentina
- ²⁸ Cavendish Laboratory, University of Cambridge, Cambridge, United Kingdom
- ²⁹ Department of Physics, Carleton University, Ottawa, ON, Canada
- ³⁰ CERN, Geneva, Switzerland
- ³¹ Enrico Fermi Institute, University of Chicago, Chicago, IL, United States
- ³² ^(a) Departamento de Física, Pontificia Universidad Católica de Chile, Santiago; ^(b) Departamento de Física, Universidad Técnica Federico Santa María, Valparaíso, Chile
- ³³ ^(a) Institute of High Energy Physics, Chinese Academy of Sciences, Beijing; ^(b) Department of Modern Physics, University of Science and Technology of China, Anhui; ^(c) Department of Physics, Nanjing University, Jiangsu; ^(d) School of Physics, Shandong University, Shandong; ^(e) Department of Physics and Astronomy, Shanghai Key Laboratory for Particle Physics and Cosmology, Shanghai Jiao Tong University, Shanghai; ^(f) Physics Department, Tsinghua University, Beijing 100084, China
- ³⁴ Laboratoire de Physique Corpusculaire, Clermont Université and Université Blaise Pascal and CNRS/IN2P3, Clermont-Ferrand, France
- ³⁵ Nevis Laboratory, Columbia University, Irvington, NY, United States
- ³⁶ Niels Bohr Institute, University of Copenhagen, Copenhagen, Denmark
- ³⁷ ^(a) INFN Gruppo Collegato di Cosenza, Laboratori Nazionali di Frascati; ^(b) Dipartimento di Fisica, Università della Calabria, Rende, Italy
- ³⁸ ^(a) AGH University of Science and Technology, Faculty of Physics and Applied Computer Science, Krakow; ^(b) Marian Smoluchowski Institute of Physics, Jagiellonian University, Krakow, Poland
- ³⁹ Institute of Nuclear Physics Polish Academy of Sciences, Krakow, Poland
- ⁴⁰ Physics Department, Southern Methodist University, Dallas, TX, United States
- ⁴¹ Physics Department, University of Texas at Dallas, Richardson, TX, United States
- ⁴² DESY, Hamburg and Zeuthen, Germany
- ⁴³ Institut für Experimentelle Physik IV, Technische Universität Dortmund, Dortmund, Germany
- ⁴⁴ Institut für Kern- und Teilchenphysik, Technische Universität Dresden, Dresden, Germany
- ⁴⁵ Department of Physics, Duke University, Durham, NC, United States
- ⁴⁶ SUPA – School of Physics and Astronomy, University of Edinburgh, Edinburgh, United Kingdom
- ⁴⁷ INFN Laboratori Nazionali di Frascati, Frascati, Italy
- ⁴⁸ Fakultät für Mathematik und Physik, Albert-Ludwigs-Universität, Freiburg, Germany
- ⁴⁹ Section de Physique, Université de Genève, Geneva, Switzerland
- ⁵⁰ ^(a) INFN Sezione di Genova; ^(b) Dipartimento di Fisica, Università di Genova, Genova, Italy
- ⁵¹ ^(a) E. Andronikashvili Institute of Physics, Iv. Javakishvili Tbilisi State University, Tbilisi; ^(b) High Energy Physics Institute, Tbilisi State University, Tbilisi, Georgia
- ⁵² II Physikalisches Institut, Justus-Liebig-Universität Giessen, Giessen, Germany
- ⁵³ SUPA – School of Physics and Astronomy, University of Glasgow, Glasgow, United Kingdom
- ⁵⁴ II Physikalisches Institut, Georg-August-Universität, Göttingen, Germany
- ⁵⁵ Laboratoire de Physique Subatomique et de Cosmologie, Université Grenoble-Alpes, CNRS/IN2P3, Grenoble, France
- ⁵⁶ Department of Physics, Hampton University, Hampton, VA, United States
- ⁵⁷ Laboratory for Particle Physics and Cosmology, Harvard University, Cambridge, MA, United States
- ⁵⁸ ^(a) Kirchhoff-Institut für Physik, Ruprecht-Karls-Universität Heidelberg, Heidelberg; ^(b) Physikalisches Institut, Ruprecht-Karls-Universität Heidelberg, Heidelberg; ^(c) ZITI Institut für technische Informatik, Ruprecht-Karls-Universität Heidelberg, Mannheim, Germany
- ⁵⁹ Faculty of Applied Information Science, Hiroshima Institute of Technology, Hiroshima, Japan
- ⁶⁰ ^(a) Department of Physics, The Chinese University of Hong Kong, Shatin, N.T., Hong Kong; ^(b) Department of Physics, The University of Hong Kong, Hong Kong; ^(c) Department of Physics, The Hong Kong University of Science and Technology, Clear Water Bay, Kowloon, Hong Kong, China
- ⁶¹ Department of Physics, Indiana University, Bloomington, IN, United States
- ⁶² Institut für Astro- und Teilchenphysik, Leopold-Franzens-Universität, Innsbruck, Austria
- ⁶³ University of Iowa, Iowa City, IA, United States
- ⁶⁴ Department of Physics and Astronomy, Iowa State University, Ames, IA, United States
- ⁶⁵ Joint Institute for Nuclear Research, JINR Dubna, Dubna, Russia
- ⁶⁶ KEK, High Energy Accelerator Research Organization, Tsukuba, Japan
- ⁶⁷ Graduate School of Science, Kobe University, Kobe, Japan
- ⁶⁸ Faculty of Science, Kyoto University, Kyoto, Japan
- ⁶⁹ Kyoto University of Education, Kyoto, Japan
- ⁷⁰ Department of Physics, Kyushu University, Fukuoka, Japan
- ⁷¹ Instituto de Física La Plata, Universidad Nacional de La Plata and CONICET, La Plata, Argentina
- ⁷² Physics Department, Lancaster University, Lancaster, United Kingdom
- ⁷³ ^(a) INFN Sezione di Lecce; ^(b) Dipartimento di Matematica e Fisica, Università del Salento, Lecce, Italy
- ⁷⁴ Oliver Lodge Laboratory, University of Liverpool, Liverpool, United Kingdom
- ⁷⁵ Department of Physics, Jožef Stefan Institute and University of Ljubljana, Ljubljana, Slovenia
- ⁷⁶ School of Physics and Astronomy, Queen Mary University of London, London, United Kingdom
- ⁷⁷ Department of Physics, Royal Holloway University of London, Surrey, United Kingdom
- ⁷⁸ Department of Physics and Astronomy, University College London, London, United Kingdom
- ⁷⁹ Louisiana Tech University, Ruston, LA, United States
- ⁸⁰ Laboratoire de Physique Nucléaire et de Hautes Energies, UPMC and Université Paris-Diderot and CNRS/IN2P3, Paris, France
- ⁸¹ Fysiska institutionen, Lunds universitet, Lund, Sweden
- ⁸² Departamento de Física Teórica C-15, Universidad Autonoma de Madrid, Madrid, Spain
- ⁸³ Institut für Physik, Universität Mainz, Mainz, Germany

- ⁸⁴ School of Physics and Astronomy, University of Manchester, Manchester, United Kingdom
- ⁸⁵ CPPM, Aix-Marseille Université and CNRS/IN2P3, Marseille, France
- ⁸⁶ Department of Physics, University of Massachusetts, Amherst, MA, United States
- ⁸⁷ Department of Physics, McGill University, Montreal, QC, Canada
- ⁸⁸ School of Physics, University of Melbourne, Victoria, Australia
- ⁸⁹ Department of Physics, The University of Michigan, Ann Arbor, MI, United States
- ⁹⁰ Department of Physics and Astronomy, Michigan State University, East Lansing, MI, United States
- ⁹¹ ^(a) INFN Sezione di Milano; ^(b) Dipartimento di Fisica, Università di Milano, Milano, Italy
- ⁹² B.I. Stepanov Institute of Physics, National Academy of Sciences of Belarus, Minsk, Belarus
- ⁹³ National Scientific and Educational Centre for Particle and High Energy Physics, Minsk, Belarus
- ⁹⁴ Department of Physics, Massachusetts Institute of Technology, Cambridge, MA, United States
- ⁹⁵ Group of Particle Physics, University of Montreal, Montreal, QC, Canada
- ⁹⁶ P.N. Lebedev Institute of Physics, Academy of Sciences, Moscow, Russia
- ⁹⁷ Institute for Theoretical and Experimental Physics (ITEP), Moscow, Russia
- ⁹⁸ National Research Nuclear University MEPhI, Moscow, Russia
- ⁹⁹ D.V. Skobel'syn Institute of Nuclear Physics, M.V. Lomonosov Moscow State University, Moscow, Russia
- ¹⁰⁰ Fakultät für Physik, Ludwig-Maximilians-Universität München, München, Germany
- ¹⁰¹ Max-Planck-Institut für Physik (Werner-Heisenberg-Institut), München, Germany
- ¹⁰² Nagasaki Institute of Applied Science, Nagasaki, Japan
- ¹⁰³ Graduate School of Science and Kobayashi-Maskawa Institute, Nagoya University, Nagoya, Japan
- ¹⁰⁴ ^(a) INFN Sezione di Napoli; ^(b) Dipartimento di Fisica, Università di Napoli, Napoli, Italy
- ¹⁰⁵ Department of Physics and Astronomy, University of New Mexico, Albuquerque, NM, United States
- ¹⁰⁶ Institute for Mathematics, Astrophysics and Particle Physics, Radboud University Nijmegen/Nikhef, Nijmegen, Netherlands
- ¹⁰⁷ Nikhef National Institute for Subatomic Physics and University of Amsterdam, Amsterdam, Netherlands
- ¹⁰⁸ Department of Physics, Northern Illinois University, DeKalb, IL, United States
- ¹⁰⁹ Budker Institute of Nuclear Physics, SB RAS, Novosibirsk, Russia
- ¹¹⁰ Department of Physics, New York University, New York, NY, United States
- ¹¹¹ Ohio State University, Columbus, OH, United States
- ¹¹² Faculty of Science, Okayama University, Okayama, Japan
- ¹¹³ Homer L. Dodge Department of Physics and Astronomy, University of Oklahoma, Norman, OK, United States
- ¹¹⁴ Department of Physics, Oklahoma State University, Stillwater, OK, United States
- ¹¹⁵ Palacký University, RCPTM, Olomouc, Czech Republic
- ¹¹⁶ Center for High Energy Physics, University of Oregon, Eugene, OR, United States
- ¹¹⁷ LAL, Université Paris-Sud and CNRS/IN2P3, Orsay, France
- ¹¹⁸ Graduate School of Science, Osaka University, Osaka, Japan
- ¹¹⁹ Department of Physics, University of Oslo, Oslo, Norway
- ¹²⁰ Department of Physics, Oxford University, Oxford, United Kingdom
- ¹²¹ ^(a) INFN Sezione di Pavia; ^(b) Dipartimento di Fisica, Università di Pavia, Pavia, Italy
- ¹²² Department of Physics, University of Pennsylvania, Philadelphia, PA, United States
- ¹²³ National Research Centre "Kurchatov Institute" B.P. Konstantinov Petersburg Nuclear Physics Institute, St. Petersburg, Russia
- ¹²⁴ ^(a) INFN Sezione di Pisa; ^(b) Dipartimento di Fisica E. Fermi, Università di Pisa, Pisa, Italy
- ¹²⁵ Department of Physics and Astronomy, University of Pittsburgh, Pittsburgh, PA, United States
- ¹²⁶ ^(a) Laboratório de Instrumentação e Física Experimental de Partículas – LIP, Lisboa; ^(b) Faculdade de Ciências, Universidade de Lisboa, Lisboa; ^(c) Department of Physics, University of Coimbra, Coimbra; ^(d) Centro de Física Nuclear da Universidade de Lisboa, Lisboa; ^(e) Departamento de Física, Universidade do Minho, Braga; ^(f) Departamento de Física Teórica y del Cosmos and CAFPE, Universidad de Granada, Granada (Spain); ^(g) Dep Física and CEFITEC de Faculdade de Ciências e Tecnologia, Universidade Nova de Lisboa, Caparica, Portugal
- ¹²⁷ Institute of Physics, Academy of Sciences of the Czech Republic, Praha, Czech Republic
- ¹²⁸ Czech Technical University in Prague, Praha, Czech Republic
- ¹²⁹ Faculty of Mathematics and Physics, Charles University in Prague, Praha, Czech Republic
- ¹³⁰ State Research Center Institute for High Energy Physics, Protvino, Russia
- ¹³¹ Particle Physics Department, Rutherford Appleton Laboratory, Didcot, United Kingdom
- ¹³² ^(a) INFN Sezione di Roma; ^(b) Dipartimento di Fisica, Sapienza Università di Roma, Roma, Italy
- ¹³³ ^(a) INFN Sezione di Roma Tor Vergata; ^(b) Dipartimento di Fisica, Università di Roma Tor Vergata, Roma, Italy
- ¹³⁴ ^(a) INFN Sezione di Roma Tre; ^(b) Dipartimento di Matematica e Fisica, Università Roma Tre, Roma, Italy
- ¹³⁵ ^(a) Faculté des Sciences Ain Chock, Réseau Universitaire de Physique des Hautes Energies – Université Hassan II, Casablanca; ^(b) Centre National de l'Energie des Sciences Techniques Nucleaires, Rabat; ^(c) Faculté des Sciences Semlalia, Université Cadi Ayyad, LPHEA, Marrakech; ^(d) Faculté des Sciences, Université Mohamed Premier and LPTPM, Oujda; ^(e) Faculté des sciences, Université Mohammed V-Agdal, Rabat, Morocco
- ¹³⁶ DSM/IRFU (Institut de Recherches sur les Lois Fondamentales de l'Univers), CEA Saclay (Commissariat à l'Energie Atomique et aux Energies Alternatives), Gif-sur-Yvette, France
- ¹³⁷ Santa Cruz Institute for Particle Physics, University of California Santa Cruz, Santa Cruz, CA, United States
- ¹³⁸ Department of Physics, University of Washington, Seattle, WA, United States
- ¹³⁹ Department of Physics and Astronomy, University of Sheffield, Sheffield, United Kingdom
- ¹⁴⁰ Department of Physics, Shinshu University, Nagano, Japan
- ¹⁴¹ Fachbereich Physik, Universität Siegen, Siegen, Germany
- ¹⁴² Department of Physics, Simon Fraser University, Burnaby, BC, Canada
- ¹⁴³ SLAC National Accelerator Laboratory, Stanford, CA, United States
- ¹⁴⁴ ^(a) Faculty of Mathematics, Physics & Informatics, Comenius University, Bratislava; ^(b) Department of Subnuclear Physics, Institute of Experimental Physics of the Slovak Academy of Sciences, Kosice, Slovak Republic
- ¹⁴⁵ ^(a) Department of Physics, University of Cape Town, Cape Town; ^(b) Department of Physics, University of Johannesburg, Johannesburg; ^(c) School of Physics, University of the Witwatersrand, Johannesburg, South Africa
- ¹⁴⁶ ^(a) Department of Physics, Stockholm University; ^(b) The Oskar Klein Centre, Stockholm, Sweden
- ¹⁴⁷ Physics Department, Royal Institute of Technology, Stockholm, Sweden
- ¹⁴⁸ Departments of Physics & Astronomy and Chemistry, Stony Brook University, Stony Brook, NY, United States
- ¹⁴⁹ Department of Physics and Astronomy, University of Sussex, Brighton, United Kingdom
- ¹⁵⁰ School of Physics, University of Sydney, Sydney, Australia
- ¹⁵¹ Institute of Physics, Academia Sinica, Taipei, Taiwan
- ¹⁵² Department of Physics, Technion: Israel Institute of Technology, Haifa, Israel
- ¹⁵³ Raymond and Beverly Sackler School of Physics and Astronomy, Tel Aviv University, Tel Aviv, Israel
- ¹⁵⁴ Department of Physics, Aristotle University of Thessaloniki, Thessaloniki, Greece
- ¹⁵⁵ International Center for Elementary Particle Physics and Department of Physics, The University of Tokyo, Tokyo, Japan
- ¹⁵⁶ Graduate School of Science and Technology, Tokyo Metropolitan University, Tokyo, Japan

- ¹⁵⁷ Department of Physics, Tokyo Institute of Technology, Tokyo, Japan
¹⁵⁸ Department of Physics, University of Toronto, Toronto, ON, Canada
¹⁵⁹ ^(a) TRIUMF, Vancouver, BC; ^(b) Department of Physics and Astronomy, York University, Toronto, ON, Canada
¹⁶⁰ Faculty of Pure and Applied Sciences, University of Tsukuba, Tsukuba, Japan
¹⁶¹ Department of Physics and Astronomy, Tufts University, Medford, MA, United States
¹⁶² Centro de Investigaciones, Universidad Antonio Narino, Bogota, Colombia
¹⁶³ Department of Physics and Astronomy, University of California Irvine, Irvine, CA, United States
¹⁶⁴ ^(a) INFN Gruppo Collegato di Udine, Sezione di Trieste, Udine; ^(b) ICTP, Trieste; ^(c) Dipartimento di Chimica, Fisica e Ambiente, Università di Udine, Udine, Italy
¹⁶⁵ Department of Physics, University of Illinois, Urbana, IL, United States
¹⁶⁶ Department of Physics and Astronomy, University of Uppsala, Uppsala, Sweden
¹⁶⁷ Instituto de Física Corpuscular (IFIC) and Departamento de Física Atómica, Molecular y Nuclear and Departamento de Ingeniería Electrónica and Instituto de Microelectrónica de Barcelona (IMB-CNM), University of Valencia and CSIC, Valencia, Spain
¹⁶⁸ Department of Physics, University of British Columbia, Vancouver, BC, Canada
¹⁶⁹ Department of Physics and Astronomy, University of Victoria, Victoria, BC, Canada
¹⁷⁰ Department of Physics, University of Warwick, Coventry, United Kingdom
¹⁷¹ Waseda University, Tokyo, Japan
¹⁷² Department of Particle Physics, The Weizmann Institute of Science, Rehovot, Israel
¹⁷³ Department of Physics, University of Wisconsin, Madison, WI, United States
¹⁷⁴ Fakultät für Physik und Astronomie, Julius-Maximilians-Universität, Würzburg, Germany
¹⁷⁵ Fachbereich C Physik, Bergische Universität Wuppertal, Wuppertal, Germany
¹⁷⁶ Department of Physics, Yale University, New Haven, CT, United States
¹⁷⁷ Yerevan Physics Institute, Yerevan, Armenia
¹⁷⁸ Centre de Calcul de l'Institut National de Physique Nucléaire et de Physique des Particules (IN2P3), Villeurbanne, France

^a Also at Department of Physics, King's College London, London, United Kingdom.

^b Also at Institute of Physics, Azerbaijan Academy of Sciences, Baku, Azerbaijan.

^c Also at Novosibirsk State University, Novosibirsk, Russia.

^d Also at TRIUMF, Vancouver, BC, Canada.

^e Also at Department of Physics, California State University, Fresno, CA, United States.

^f Also at Department of Physics, University of Fribourg, Fribourg, Switzerland.

^g Also at Departamento de Física e Astronomia, Faculdade de Ciências, Universidade do Porto, Portugal.

^h Also at Tomsk State University, Tomsk, Russia.

ⁱ Also at CPPM, Aix-Marseille Université and CNRS/IN2P3, Marseille, France.

^j Also at Università di Napoli Parthenope, Napoli, Italy.

^k Also at Institute of Particle Physics (IPP), Canada.

^l Also at Particle Physics Department, Rutherford Appleton Laboratory, Didcot, United Kingdom.

^m Also at Department of Physics, St. Petersburg State Polytechnical University, St. Petersburg, Russia.

ⁿ Also at Louisiana Tech University, Ruston, LA, United States.

^o Also at Institutio Catalana de Recerca i Estudis Avancats, ICREA, Barcelona, Spain.

^p Also at Department of Physics, National Tsing Hua University, Taiwan.

^q Also at Department of Physics, The University of Texas at Austin, Austin, TX, United States.

^r Also at Institute of Theoretical Physics, Ilia State University, Tbilisi, Georgia.

^s Also at CERN, Geneva, Switzerland.

^t Also at Georgian Technical University (GTU), Tbilisi, Georgia.

^u Also at Ochadai Academic Production, Ochanomizu University, Tokyo, Japan.

^v Also at Manhattan College, New York, NY, United States.

^w Also at Hellenic Open University, Patras, Greece.

^x Also at Institute of Physics, Academia Sinica, Taipei, Taiwan.

^y Also at LAL, Université Paris-Sud and CNRS/IN2P3, Orsay, France.

^z Also at Academia Sinica Grid Computing, Institute of Physics, Academia Sinica, Taipei, Taiwan.

^{aa} Also at School of Physics, Shandong University, Shandong, China.

^{ab} Also at Moscow Institute of Physics and Technology State University, Dolgoprudny, Russia.

^{ac} Also at Section de Physique, Université de Genève, Geneva, Switzerland.

^{ad} Also at International School for Advanced Studies (SISSA), Trieste, Italy.

^{ae} Also at Department of Physics and Astronomy, University of South Carolina, Columbia, SC, United States.

^{af} Also at School of Physics and Engineering, Sun Yat-sen University, Guangzhou, China.

^{ag} Also at Faculty of Physics, M.V. Lomonosov Moscow State University, Moscow, Russia.

^{ah} Also at National Research Nuclear University MEPhI, Moscow, Russia.

^{ai} Also at Department of Physics, Stanford University, Stanford, CA, United States.

^{aj} Also at Institute for Particle and Nuclear Physics, Wigner Research Centre for Physics, Budapest, Hungary.

^{ak} Also at Department of Physics, The University of Michigan, Ann Arbor, MI, United States.

^{al} Also at Discipline of Physics, University of KwaZulu-Natal, Durban, South Africa.

^{am} Also at University of Malaya, Department of Physics, Kuala Lumpur, Malaysia.

* Deceased.